**EUROPEAN COMMISSION**
**5th EURATOM FRAMEWORK PROGRAMME 1998-2002**
**KEY ACTION : NUCLEAR FISSION**

# VALCO

**FIKS-CT-2001-00166**

## Deliverable D07:

# RESULTS OF COUPLED CODE VALIDATION CALCULATIONS

VALCO/WP1/D7.2

Anitta Hämäläinen, Timo Vanttola
VTT Processes
Finland

# SUMMARY

In work package one of the VALCO project five VVER transients were collected into a data base, that is used for validation of coupled neutronics thermal-hydraulics codes. This report focuses on the coupled code validation performed with several code combinations for two transients that were selected in first phase of the project. The transients were 'Drop of control rod at nominal power at Bohunice-3' for VVER-440 reactors and 'Coast-down of 1 from 3 MCPs at Kozloduy-6' for VVER –1000 reactors.

In the report the transients are at first shortly described. The comparison between the calculations and the measured data are given in figures and tables. Some conclusion are made and the problems come up during the validation are discussed. Five calculations were made for both the cases. The detailed validation reports of each calculation are appended to this report.

# CONTENTS



APPENDICES: CODE VALIDATION REPORTS IN VALCO:

1) Hämäläinen, A., Vanttola, T., Recommendations for Calculations and Calculated Parameters for Comparisons from Bohunice and Kozloduy Transient, VALCO/WP1/GUIDE-3, 2002. VTT Processes, Finland.

2) Hämäläinen, A., Kaloinen, E., Vanttola, T., VTT Calculations of the Bohunice Rod Drop Transient, VALCO/WP1/VTT-BO-CALC, 2003. VTT processes, Finland.

3) Strmensky, C., Darilék, P., Kvizda, B., Suchon, M., Hlbocky, P., VUJE Calculations Of The Bohunice Rod Drop Transient, VALCO/WP1/VUJE-BO-CALC, 2003. VUJE ltd., SE EBO ltd., Slovakia.

4) Hádek. J., Lahovský, F., Macek. J., NRI Calculations of the Bohunice Rod Drop Transient, VALCO/WP1/NRI-BO-CALC-1, 2003. Nuclear Research Institute Řež plc, Czech Republic.

5) Hegyi, G, Keresztúri, A., Trosztel, I, Aeki Calculations Of The Bohunice Rod Drop Transient, VALCO/WP1/AEKI-BO-CALC, 2003. KFKI-AEKI-RAL, Hungary

6) Danilin, S., Nikonov, S., Lizorkin, M., KI Calculations Of The Bohunice Rod Drop Transient, VALCO/WP1/KI-BO-CALC, 2003. RRC “Kurchatov Institute”, Institute of Nuclear Reactors, Russia.

7) Hämäläinen, A., Kaloinen, E., Vanttola, T., VTT Calculations of the Kozloduy Pump Trip Transient, VALCO/WP1/VTT-KO-CALC, 2003. VTT Processes, Finland

8) Danilin, S., Nikonov, S., Lizorkin, M., KI Calculations of the Kozloduy Pump Trip Transient, VALCO/WP1/KI-KO-CALC, 2003. RRC “Kurchatov Institute”, Institute of Nuclear Reactors, Russia

9) Kliem, S., Kozmenkov, Y., Mittag, S., Weiss, F.-P., FZR Calculations of the Kozloduy MCP Switching off Transient, VALCO/WP1/FZR-K6-CALC, 2003. FZR, Germany

10) Kuchin, A., Khalimonchuk, V., SSTC NRS Calculations Of Coast-down of one of three working MCPs at Kozloduy, unit 6, VALCO/WP1/SSTC NRS-KOZ-CALC, 2003. SSTC NRS, Ukraine

11) Stefanova, S., INRNE Calculations of the Kozloduy Pump Trip Transient, VALCO/WP1/INRNE-KO-CALC, 2003. INRNE, Bulgaria. Not ready.

# TABLE OF FIGURES

# 1 INTRODUCTION

The collection of measured data from NPP transients is of key importance for the validation of coupled thermal hydraulics / neutron kinetics codes. The first efforts in code validation concerning VVER reactors have already been going on for a number of years among the VVER users and analyzers. In the previous PHARE project SRR1/95 a first systematic effort was taken to search validation cases among occurred VVER plant transients and tests /refs. 6-7/. In the VALCO project this task is extended to new types of transients and new data.

In the beginning Work Package 1 of the VALCO project, a collection of five transients was made /ref.1/, three concerning VVER-440 plants and two of VVER-1000 type. Table 1.1 summarises all the collected transients in VALCO and in the previous PHARE project SRR1/95. The transients may be classified into four types: main coolant pump trips (5 pieces), control rod movements (2), turbine trips (2) and feed water pump trips (1). In the SRR1/95 project two secondary side originated transients: turbine trip and feed water trip, were selected for code validation. Two transients were selected for coupled code validation also in VALCO, this time of primary side origin. They were 'Drop of control rod at nominal power at Bohunice-3' for VVER-440 reactors and 'Coast-down of 1 from 3 working MCPs at Kozloduy-6' for VVER-1000 reactors. The first is an unexpected event and the latter one part of start up tests. So all the collected transient types have now been used for code validation.

**Table 1.1 Transients for data collection in VALCO and SRR1/95 projects**

| | **1. TRANSIENTS REPORTED IN SRR1/95:** | year |
|---|---|---|
| VVER-440 | Drop of one turbine to house load level experiment at the Loviisa-1 | 1997 |
| | Shutdown of 3 from 6 working main coolant pumps at the Dukovany-2 | 1986 |
| VVER-1000 | Turn-off of one from two working SG feed water pumps at the Balakovo-4 | |
| | Decrease of the turbo-generator power from 1000 MW down to the house load level at the Zaporoshye NPP | 1996 |
| | Switch-off of two neighbouring main coolant pumps at the Kozloduy-6 | 1992 |
| | **2. TRANSIENTS REPORTED IN VALCO:** | |
| VVER-440 | Drop of control rod No. 287 at 100% $N_{nom}$ at the Bohunice-3 | 1999 |
| | Outage of three main coolant pumps at N=95,4% $N_{nom}$ at the Mochovce-1 | 2000 |
| | Shutdown of 2 from 6 working MCPs at 100 % at the Dukovany-2 followed by reactor trip | 1997 |
| VVER-1000 | Main coolant pump 3 switch-off (1 of 4) at 100 % $N_{nom}$ followed with MCP 1 switch-off (1 of 3) at 65 % $N_{nom}$ at the Kozloduy-6 | 1992 |
| | Several single control rod insertions / withdrawals at the Rivne-3 | 2001 |

In VALCO eight institutes participated for the code validation with five different coupled codes. The institutes were Forschungszentrum Rossendorf in Germany (FZR), Technical Research Centre of Finland (VTT), KFKI Atomic Energy Research Institute in Hungary (AEKI), Nuclear Research Institute Rez, plc in Czech Republic (NRI), Institute for Nuclear Research and Nuclear Energy in Bulgaria (INRNE), VUJE Trnava a.s. in Slovakia (VUJE), State Scientific and Technical Centre on Nuclear and Radiation Safety in Ukraine (SSTCN) and Russian Research Center 'Kurchatov Institute' (KI).

Six teams applied ATHLET as thermal-hydraulic code and five teams DYN3D as neutronics code. The combination of ATHLET and DYN3D was applied by four teams. The participants, codes and calculated transients are summarized in Table 1.2.

**Table 1.2 Participants, used coupled codes and calculated cases in VALCO code validation.**

| Participant | Coupled code | VVER-440 Bohunice | VVER-1000, Kozloduy |
|---|---|---|---|
| FZR | ATHLET-DYN3D | | + |
| VTT | HEXTRAN-SMABRE | + | + |
| KFKI | ATHLET-KIKO3D | + | |
| NRI | ATHLET-DYN3D | + | |
| INRNE | ATHLET-DYN3D | | + |
| VUJE | RELAP5-DYN3D | + | |
| SSTC NRS | ATHLET-DYN3D | | + |
| KI | ATHLET-BIPR8 | + | + |

In the following chapters 2 and 3 the Bohunice and the Kozloduy transients are shortly described according to /refs. 1-3/. The comparison of calculations and the conclusions are in chapter 4. Nearly all the requested data for comparison is attached here as figures.

The code validation against measurements and not just between the codes, differs from benchmarking, because each participant also has to interpret the real measurements. In order to avoid excessive discrepancies, some recommendations for data interpretation were still needed. The recommendations and the code validation reports by each participant are appended to this report.

A further limitation to the validation task emerges from the restricted resources of the project: each participant applied a ready made model in the simulations. This implied certain shortcomings in the modelling of some specific features of the transients. Some of these issues are discussed in the report.

# 2 BOHUNICE TRANSIENT

## *2.1 Transient description*

In the Bohunice unit 3, control rod No. 287 from group 2 dropped during normal full power operation 6.1.1999. The level of power was reduced to 89% $N_{nom}$. The control rod reached lower-end position. Protection system HO-4 was activated (rod withdrawal blocked). Operator reduced the unit power to 85% $N_{nom}$ and all parameters were stabilised. Most information of the reactor core and thermal-hydraulic data within the transient are available. Some parameters are calculated from obtained data. The recording also includes restoration of the full power state. The transient was continued by power increase to nominal state after half an hour when rod withdrawal blocking was removed. For the code validation in VALCO only 1000 seconds after rod drop was used as reference measured data.

According to the external ionization chamber recordings the power distribution was remarkably skewed. This also reflected to marked variation of the hot leg temperatures and fuel assembly outlet temperatures. The observed phenomena enable model evaluation of reactivity effects of rod movements and consequent power redistribution calculations. The changes in the hot leg temperatures also enable evaluation of mixing process in the upper plenum. Because of the fairly sparse recording steps of some parameters, it is not possible to get a detailed picture of all aspects of the transient process, but it has been valuable to evaluate the difference between the initial and the stabilised state 1000 seconds after the rod drop.

## *2.2 Calculation specification*

The Bohunice data collection report /ref. 2/ gave the main ideas how to perform the validation calculations. However, because interpretation of the measured data may lead to several directions in this transient, some recommendations were in place (see appendix 1). In the appendix, also the variables and the parameters to be simulated were listed.

The calculated transient is initiated with control rod 287 drop at time 0.0. The position of dropped rod is shown in Figure 2.1. According to measured data set from the plant, the last unchanged measured time point is 18:37:47, and the first changed time point is 18:37:59. The rod drop can be expected to have started between these two points. In the following comparison it is assumed that the calculated time 0.0 corresponds the real time 18:37:47 at the plant. No more that 12 seconds are needed for the rod to reach the lowest position, when a typical rod drop speed of 20 cm/s is assumed.

In line with the data report, the initial position of the regulating group was fixed to 175 cm from the bottom of the core and that the protection system blocked withdrawal of the group after the incident. The data report further shows that, starting from 18:40 the operator gradually lowered the power level from 89 % to 85 %. The measured data indicate slow movement or several small control rod group actions during the next minutes. For the calculations the regulating control rod group was recommended to be inserted in two slopes, the first between 180 – 220 s and the second one between 260 – 320 s. In the first step the control rod movement was assumed to take 25 % of the total

movement, and in the second one 75 %, correspondingly. Total movement needed for the power reduction was left as a parameter to be defined by each calculator.

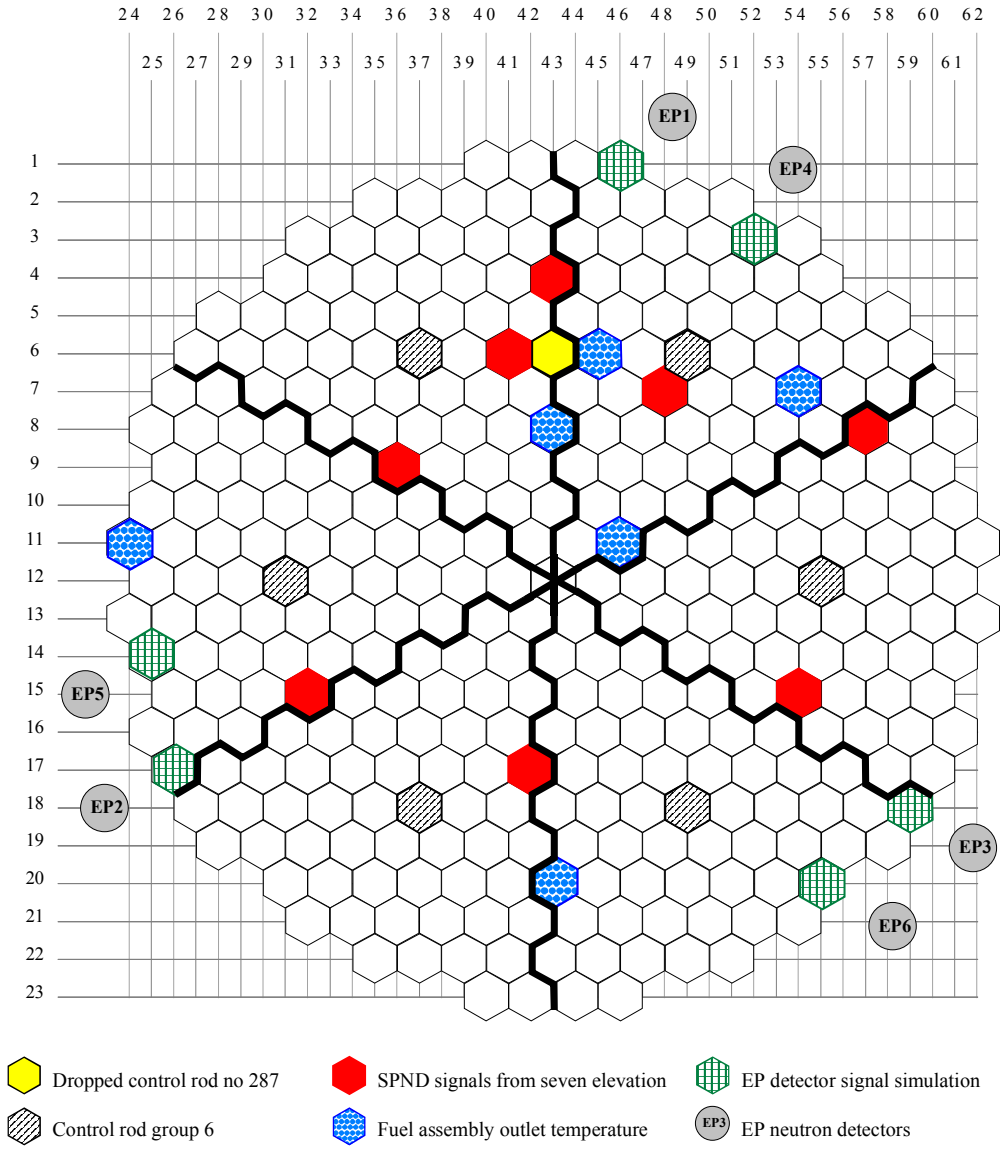


Figure 2.1 Layout of the fuel assemblies and essential control rods. The figure also shows the approximate thermal hydraulic sectors corresponding to the loops and positions of assemblies chosen for the comparison between measurements and calculations.

According to the data report the core bypass flow, totally 9.12 % of the flow to the pressure vessel, consists of several components. The main part of it, 5.45 %, is the share of the core inlet flow that diverts through the assembly lower part holes to the inter assembly space and returns through the upper holes below the assembly outlet temperature probe. Because the core outlet temperatures are important parameters for comparison of the calculated results to the measured ones, depending on the used model

the participants were recommended to determine, whether a smaller (3.67 %) bypass is used or the reported one (9.12 %). In the latter case the mixing before the temperature measurement should be considered.

In the Bohunice transient the main interest is in the core and pressure vessel phenomena. For the secondary side modelling it was recommended that the participants should determine by themselves what kind of boundary conditions to apply. They are highly dependent on the extent of the used plant model, that varied considerably between the participants.

### *2.3 Used codes and type of coupling*

The Bohunice transient was calculated in five institutes (VTT, KFKI, VUJE, NRI and KI) with five different code couplings. The ATHLET code was used as thermal hydraulic code in three combinations. The others were SMABRE and RELAP5 codes. The DYN3D code was the neutron kinetic code in two combinations and the others were HEXTRAN, KIKO3D and BIPR8. In table 2.1 the used codes and the basic models are summarised.

**Table 2.1 Basic data in Bohunice calculations**

| | VTT | VUJE | NRI | KFKI | KI |
|---|---|---|---|---|---|
| Neutron kinetic code, version | HEXTRAN 2.8 | DYN3D /H1.1 | DYN3D2 000/M1 | KIKO3D | BIBR8 |
| Thermal hydraulic code, version | SMABRE 4.7 | RELAP5/ MOD3 | ATHLET 1.2a | ATHLET | ATHLET |
| Type of coupling | Parallel | Parallel | External | Internal | Internal |
| Number of core fluid channels in the thermal hydraulic code | 6 | 6 | - | 25 | 349 |
| Number of core fluid channels in neutron-kinetic code | 349 | 349 | 349 | - | - |
| Number of assemblies in neutron kinetic code | 349 | 349 | 349 | 349 | 349 |
| Total core bypass flow in the active part of the core (%) | 3.64 | 9.112 | 3.67 | 9.12 | 9. |
| Degree of mixing in reactor pressure vessel before core / after core (%) | 30. / 0. | 100./100. | 100./100. | 25. / 0. | 100./100. |
| Number of circulation loops | 6 | 6 | 2 | 6 | 6 |

In all the neutron kinetics models, the whole core description was used with separate 349 fuel assemblies. In the joining of a neutron kinetics code and a thermal hydraulics code, three types of coupling were used: parallel, external and internal. VTT and VUJE applied parallel coupling, where thermal hydraulics is calculated in both parts, thermal hydraulic codes SMABRE / RELAP5 and neutron-dynamic codes HEXTRAN / DYN3D. Both have six parallel fluid channels in the thermal hydraulics code and all the 349 assemblies/channels in neutron dynamics code. The distribution into six parallel fluid channels in the core is about the one showed in Figure 2.1, where a sector corresponds to a circulation loop and the dropped rod is between two sectors.

NRI used the external coupling, where all the core calculation including thermal hydraulics is calculated with neutron-dynamic code DYN3D. All the assemblies were modelled with parallel fluid channels.

KFKI and KI used the internal coupling, where thermal hydraulics of the core is calculated only with the thermal hydraulics code (ATHLET). KI modelled all 349 assemblies as parallel fluid channels and KFKI used 25 parallel channels for ATHLET. Basically the KFKI division into channels is according to sectors in Figure 2.1, but the assemblies with control rods, assemblies near the outer edge in each sector, near the dropped rod and the assembly with dropped rod are represented with separate fluid channels. Further, in KFKI results a special method has been used to get individual FA outlet temperatures. Some fluid channels describing the reflectors are included in part of the calculations.

The asymmetric transient also reflects to the loop behaviour, as can be seen in the deviation of the loop measurements. Therefore the mixing processes in the lower and upper plenum need consideration, in addition to the requirement of individual loop modelling. In the core there is practically no mixing due to the shrouds around the assemblies.

In the calculations VTT, VUJE, KFKI and KI modelled all the six circulation loops, whereas NRI used two loops. Before the core inlet, VTT and KFKI used degree of mixing of 30 and 25 %, respectively. After the core they did not assume mixing at all. VUJE and NRI assumed ideal mixing (100 %) before and after the core, which was a consequence of one-dimensional nodalisation of the corresponding pressure vessel parts.

Four codes, CASMO-4, HELIOS, KARATE-440 and KASSETA were used for cross section data preparation from the nuclear data libraries. The combinations appear in Table 2.2, where the initial state feedback coefficients are compared, too.

**Table 2.2 Reactor data in Bohunice calculations**

| | VTT | VUJE | NRI | KFKI | KI |
|---|---|---|---|---|---|
| Neutron kinetic code | HEXTRAN | DYN3D /H1.1 | DYN3D2 000/M1 | KIKO3D | BIBR8 |
| Cross section calculations | CASMO-4 | HELIOS | HELIOS | KARATE -440 | KASSETA |
| Doppler coefficient in initial state (pcm/K)* | -2.67 | | -2.48 | -2.83 (-3.28) | -2.54 |
| Moderator total temperature coefficient in initial state for uniform temperature change (pcm/K) | -39.1 | | -43.38 | -41.8 | -41.24 |
| Initial boron concentration (g/kg) | 3.0 | 2.9995 | 2.723 | 2.96 | 2.60 |

* uniform change in fuel temperature

## *2.4 Results*

At the initial state the measured cold and hot leg temperatures varies from 269.2 to 272.4 and from 299.2 to 302.4 °C, both are inside ±1.6 °C. The deviation between the loops is

partly due to measuring accuracy and partly due to asymmetry in the plant. The highest pressure in steam generator 5 leads to the highest cold leg temperature in loop 5. The largest mass flow in the same loop leads to the lowest temperature difference over the core sector and at the same time with highest cold leg temperatures to the lowest hot leg temperature.

The time histories of the Bohunice transient simulations compared to the measurements are shown in Figure 2.5 to Figure 2.31. Typically the measurements are stepwise due to reading dependent measuring system, where the values are periodically checked and recorded if recording step (aperture, change from previously recorded) has been exceeded. Otherwise the preceding 'old' value is given in the measurement. The recording step is individually set for the measurements and may also be changed during the transient. In the comparison between calculations and measurements, only the signals immediately after such a step are considered 'true' and are often marked with a square symbol on the curves. When using average values of the measurements 'true' points are somewhere between the steps.

The transient starts at time 0.0 with the rod drop at position 12-43. The rod drop is recorded immediately by the out of core neutron detectors (Figure 2.22) near to the dropped rod. In the calculations the detector response kernels are used in VTT calculations, while in the others' calculations the local fast neutron flux (closest to the detector) is used for simulation of detector readings. All the calculations in this corner at first reach and go under the recorded relative power signals 0.7 and 0.745, but then return on some higher level due to feedback effects. The detectors far from the dropped rod record only the later control action and drop down to the level 0.91 – 0.93 (Figure 2.23). The overall asymmetry of the core is illustrated in Figure 2.2 with power ratio of the final and the initial state. A more detailed power profile in a row of assemblies crossing the rod drop position appears in Figure 2.3. The profiles vary to some extent close to the dropped rod, and the same differences may also be seen in the external detector signals (Figure 2.22).

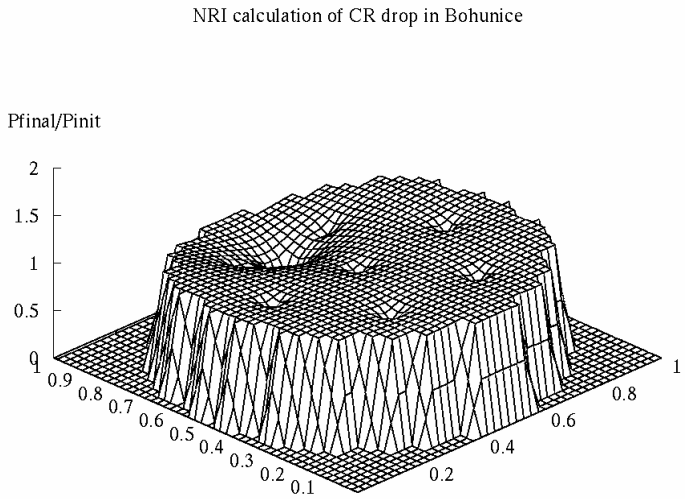


Figure 2.2 The relative radial power profile (Pfinal/Pinitial) of the core at the end of the NRI calculations.

The control action is made with control rod group 6 depicted in Figure 2.6. The final power level of 85 % is reached with very different positions of control rod group, with total movement of control rods ranging from 12.4 cm to 29.5 cm, shown in Table 2.3. This is not just a result of the different worth of control rods (KFKI the largest) but also the initial fuel temperature, shown in Table 2.3. More reactivity is released when fuel cools down more because of higher initial fuel temperature. The larger released Doppler reactivity increases power more after the rod drop, which leads to larger control rod action needed to reach the desired power level.

The power level after the initial drop needs some consideration (Figure 2.5): The power of the KFKI, VUJE and NRI calculations stabilize on a higher level than in the VTT and KI calculations. The KFKI model has the largest value of the control rod, 0.165, and a moderate fuel initial temperature, but the coolant inlet temperature cools down more that in the other simulations (Figure 2.7). In the VUJE and the NRI calculations the fuel initial temperature is relatively high, which releases more reactivity after the rod drop, and at the same time the inlet temperature decrease is some larger that in the VTT and KI calculations.

In VUJE result peculiar behaviour with power increase is shown after starting the control action. The comparison to actual power can be simulated with the average temperature difference of the loops (Figure 2.9) and with mass flows (Figure 2.10). All the calculated temperature differences are within 1.5 °C from the measurements. In the Figure 2.10 the larger values are the total primary mass flows and smaller ones the core inlet mass flows. The total mass flows are within 200 kg/s from the measurements but the core mass flows deviate much more from each other due to different assumptions of the core bypass.

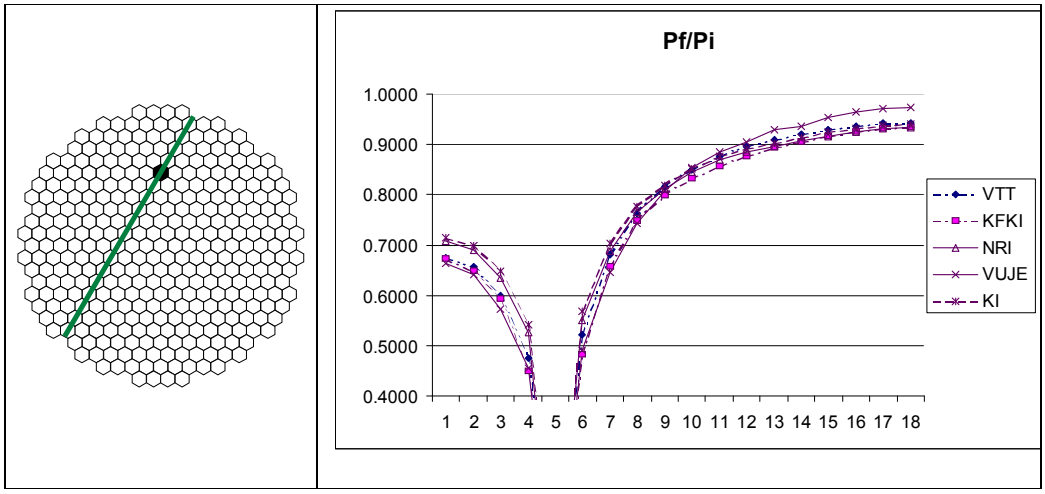


Figure 2.3 The calculated power profile in the indicated assembly row through the dropped rod at the end of the calculations.

**Table 2.3 Control rod and fuel rod modelling in Bohunice calculations**

| | VTT | VUJE | NRI | KFKI | KI |
|---|---|---|---|---|---|
| Total control rod movement (cm) | 12.4 | 21.0 | 29.5 | 18.0 | 16.0 |
| Worth of dropped rod in hot zero power critical state, T=260 °C, no Xe (%) | 0.1337 | 0.1143 | 0.12646 | 0.165 | 0.1312 |
| Critical boron concentration in hot zero power, T=260 °C, no Xe (g/kg) | 6.186 | 7.003 | 6.67108 | | |
| Fuel average temperature (ºC)<br>at initial state<br>at final state | <br>527.<br>488. | 680. | 616. | 593. | |
| Maximum fuel centerline temperature at initial state (ºC)<br>at final state (ºC) | <br>925.<br>888. | 982. | 1217. | | 1129. |
| Used gas gap model, constant ($W/m^2K$), dependencies of temperature or burnup ... | temp. and burnup dep. | constant 5600 | temp. and burnup dep. | constant 3000 | constant 3000 |

The calculated primary pressure with some measured points are shown in Figure 2.11 and the pressurizer level in Figure 2.12. The secondary side behaviour is depicted in Figure 2.13 with average steam generator pressures, with average steam line mass flows in Figure 2.14 and with average feed water mass flows in Figure 2.15.

As a result of quite stable steam generator pressures, the cold leg temperatures have changed only few degrees during the transient (Figure 2.7) and are within measuring accuracy. KFKI and VUJE calculations include dropping of cold leg temperatures and recovering just after rod drop like seen in the measurements, too.

The calculated and measured hot leg temperatures in all six loops are shown in Figure 2.8. The measured hot leg temperatures start deviating from each other just after rod drop due to asymmetric situation in the core. In the VTT and KFKI calculations the upper plenum is modelled without mixing. In these results the hot leg temperature in two loops near the dropped rod decreases 7 °C lower than the loops far from dropped rod.

The signals of the local neutron detectors inside the core and the signals of the thermo-couples are filtered due to the physical properties of the measurement instruments. In the /refs. 1 and 4/ a model was given how to handle the calculated values before the comparison to measurements. According to results of SRR1-95, the time constant of 10 second was used for calculated loop temperatures and 30 seconds for assembly outlet temperatures while comparing to measurements. The time constants for SPND simulation are discussed in chapter 2.4.1

The time histories of core outlet temperature from six assemblies are shown in Figure 2.16 to Figure 2.21. The measured temperature drop due to rod drop, from the initial values to the level about two minutes later, is in each six assemblies bigger than in the calculations. The temperature drop due to control action is on the contrary somewhat higher in the calculation than in the measurements. VTT with highest control rod worth and smallest initial fuel temperatures reaches the lowest power level and biggest temperature drop of core outlet temperature in rod drop. In some core outlet temperature figures the VUJE and KFKI results differ from the others due to less thermal hydraulic channels in the core than all the others.

The axial and radial power distributions and the core outlet temperature distributions are depicted in Figure 2.32 to Figure 2.41. The axial power profile in the VUJE calculations show clearly more peaked power in lower parts of core. The differences between calculated and measured temperatures are mainly in the measuring accuracy.

### 2.4.1 Self Power Neutron Detectors (SPND)

In the Bohunice reactor core in the 36 fuel assemblies, seven Rhodium emitter self powered neutron detectors are located at seven elevations. The three dimensional power distribution of the core may be evaluated by the signals of these detectors. The neutron detector sensitivity can be assumed to be constant during the transient, so the behaviour of local power density can be determined based on the current using its relative change during the transient. The time constant of the detector current must be taken into account, however. The delayed part of the detector signal can be normally /ref. 4/ taken as 95 % with two different half-lives T1/2 = 42 s (92 % of the delayed signal) and T1/2 = 4.4 min (8 % of the delayed signal). Thus the time constants are about 60.6 s and 380 s respectively. This has been successfully applied in previous project, but now all the calculations are well compared to measurements when clearly higher values, 178.5 s and 246.9 s, have been used.

Also another problem appeared with SPND measurements. According to measured data set from the plant, the first changed time point is 18:37:59, but the first marks in SPND measurements are at 18:39:11. Such a large difference between SPND measurements and other measurements can't be expected to be in spite of large time constants of the measurement system. That is why in the following, the time shift of one minute is used in comparison of the calculations to the measurements. This kind of time shift could be expected if the clocks are not synchronized in different measuring systems in the plant.

The general behaviour of calculated SPND signals with the above mentioned one minute time shift and modified time constants are quite good in all calculations as shown in Figure 2.4. However, a notable result is that in spite of total power decrease, the KFKI and the NRI results before the control action, and in the VUJE results also at the end of transient, indicate local power increase on the opposite side from the dropped rod. This can be seen in the topmost SPND signals. These signals mainly represent the power part of the core. The explanation to the power rise in these simulations is the reactivity effect when the coolant inlet temperature decreases more than in the VTT and KI calculations. In the VUJE calculation the phenomenon is stronger because of the more low peaked fission power that also sharpens more during the transient than in the other calculations.

The SPND signals of each assembly in the middle, the lowest and upper most positions compared to measurements are depicted in Figure 2.24 to Figure 2.31. Near the dropped rod the signals of same assembly in all elevations drop nearly equally (positions 04-43, 06-41 and 07-48 in Figure 2.24 to Figure 2.26) and the drops are the largest ones, 0.55 in relative units in neighbouring assembly to dropped rod. On the other side of the core the rod drop is not seen and in some calculations the signals even increase until the control action starts to decrease the signals, but the total changes are not as large ones. The measured and calculated signals in positions, 15-32, 15-56 and 17-42 in Figure 2.28 to Figure 2.31, differs between different elevations and also between the calculations. The signals on the upper levels of these assemblies drop more due to control group insertion.

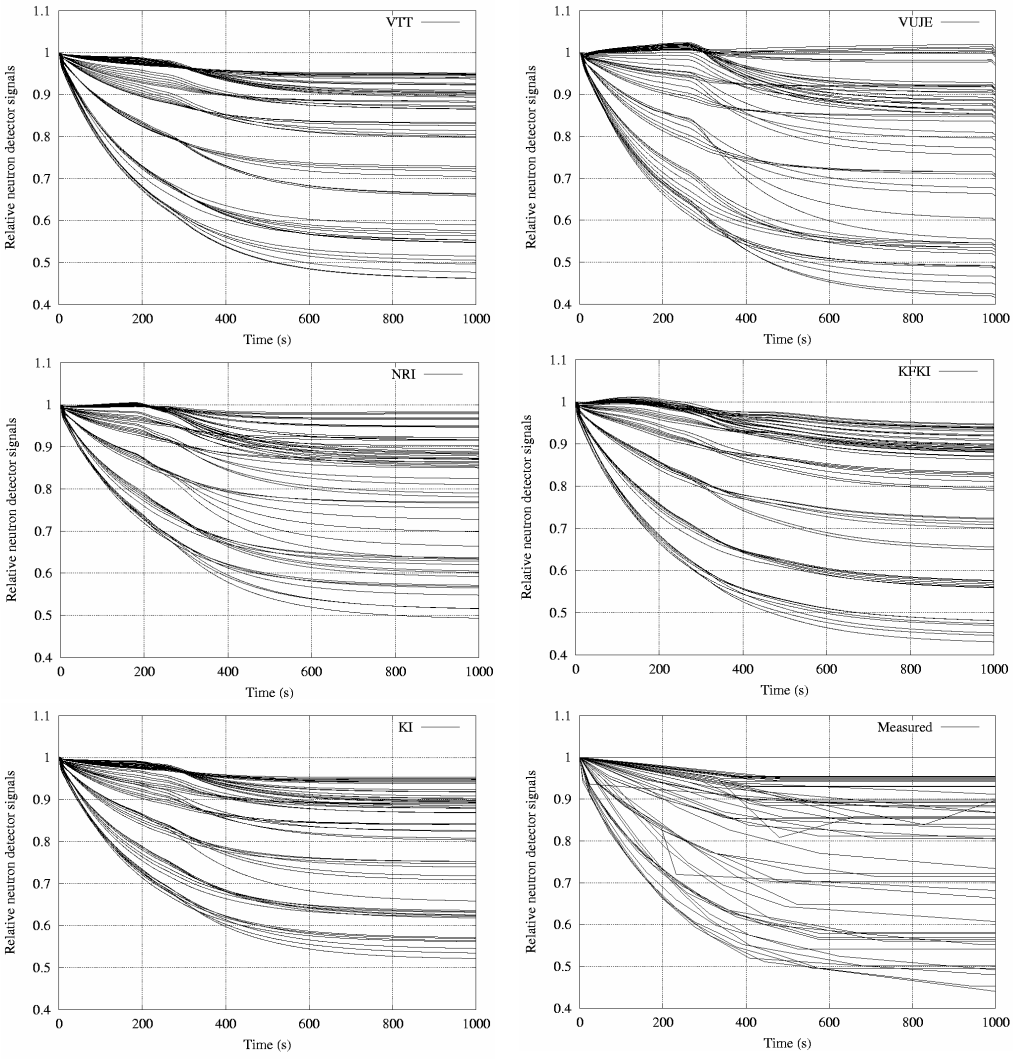


Figure 2.4 Measured and calculated SPND signals from eight assemblies and seven elevations at Bohunice rod drop case. The signals are all scaled to 1 in the beginning of the transient.

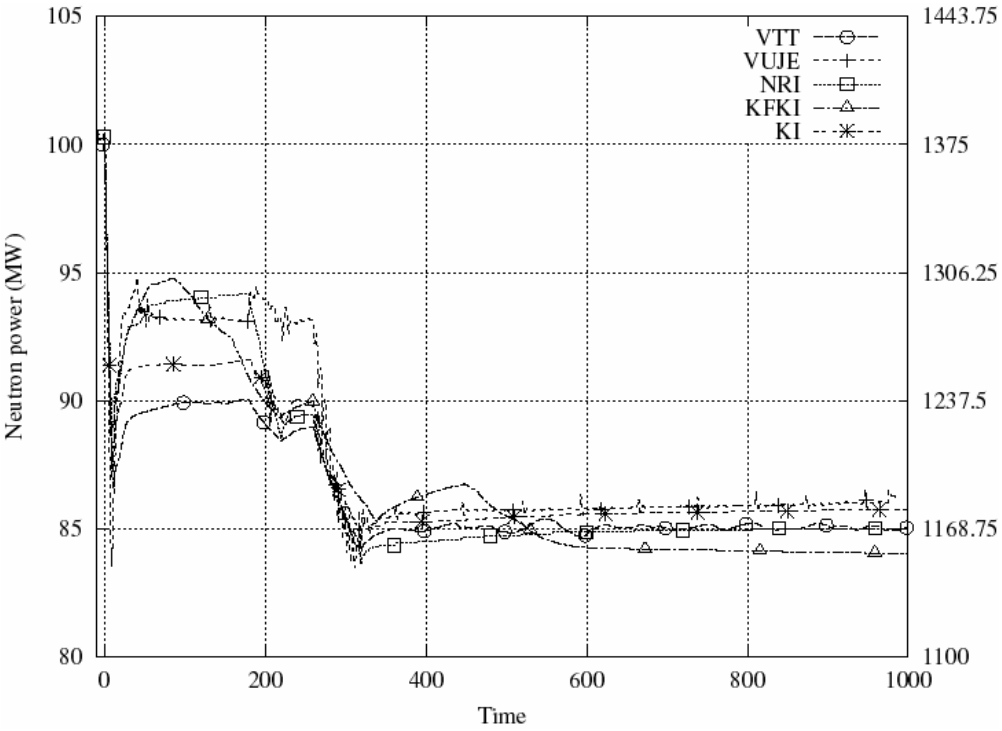


Figure 2.5 Calculated neutron power.

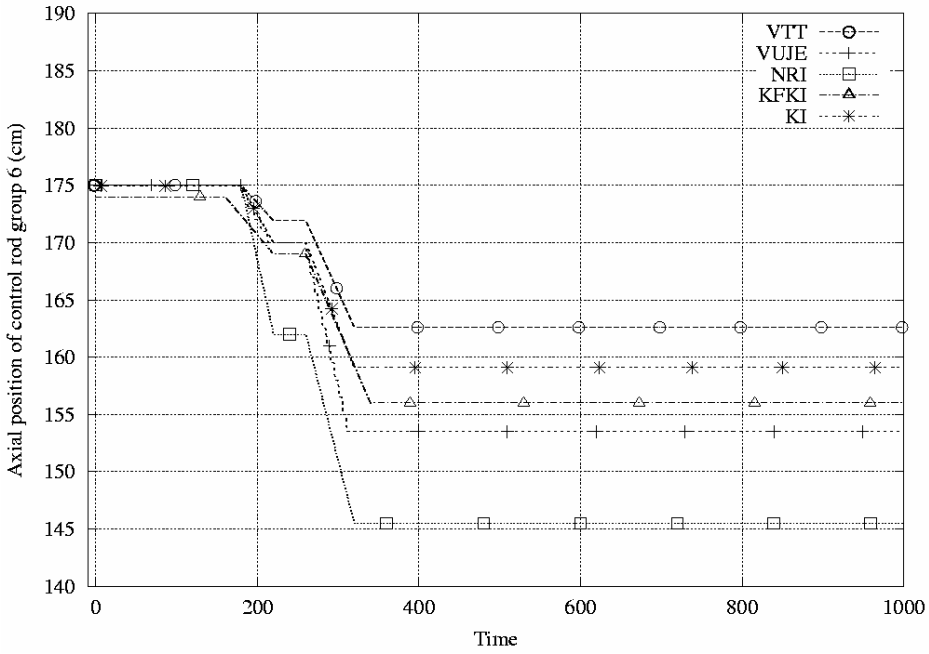


Figure 2.6 Calculated axial position of control rod group 6.

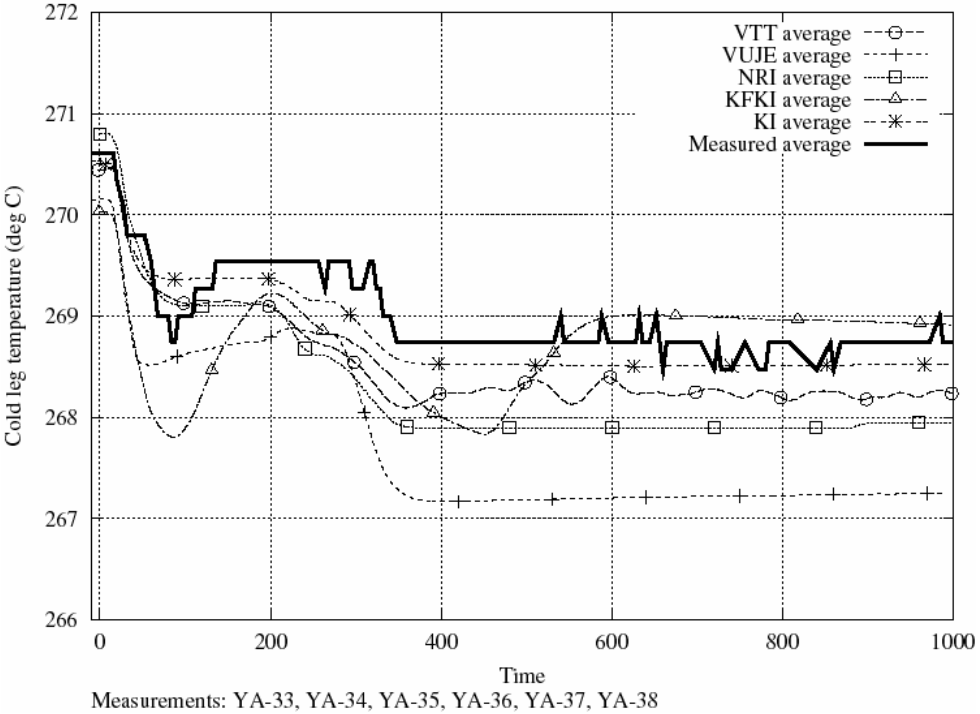


Figure 2.7 Calculated and measured average temperatures in six cold legs.

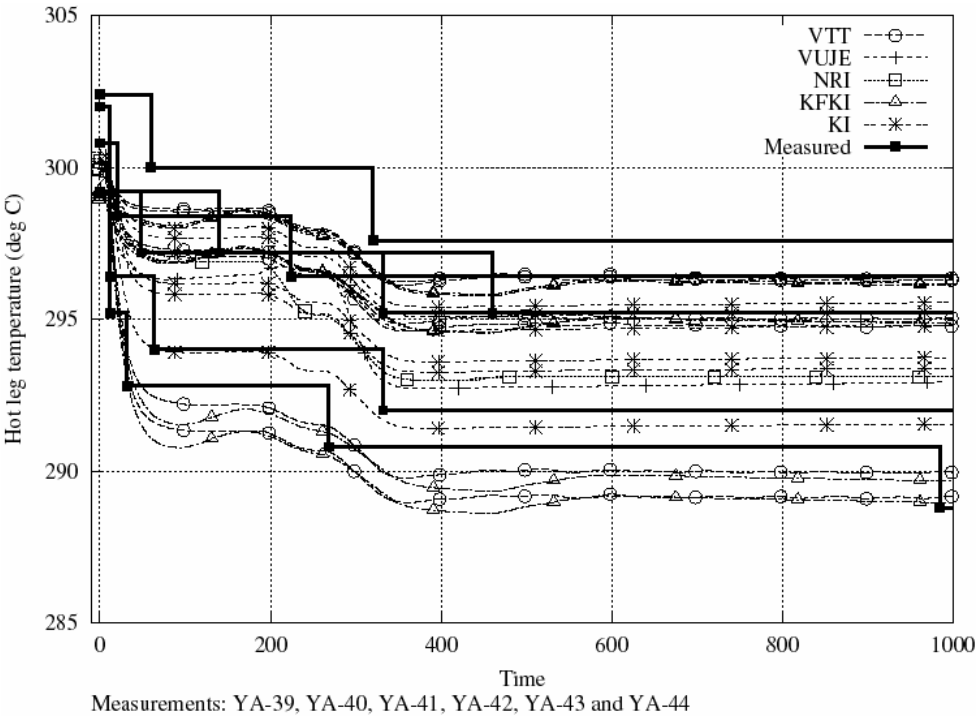


Figure 2.8 Calculated and measured temperatures in six hot legs.

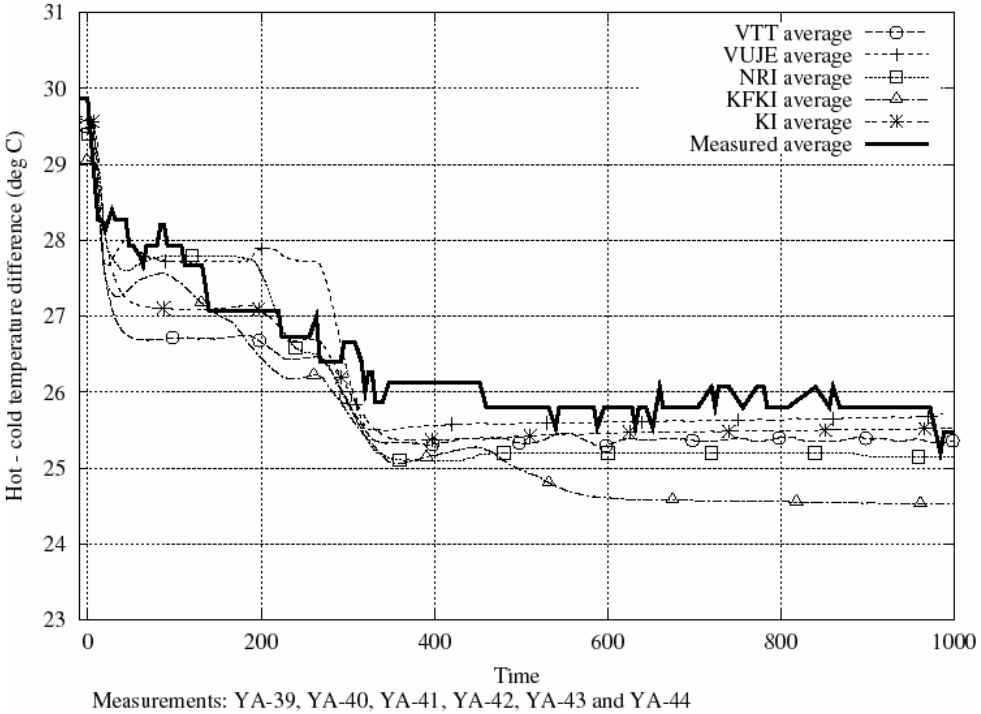


Figure 2.9 Calculated and measured average temperature difference between cold and hot legs.

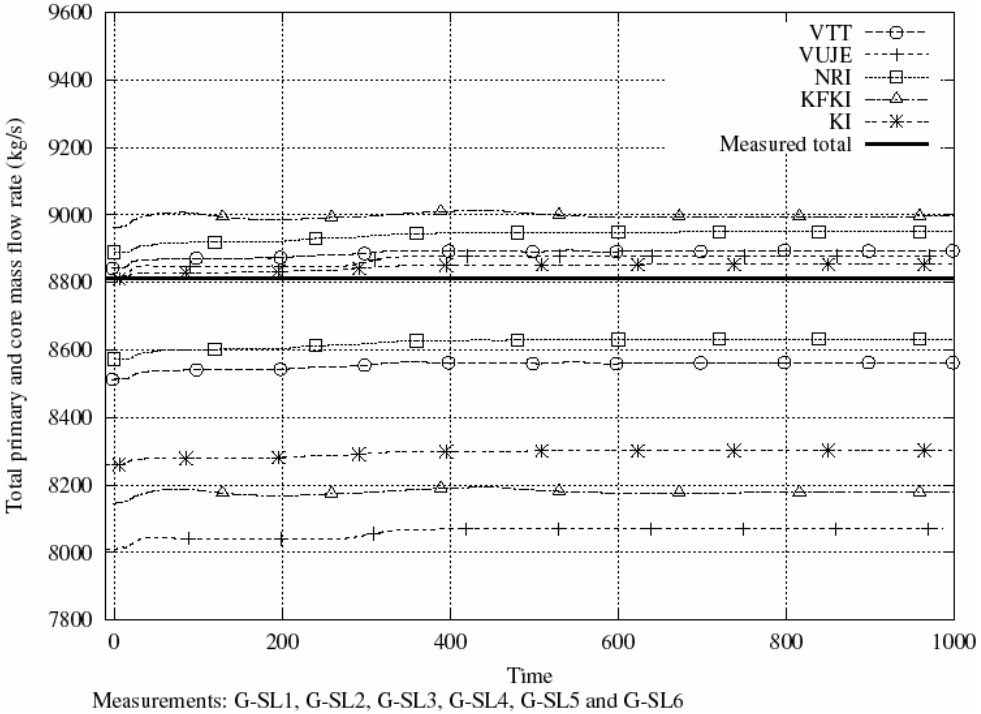


Figure 2.10 Calculated and measured total primary mass flow rates and calculated core mass flows.

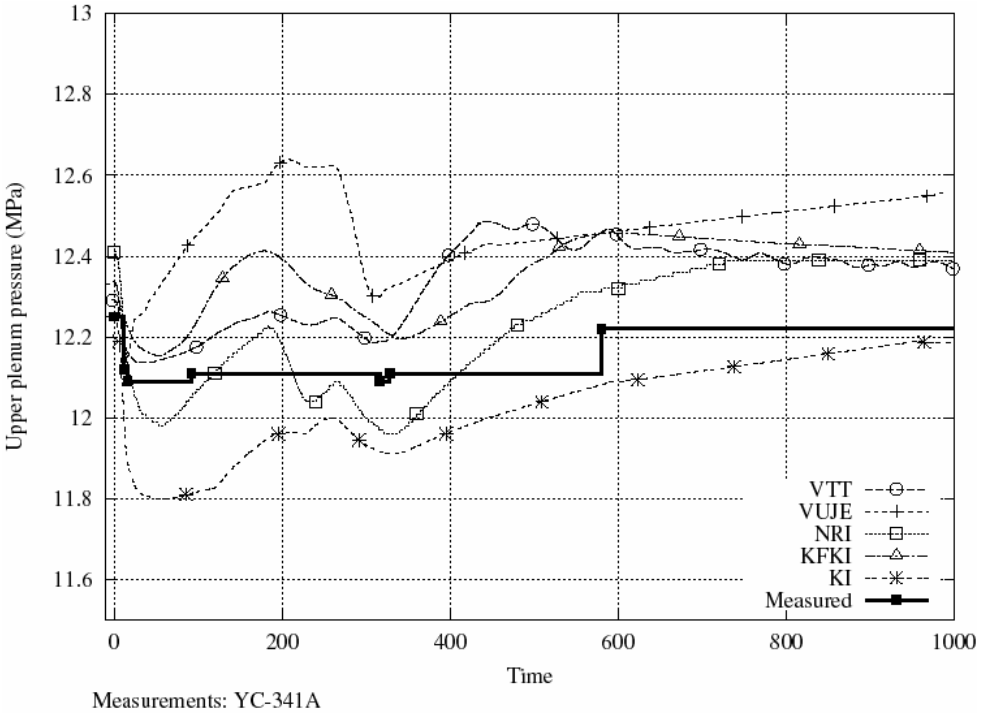


Figure 2.11 Calculated and measured upper plenum pressures.

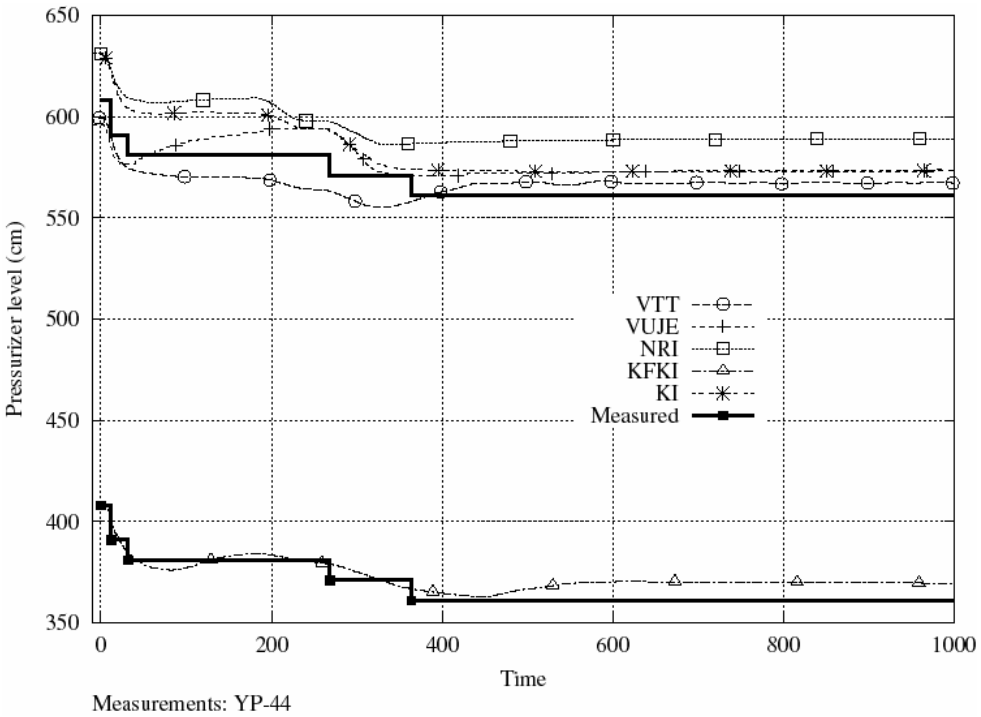


Figure 2.12 Calculated and measured water level in pressurizer.

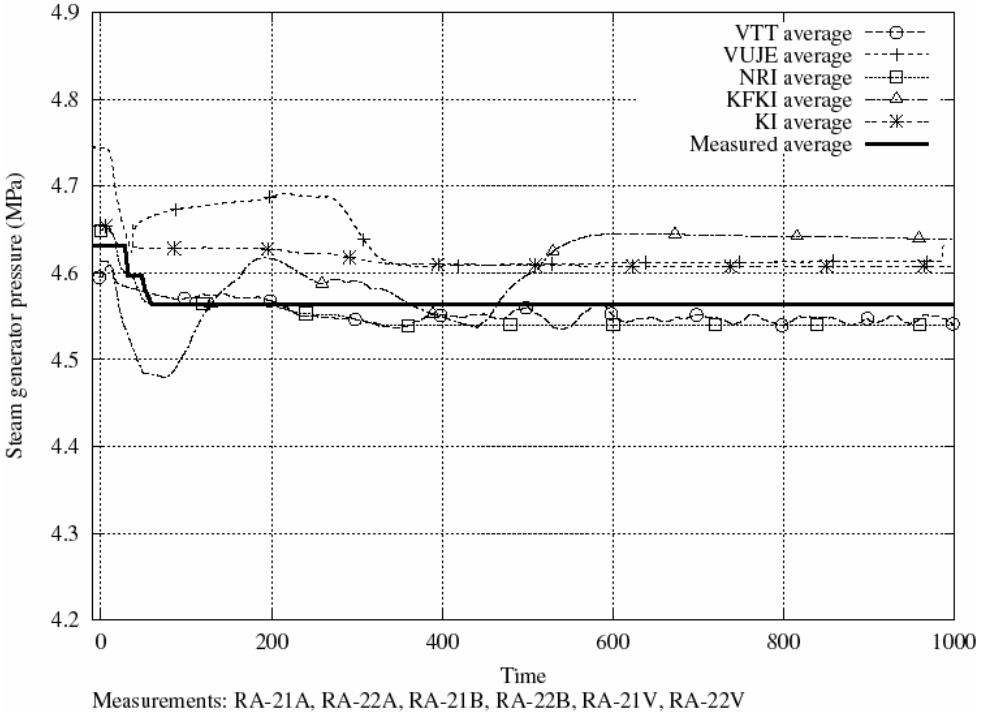


Figure 2.13 Calculated and measured average pressure at steam generator secondary side.

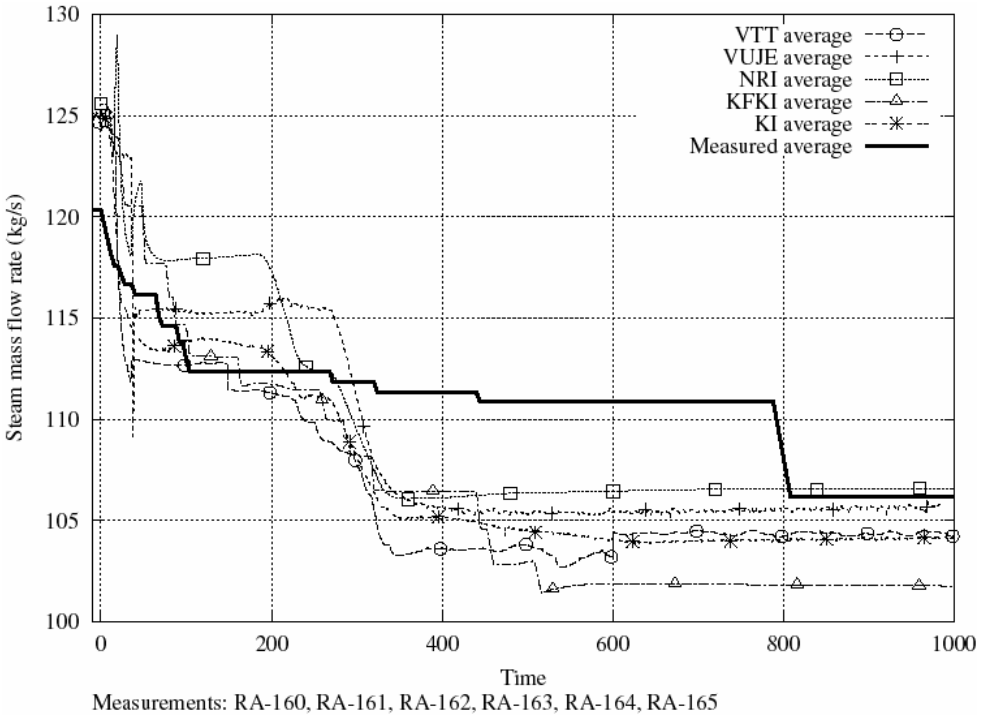


Figure 2.14 Calculated and measured average steam line mass flow rate.

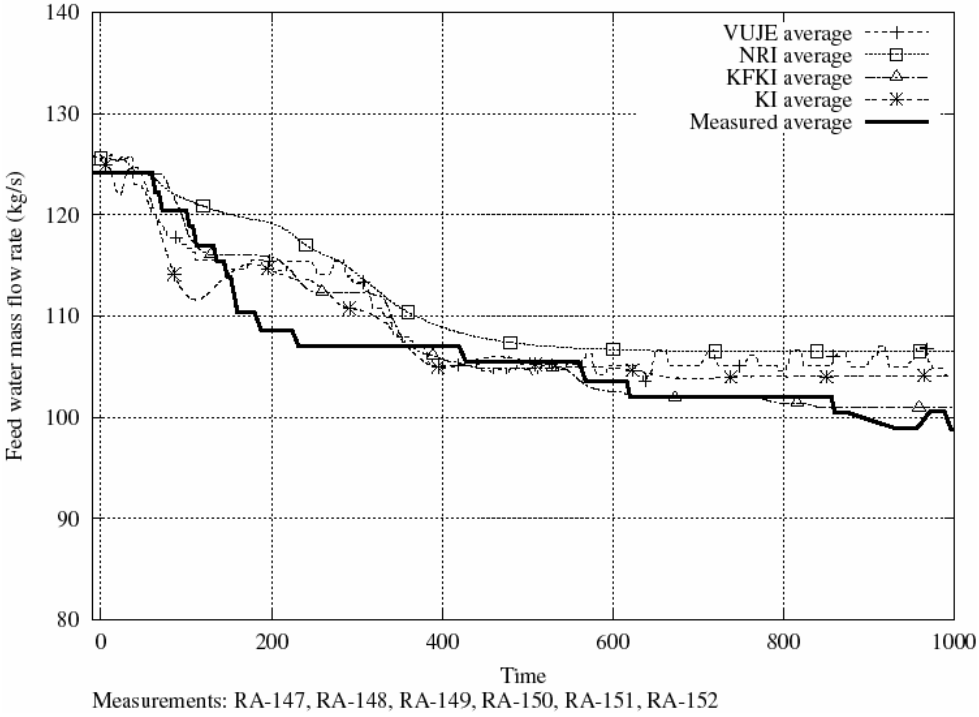


Figure 2.15 Calculated and measured average feed water mass flow rate.

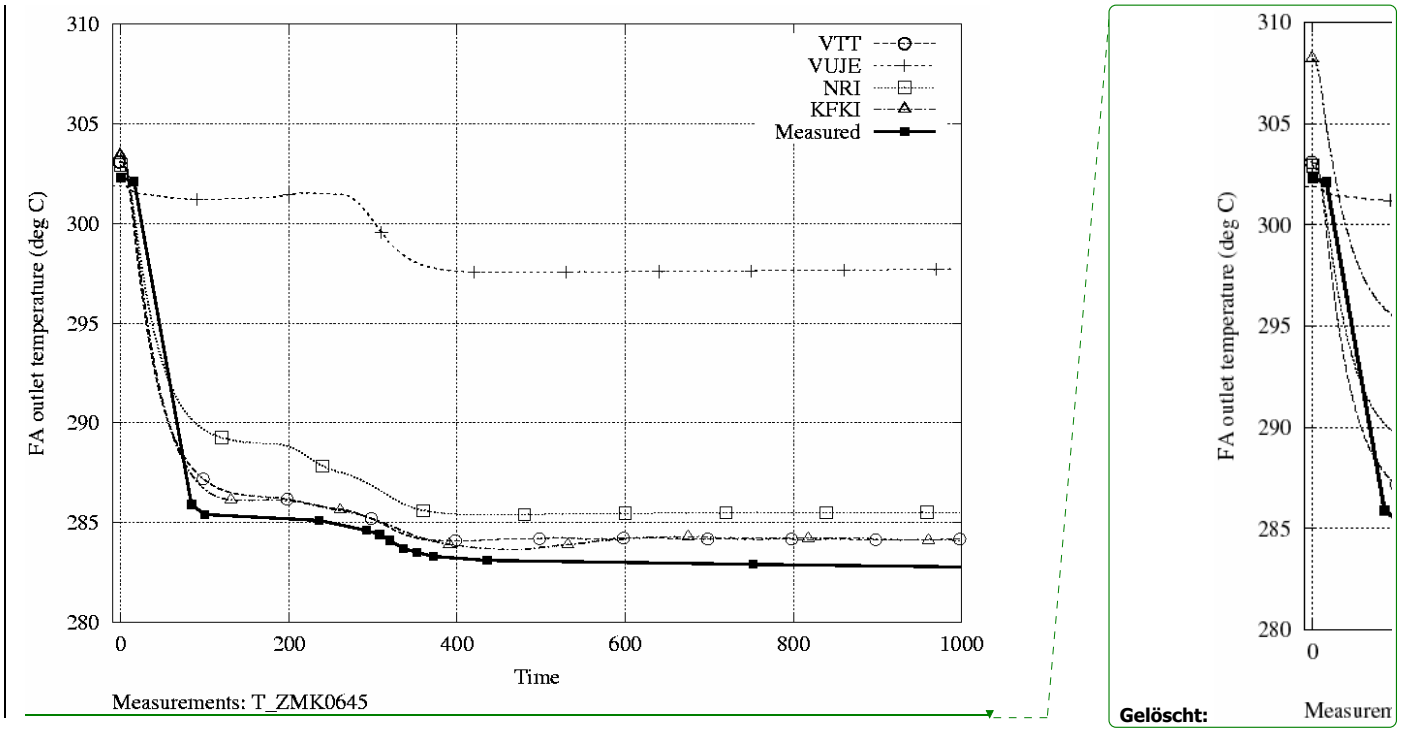


Figure 2.16 Calculated and measured fuel assembly outlet temperature at position 06-45.

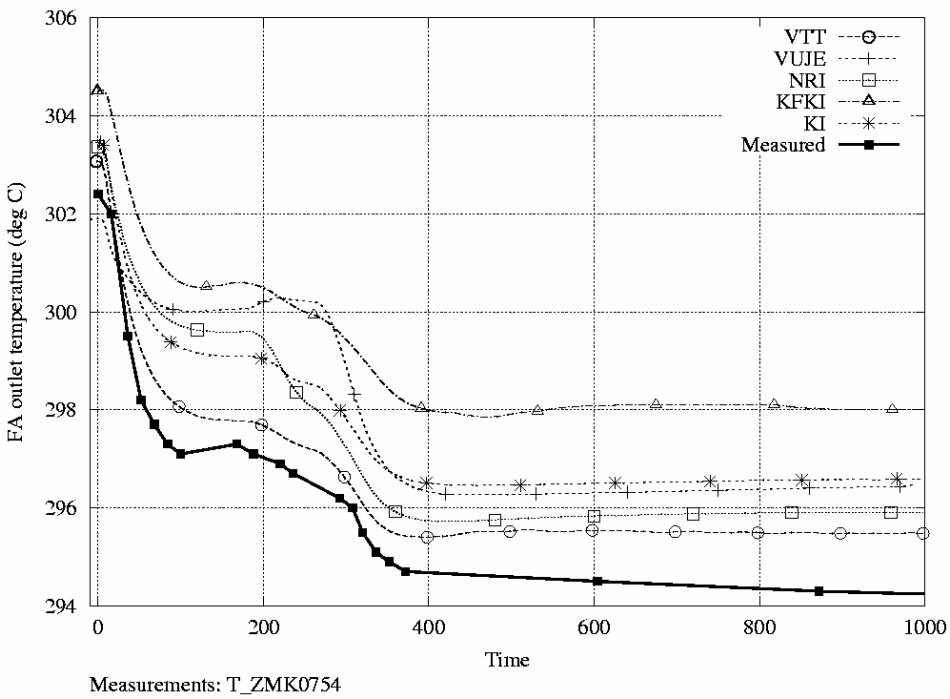


Figure 2.17 Calculated and measured fuel assembly outlet temperature at position 07-54.

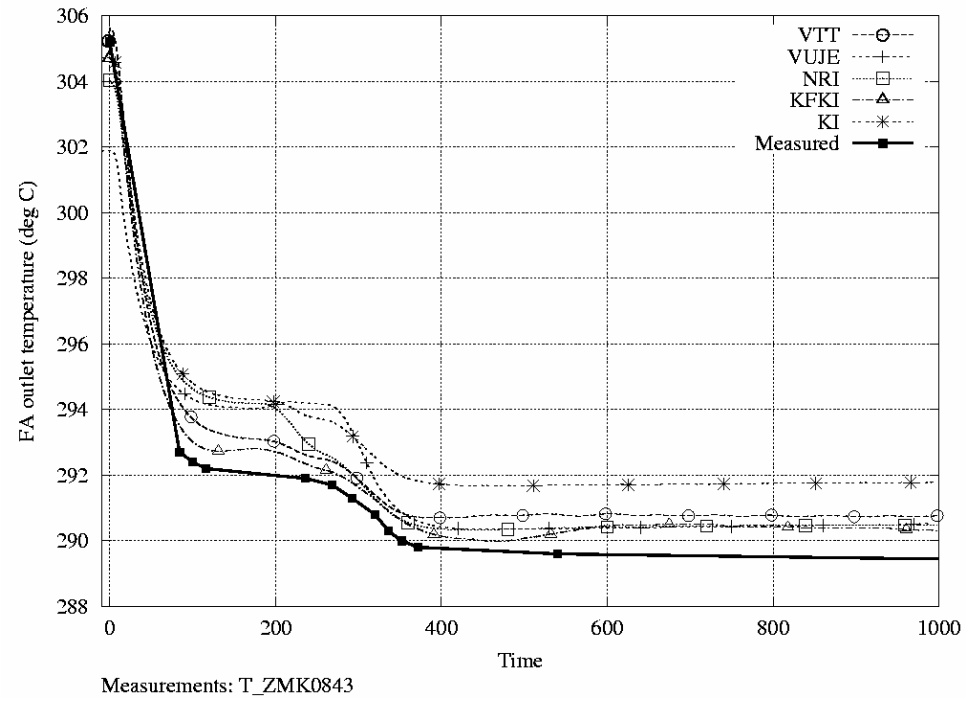


Figure 2.18 Calculated and measured fuel assembly outlet temperature at position 08-43.

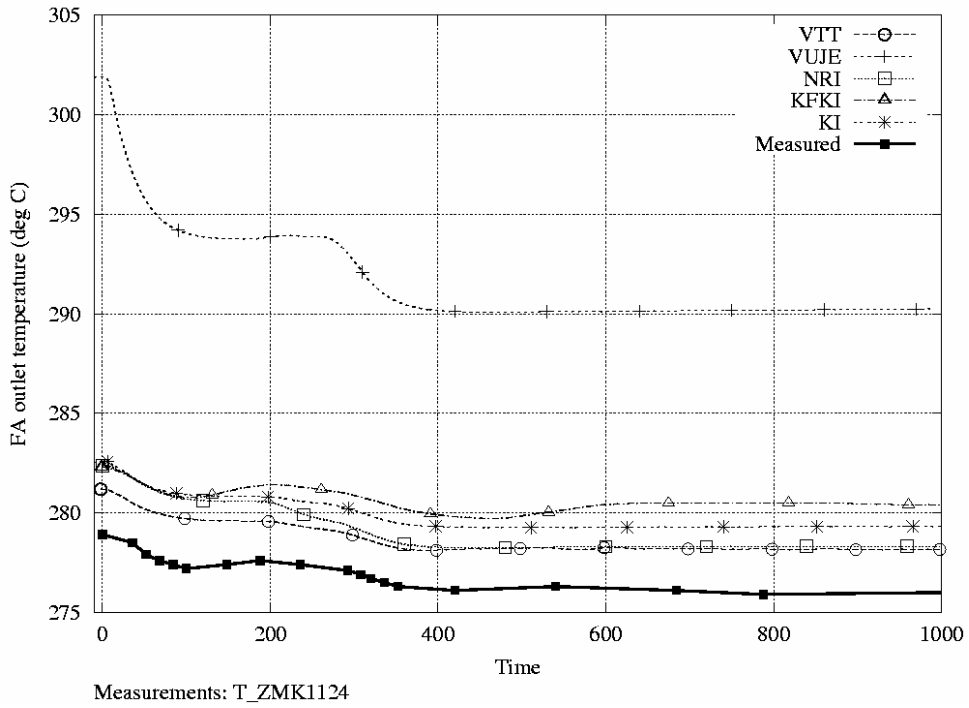


Figure 2.19 Calculated and measured fuel assembly outlet temperature at position 11-24.

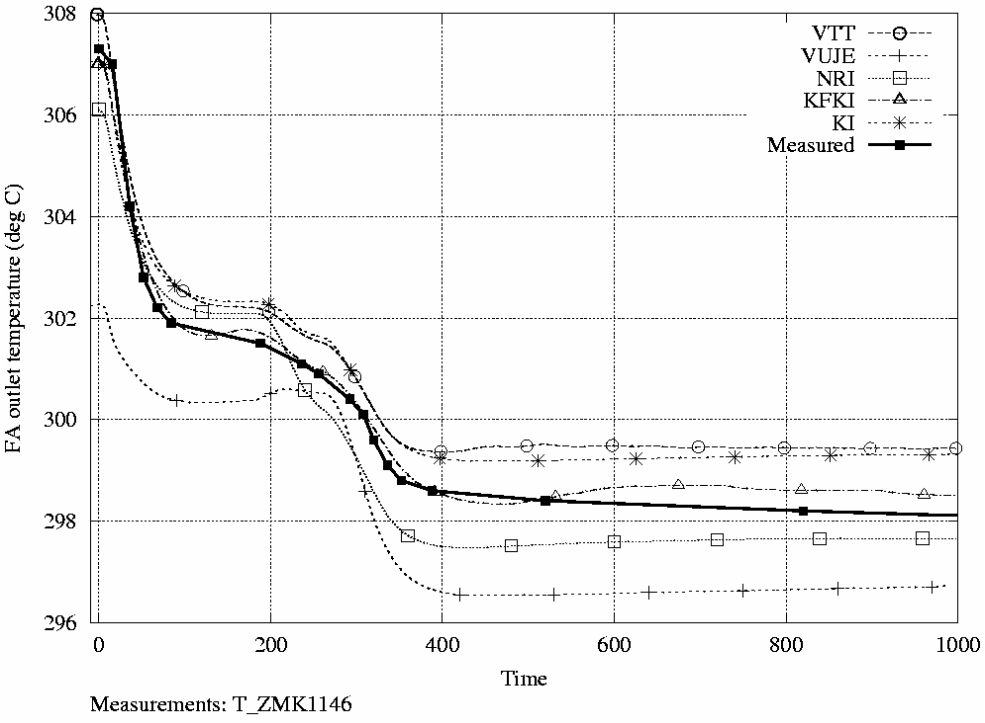


Figure 2.20 Calculated and measured fuel assembly outlet temperature at position 11-46.

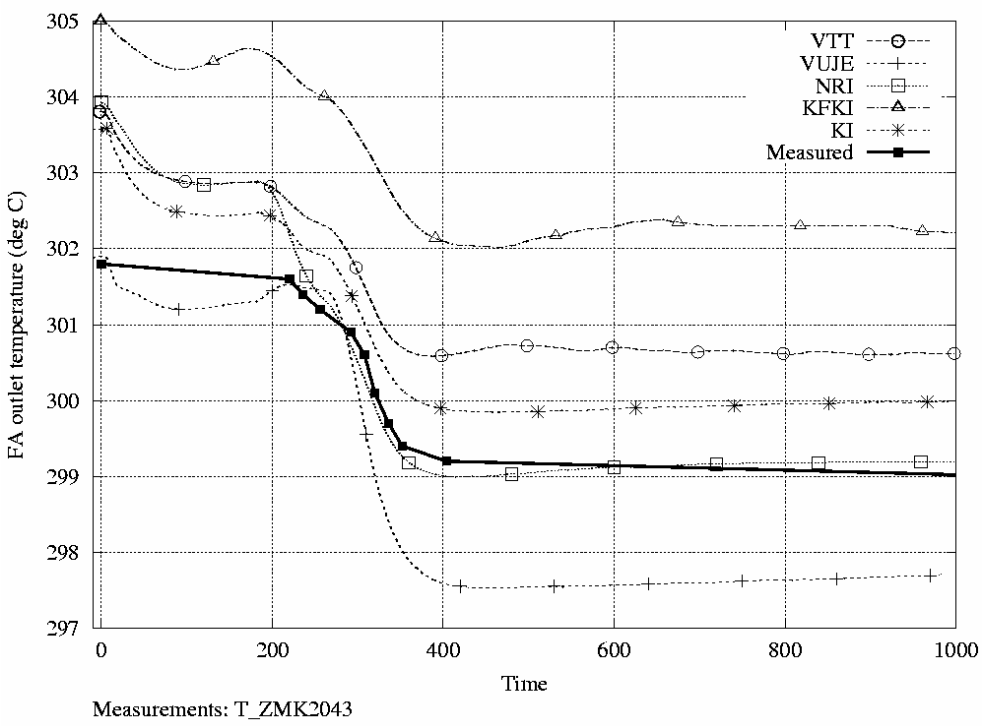


Figure 2.21 Calculated and measured fuel assembly outlet temperature at position 20-43.

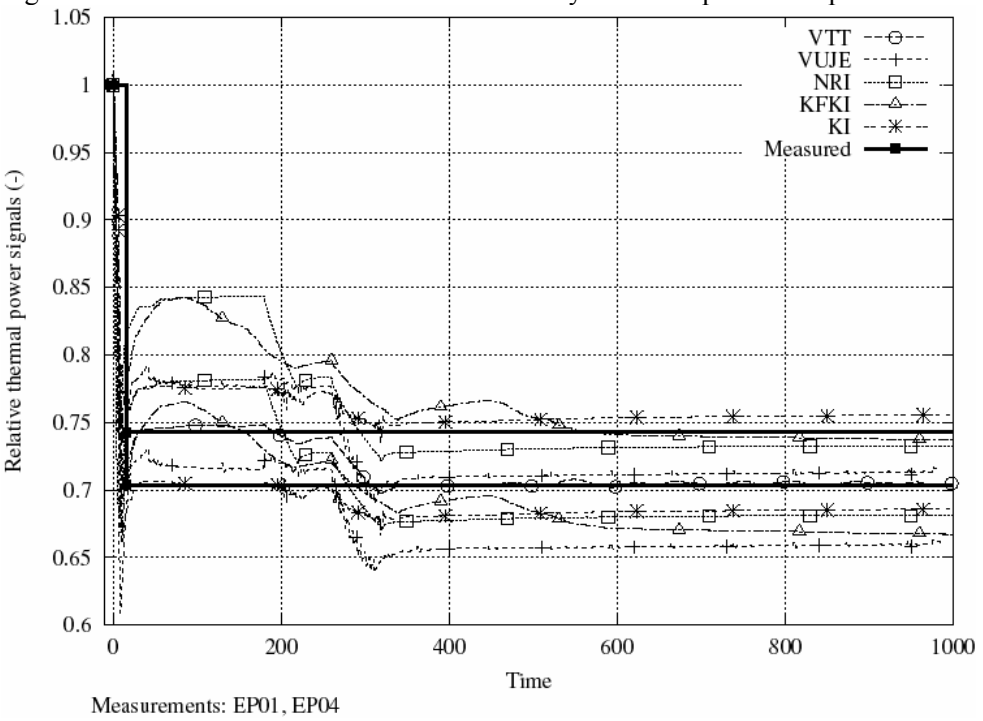


Figure 2.22 Measured out of core neutron detector signals and simulations in calculations near the dropped rod. VTT simulated only EP01.

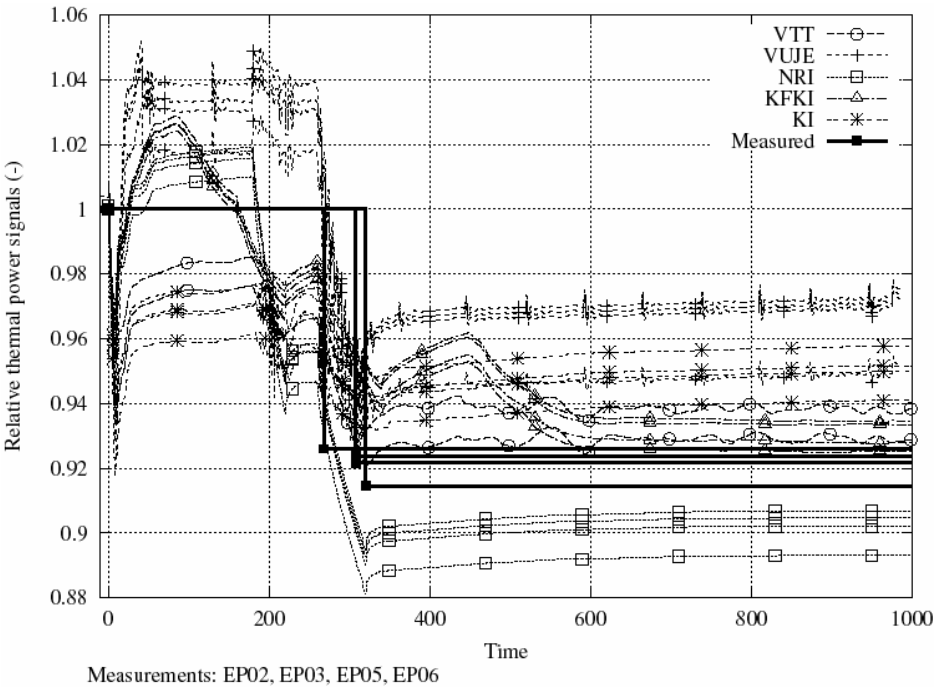


Figure 2.23 Measured out of core neutron detector signals and simulations in calculations far a way from the dropped rod. VTT simulated only EP02 and EP03.

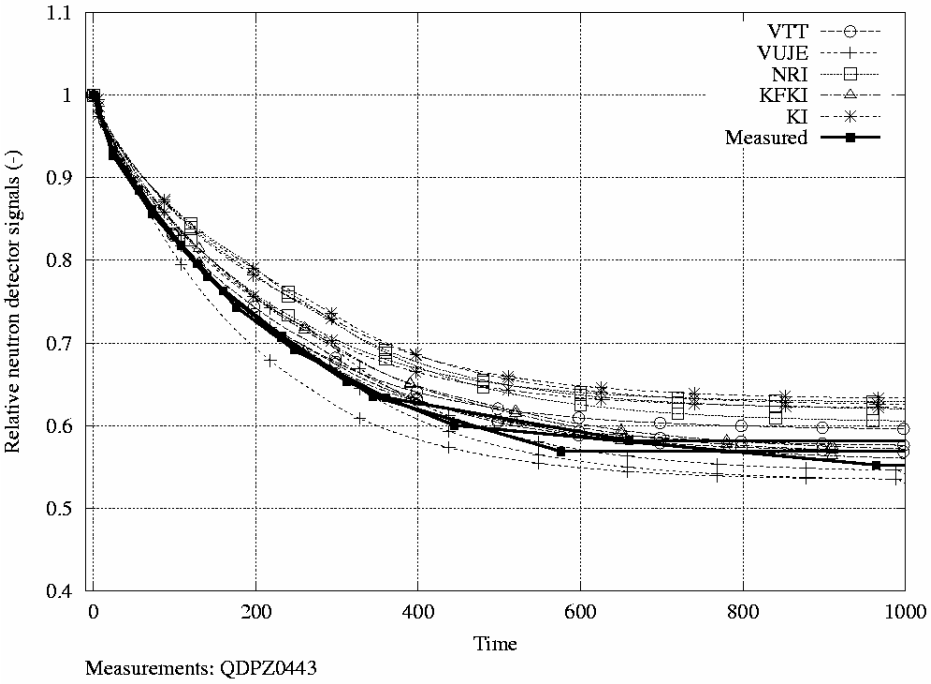


Figure 2.24 Calculated and measured relative neutron detector signals at three elevations of assembly position 04-43.

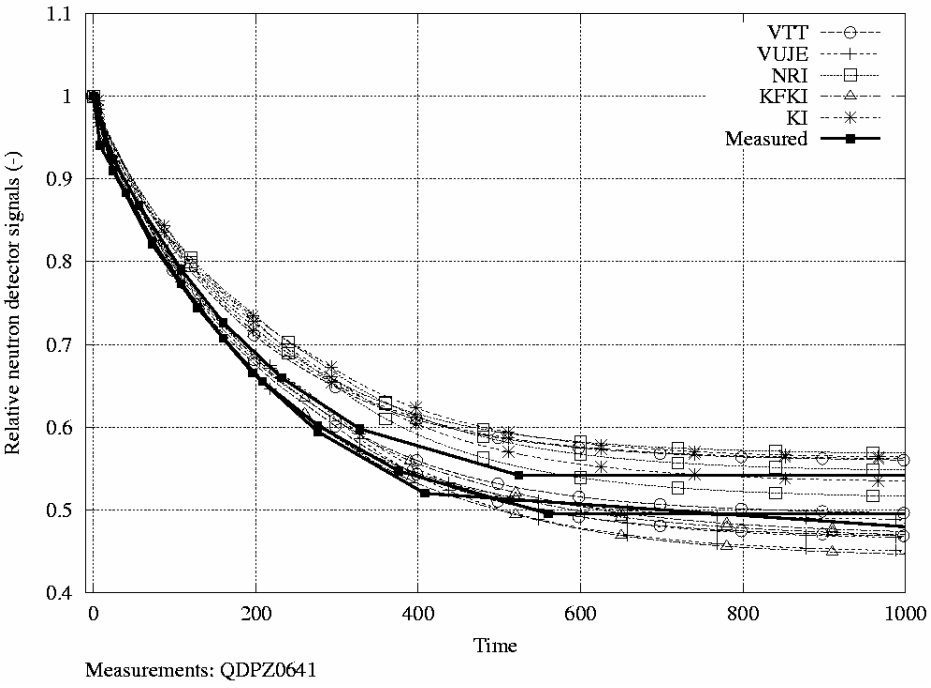


Figure 2.25 Calculated and measured relative neutron detector signals at three elevations of assembly position 06-41.

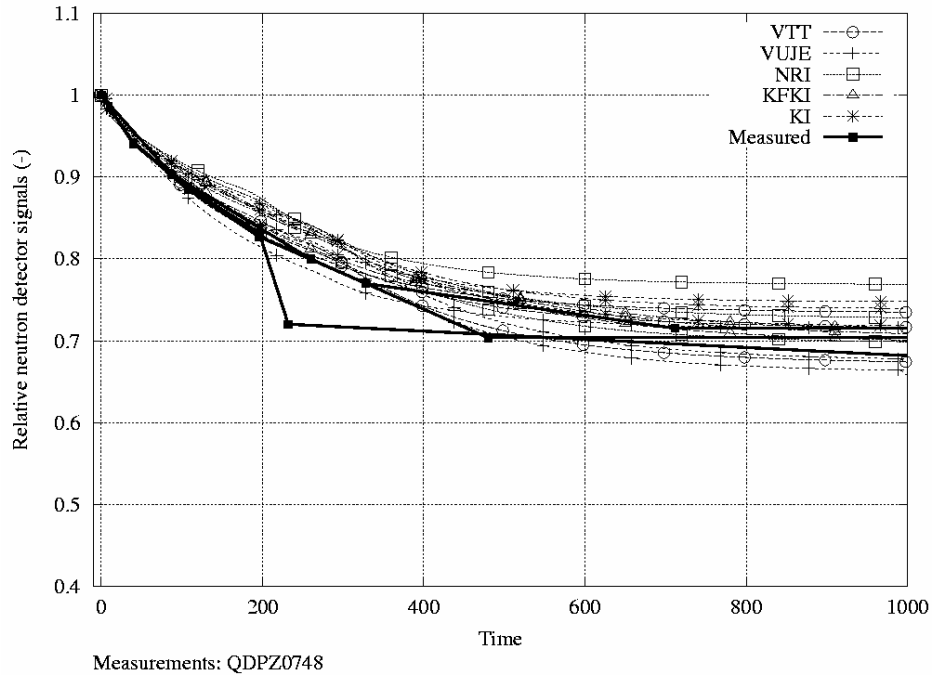


Figure 2.26 Calculated and measured relative neutron detector signals at three elevations of assembly position 07-48.

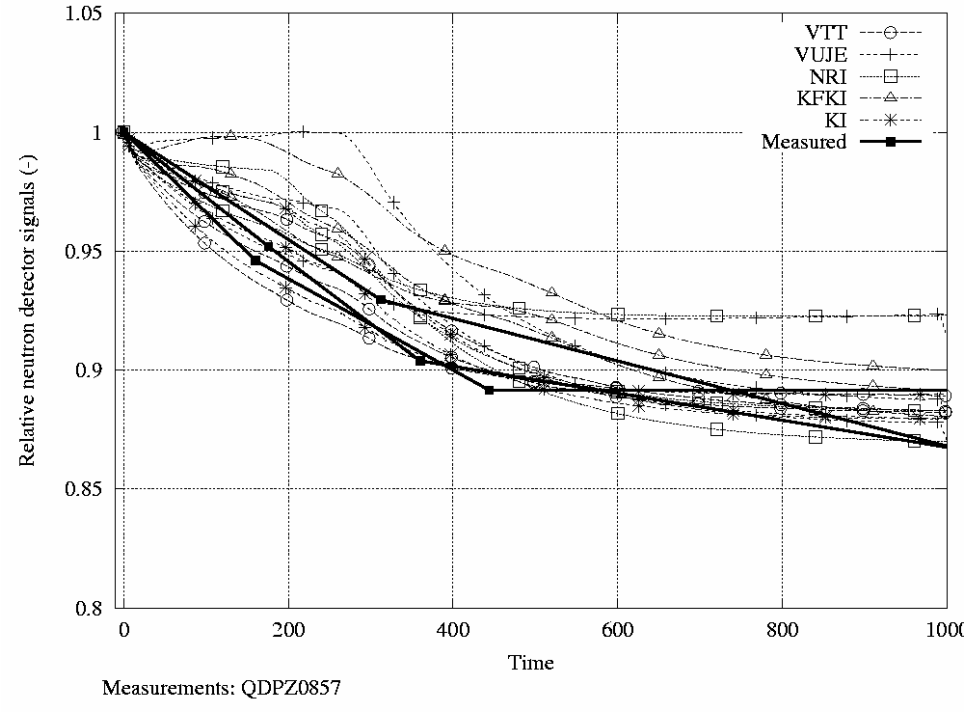


Figure 2.27 Calculated and measured relative neutron detector signals at three elevations of assembly position 08-57.

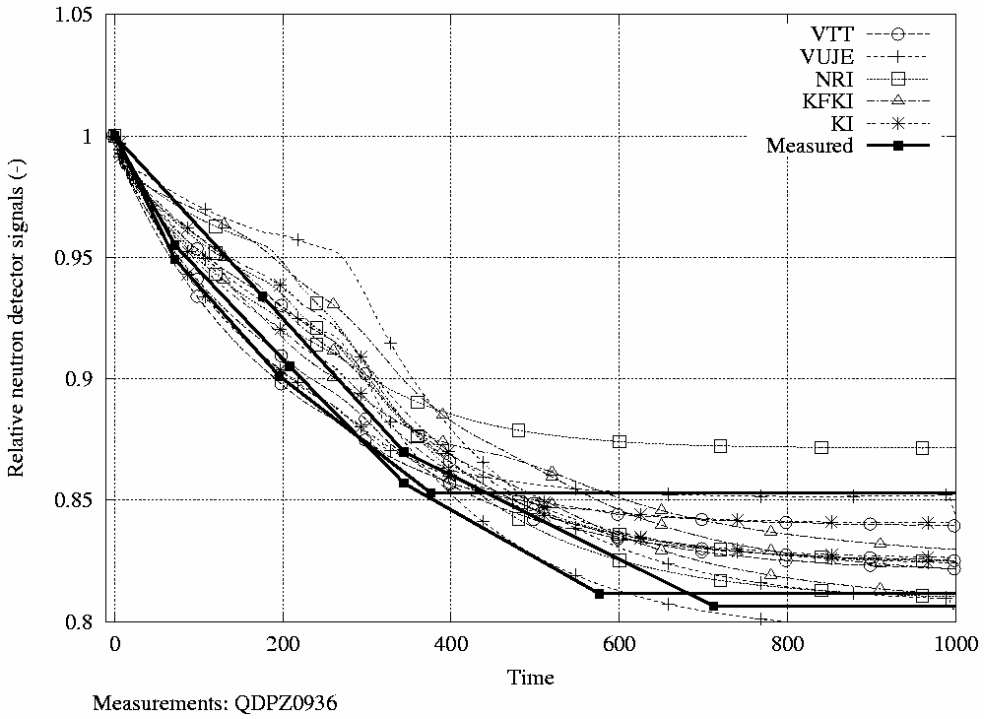


Figure 2.28 Calculated and measured relative neutron detector signals at three elevations of assembly position 09-36.

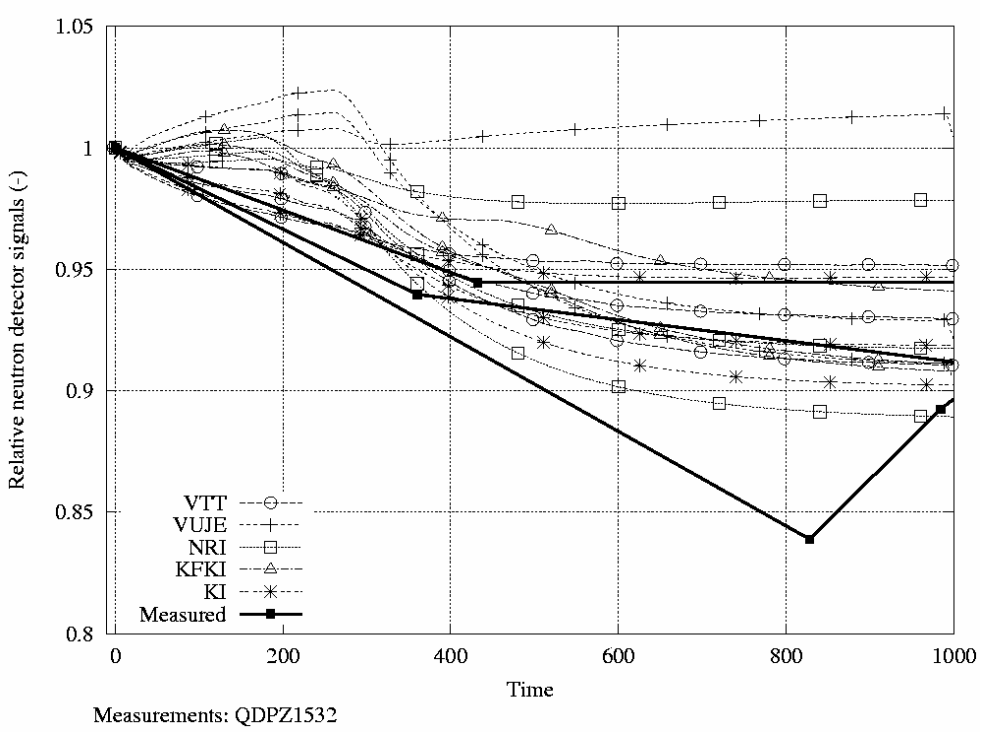


Figure 2.29 Calculated and measured relative neutron detector signals at three elevations of assembly position 15-32.

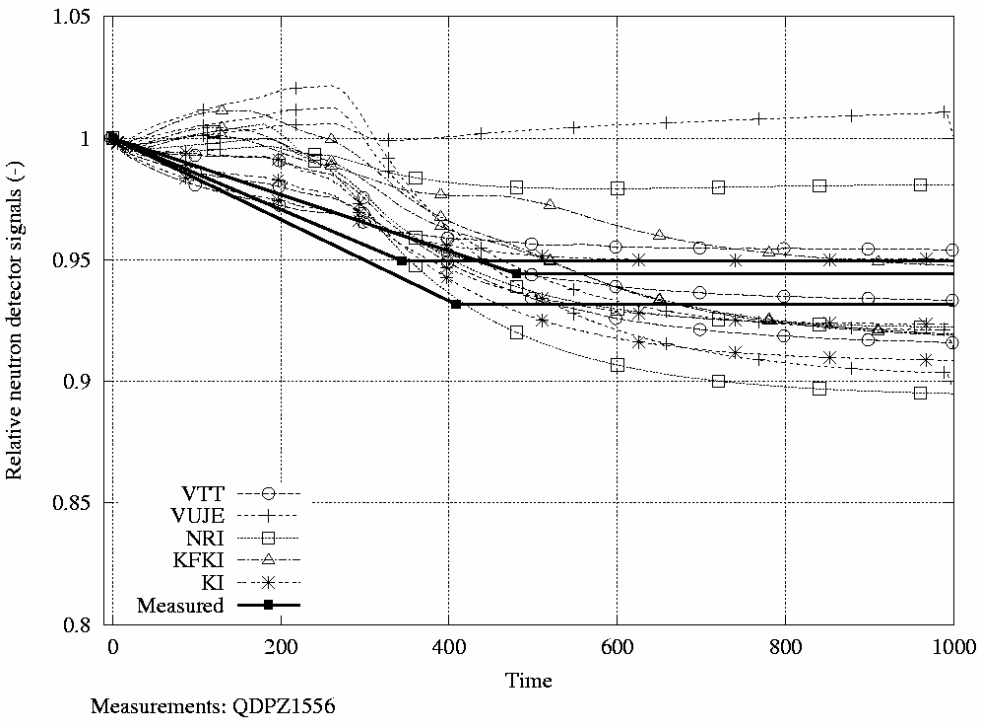


Figure 2.30 Calculated and measured relative neutron detector signals at three elevations of assembly position 15-56.

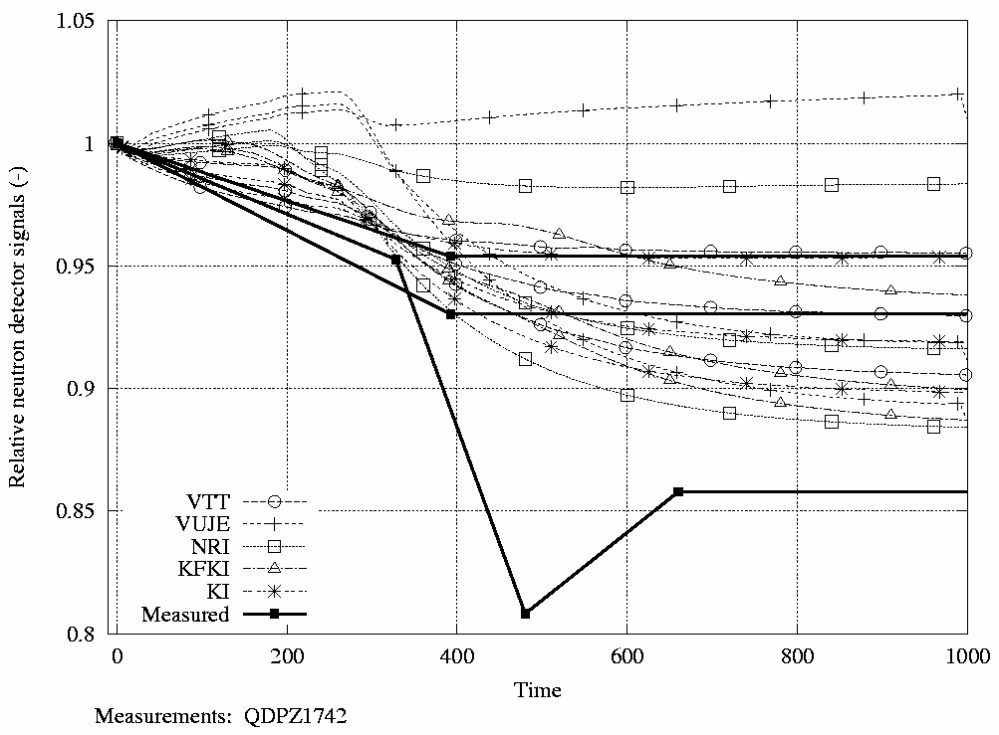


Figure 2.31 Calculated and measured relative neutron detector signals at three elevations of assembly position 17-42.

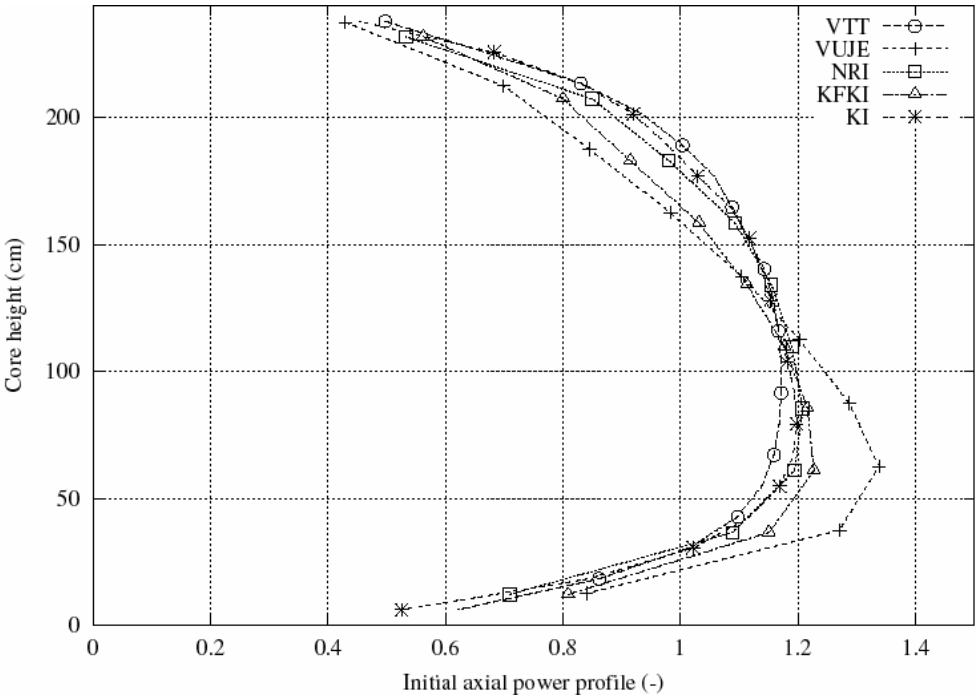


Figure 2.32 Measured and calculated initial axial power profile.

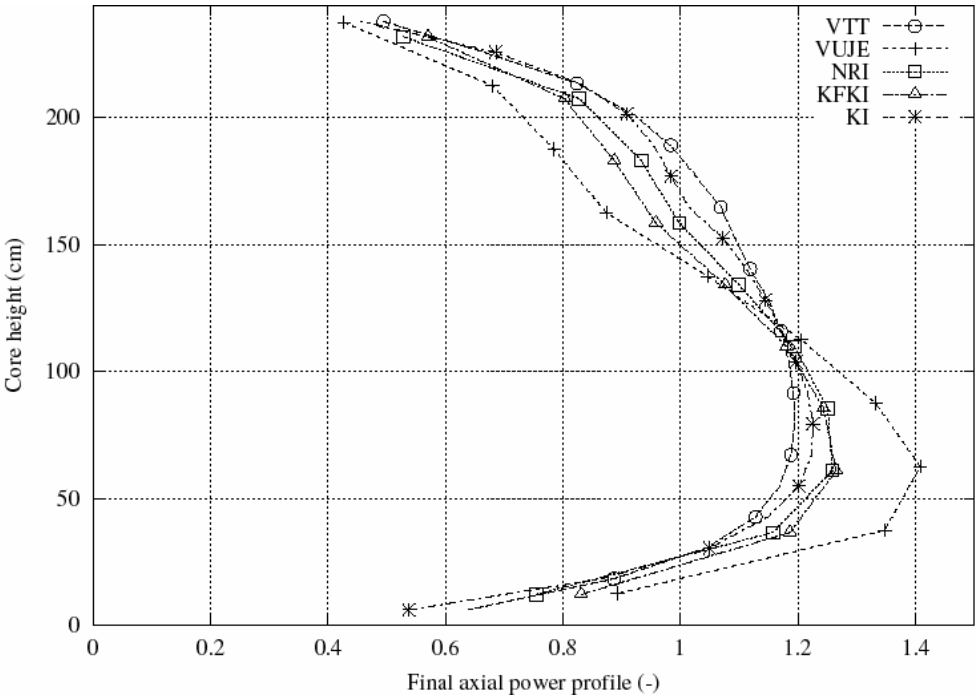


Figure 2.33 Measured and calculated final axial power profile

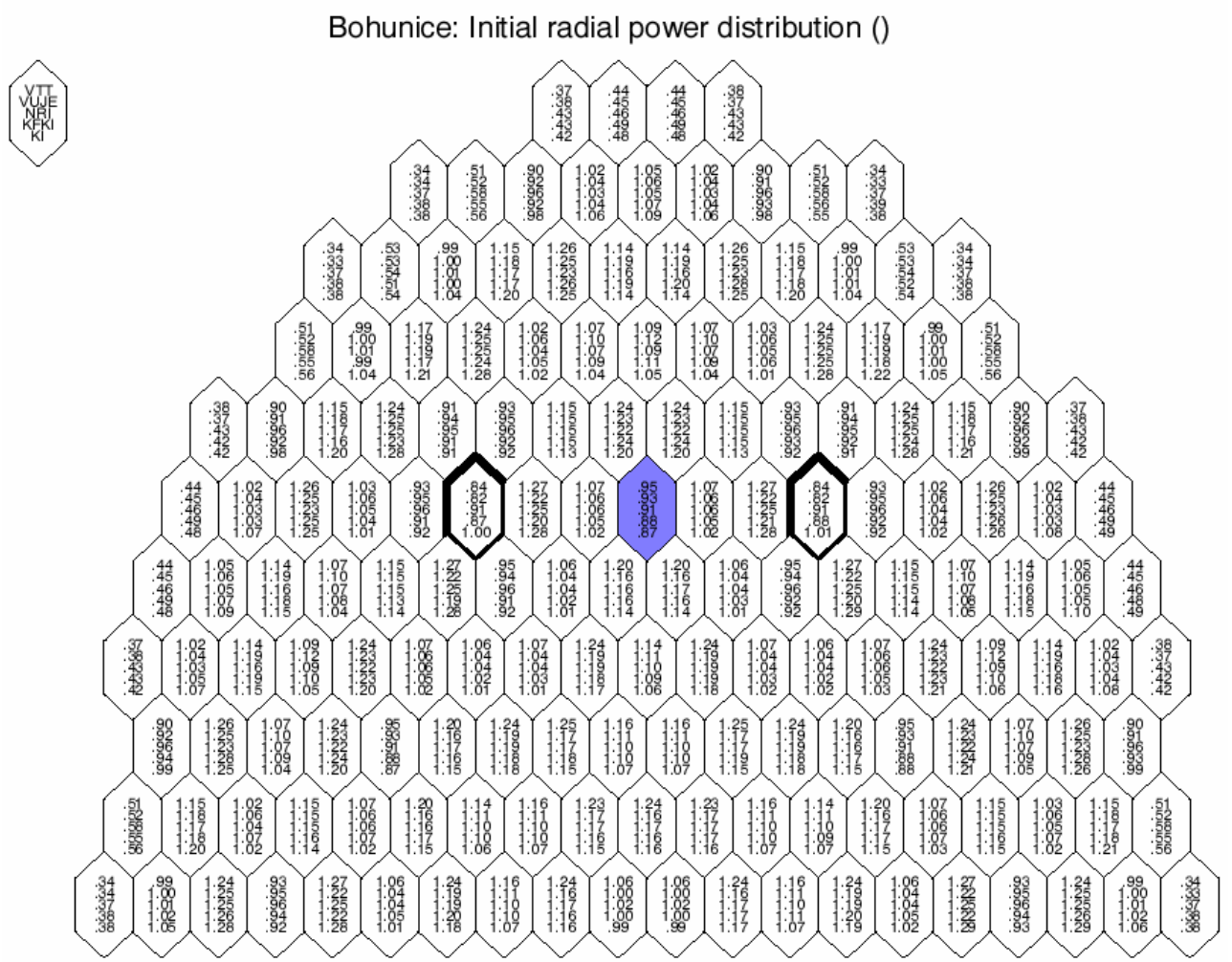


Figure 2.34 Calculated initial radial power distributions in Bohunice case, assembly with rod drop is in the middle.

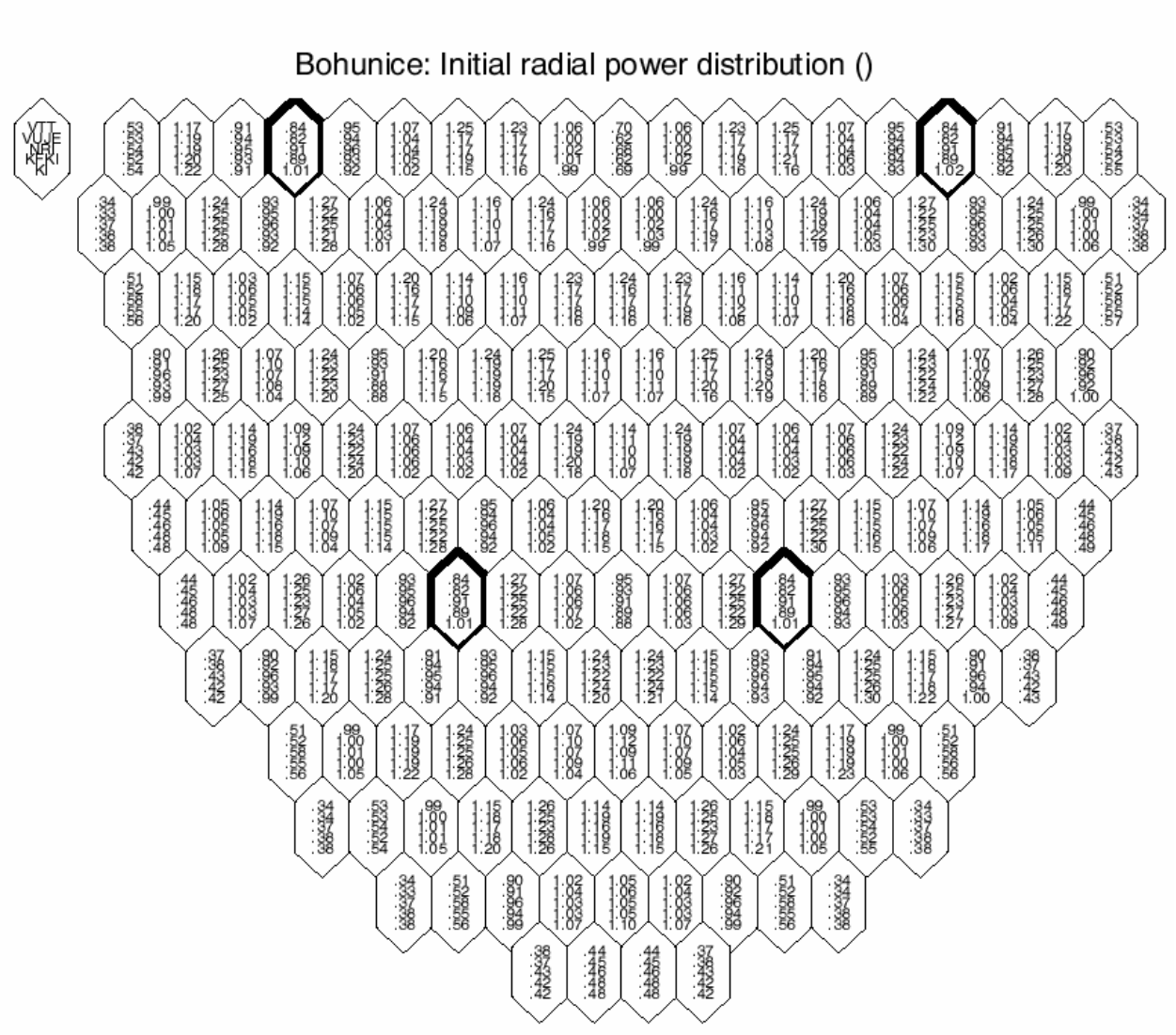


Figure 2.35 Calculated initial radial power distributions in Bohunice, far away from dropped rod.

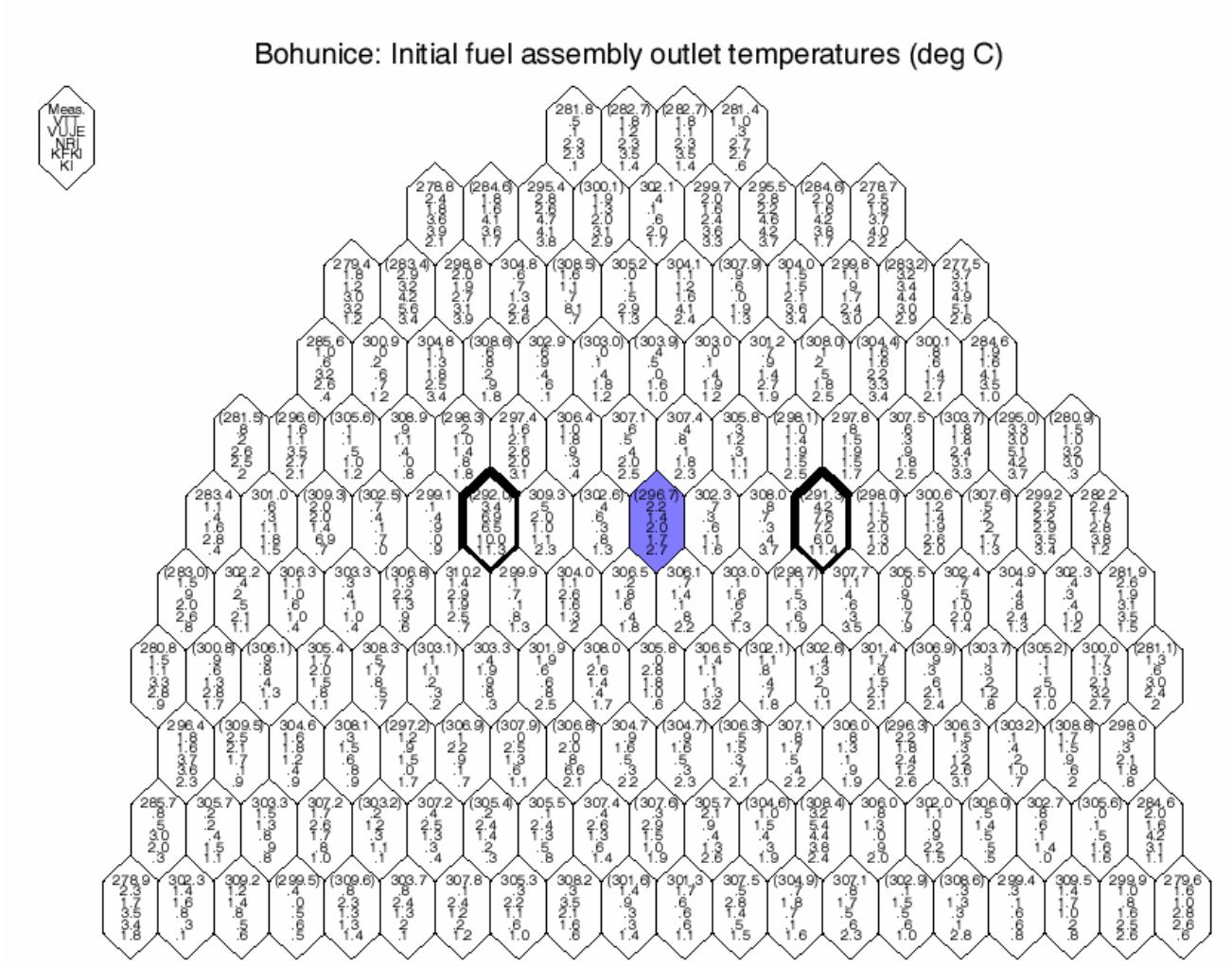


Figure 2.36 Measured core outlet temperature at initial state and difference between calculated and measured ones in Bohunice case. If there is no measurements, the comparison is made to calculated values (in brackets) given in data report. Assembly with dropped rod is in the middle.

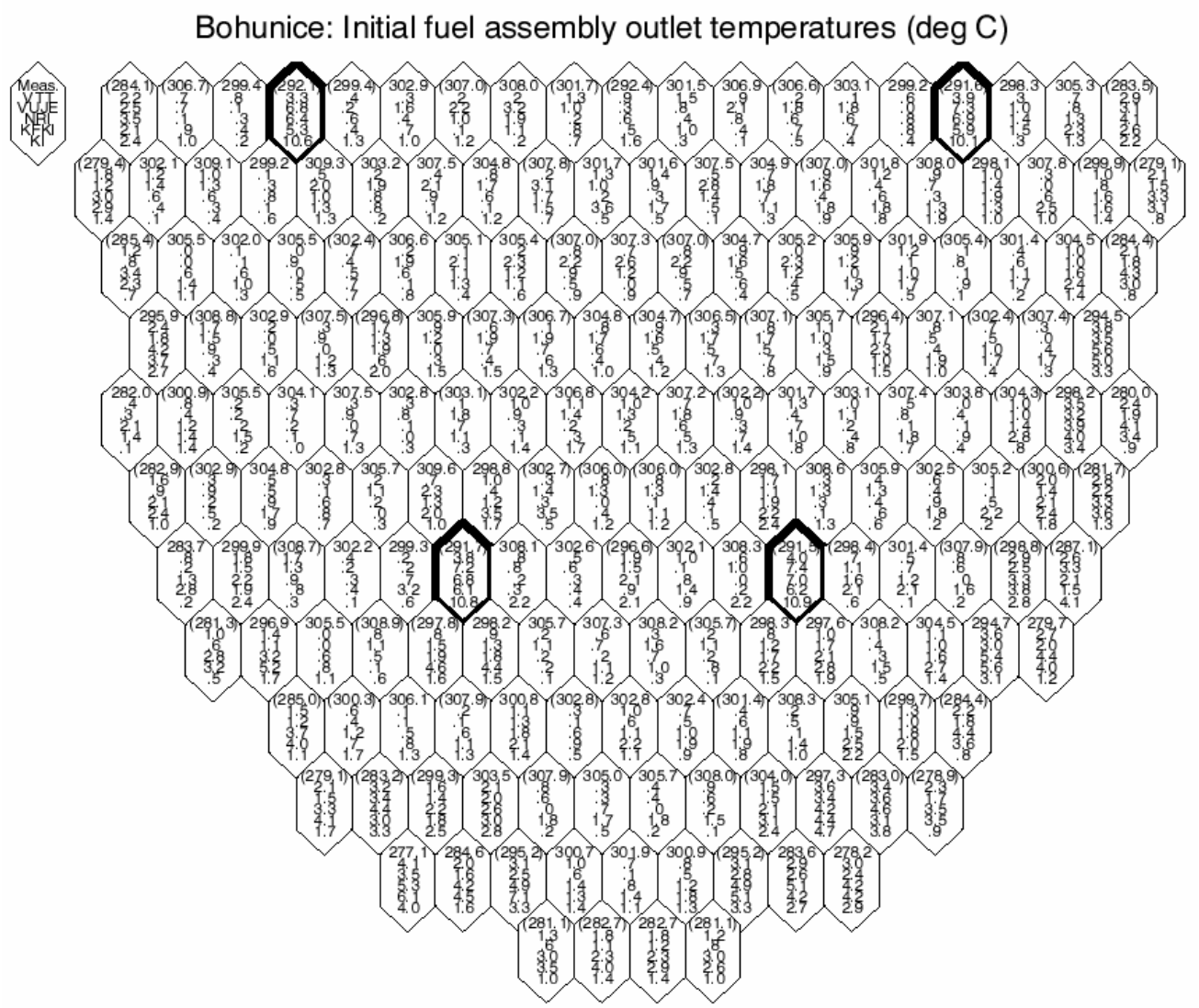


Figure 2.37 Measured core outlet temperature at initial state and difference between calculated and measured ones in Bohunice case. If there is no measurements, the comparison is made to calculated values (in brackets) given in data report.

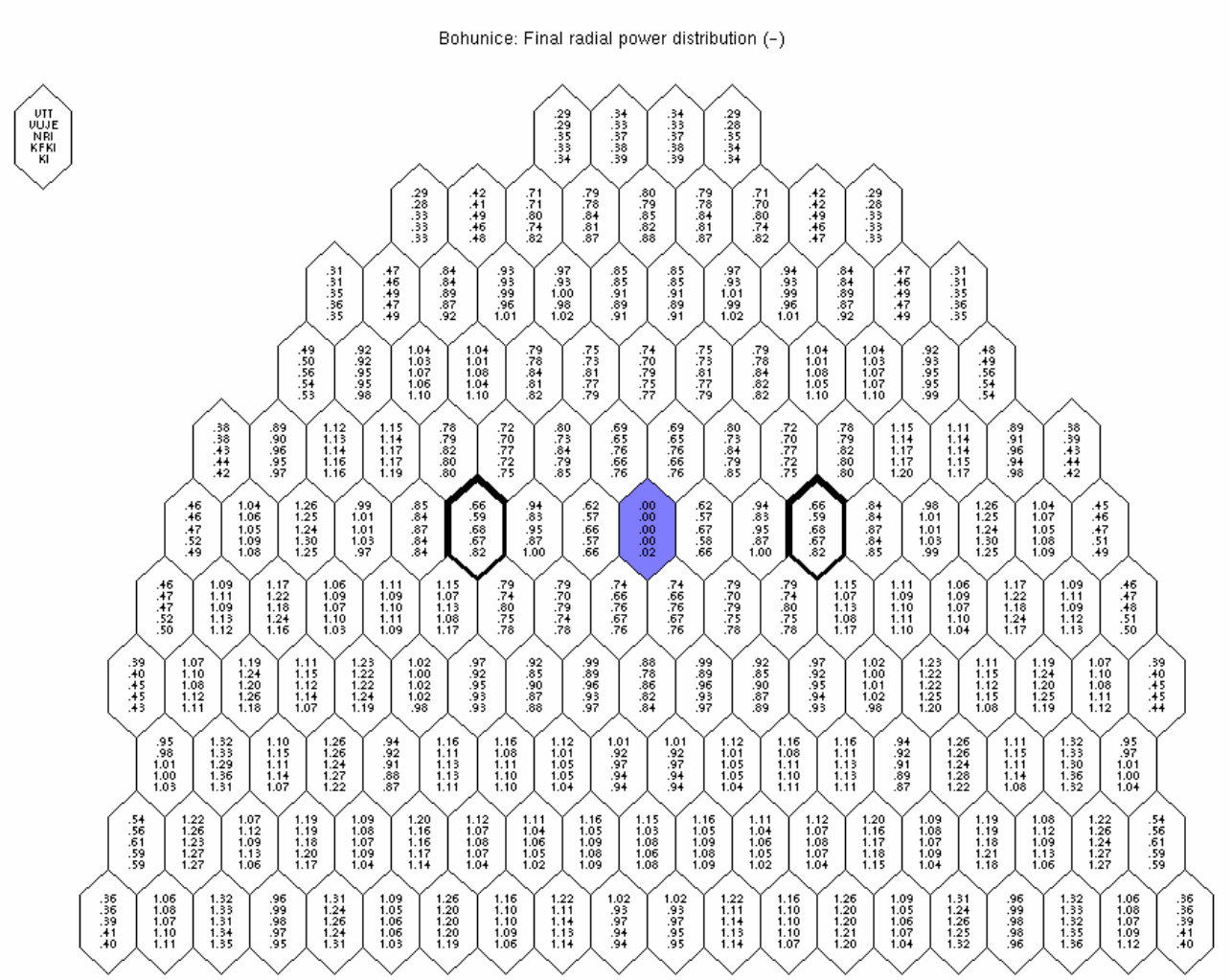


Figure 2.38 Calculated final radial power distributions in Bohunice case, assembly with rod drop is in the middle.

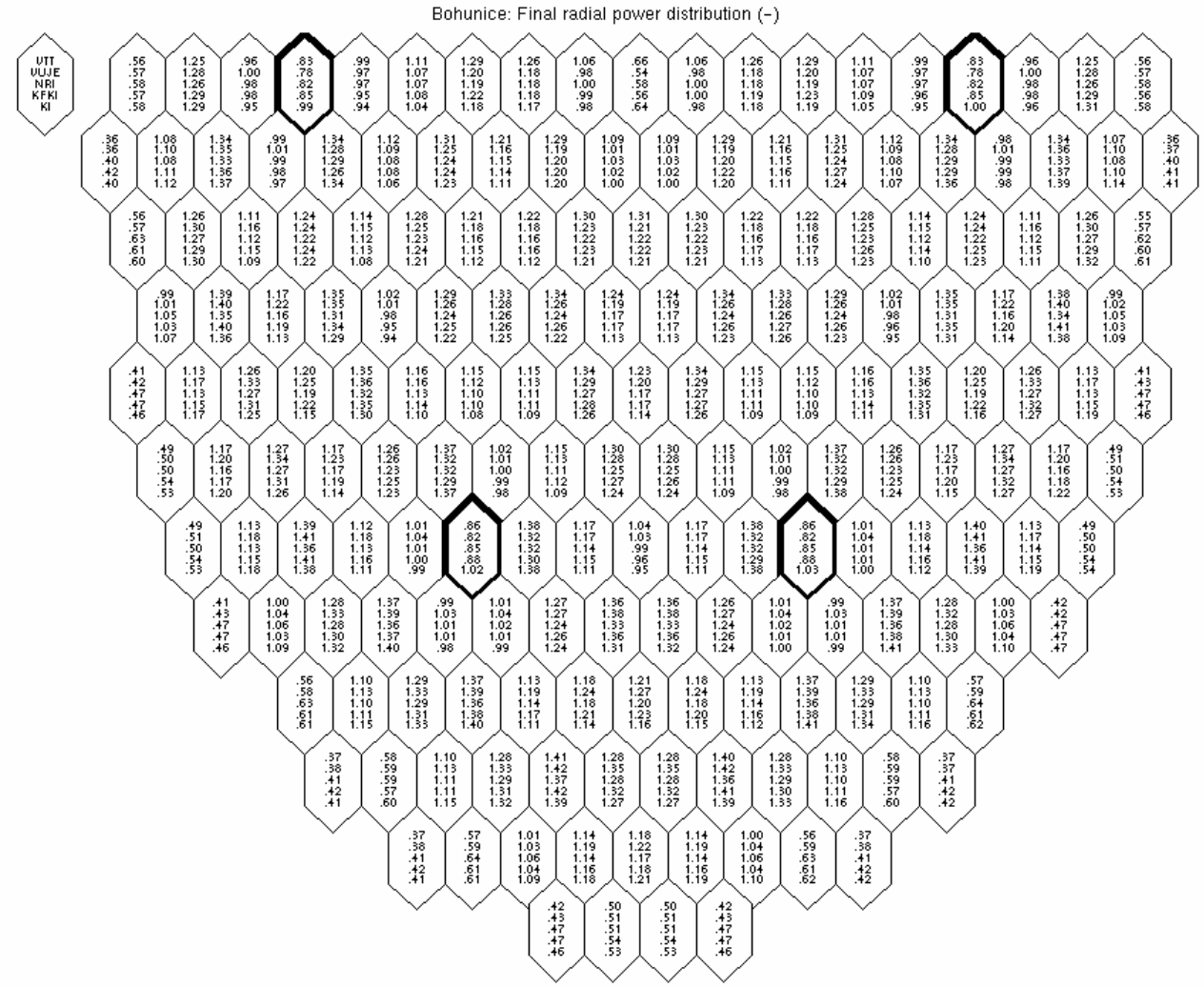


Figure 2.39 Calculated final radial power distributions in Bohunice case, far away from dropped rod.

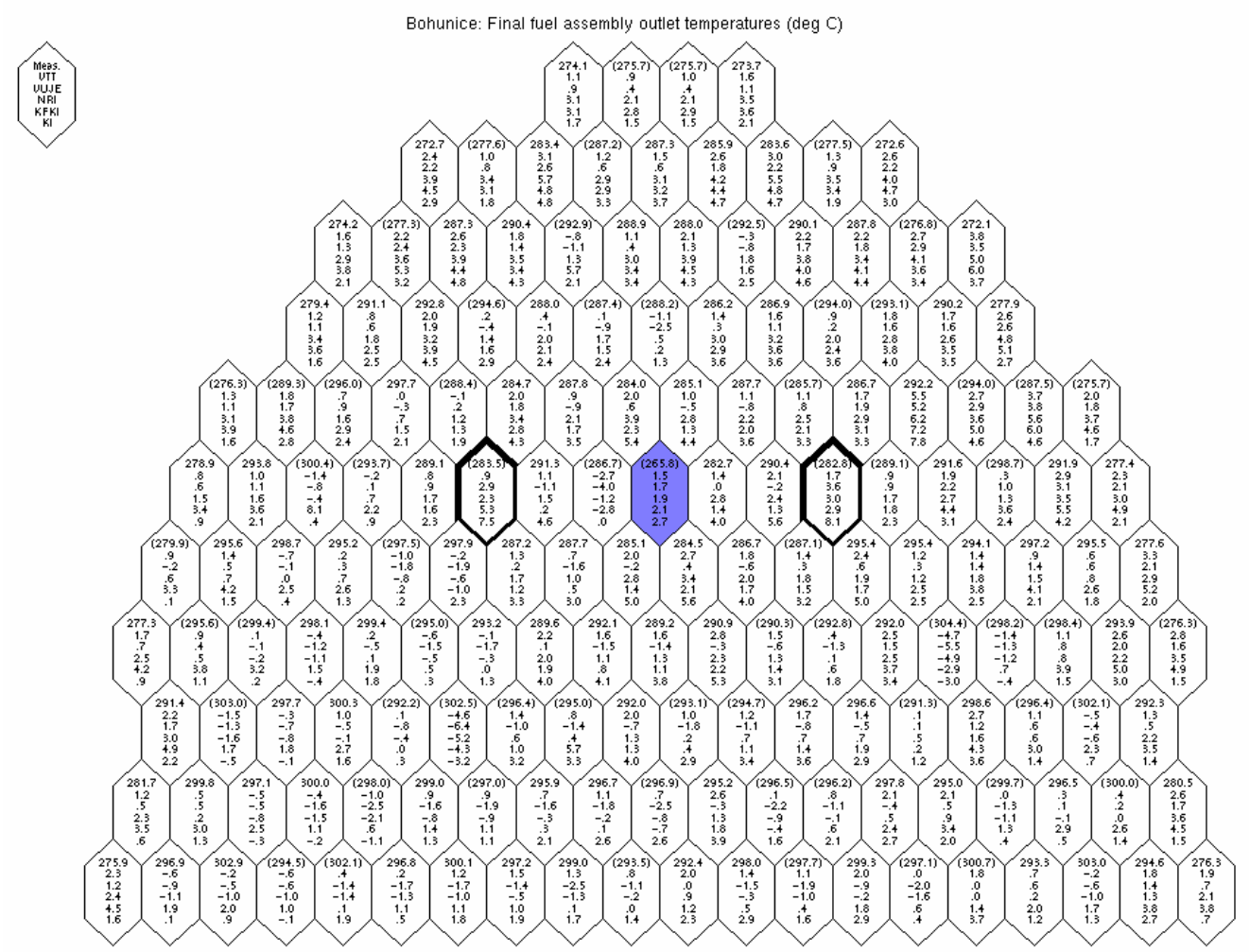


Figure 2.40 Measured core outlet temperature at final state and difference between calculated and measured ones in Bohunice case. If there is no measurements, the comparison is made to calculated values (in brackets) given in data report. Assembly with dropped rod is in the middle.

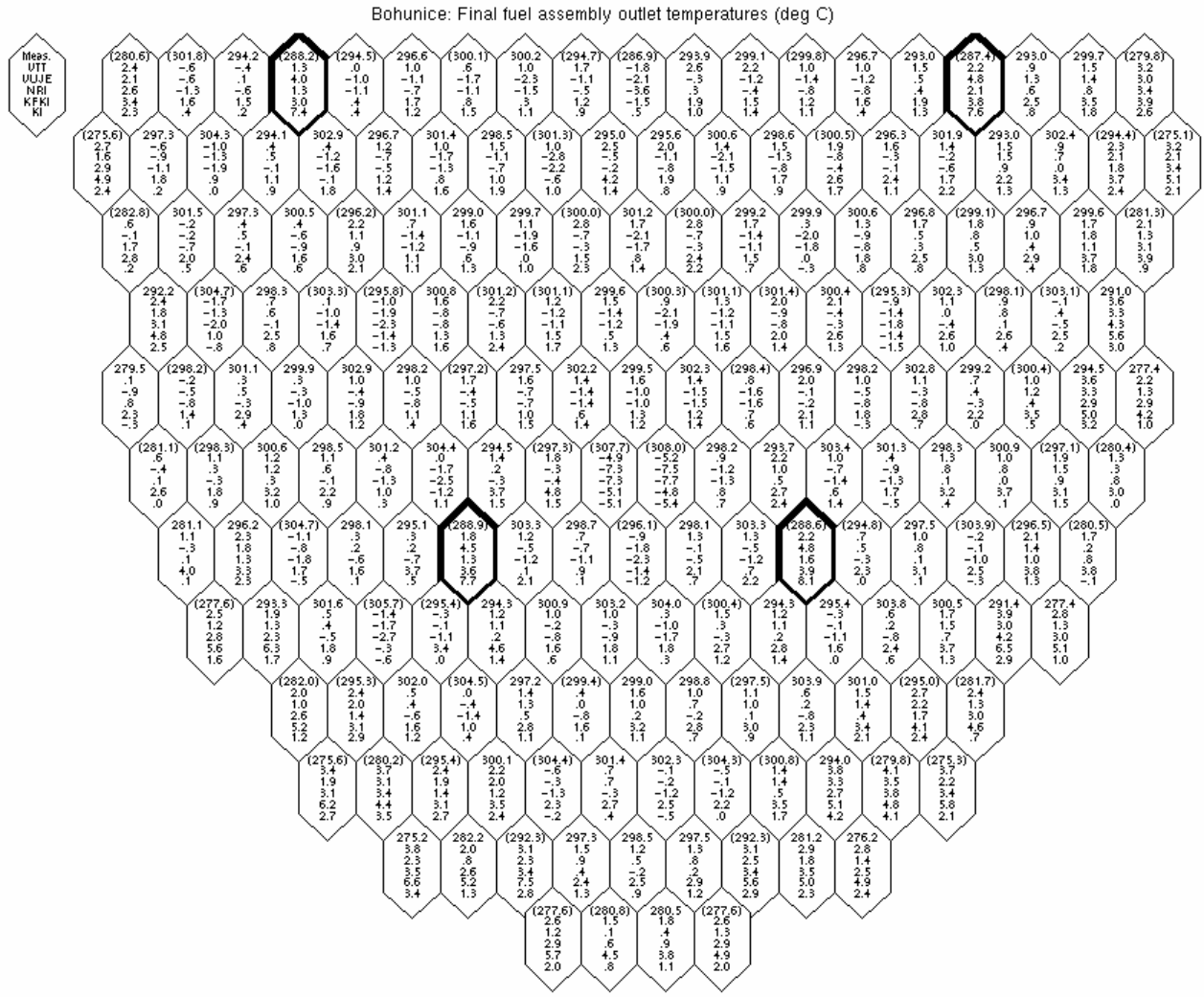


Figure 2.41 Measured core outlet temperature at final state and difference between calculated and measured ones in Bohunice case. If there is no measurements, the comparison is made to calculated values (in brackets) given in data report.

# 3 KOZLODUY TRANSIENT

## *3.1 Transient description*

Two start-up experiments with the coast-down of one of four and one of three working main coolant pumps, respectively, were conducted at the VVER-1000/V-320 type unit 6 of the Kozloduy NPP September 6th, 1992. In the VALCO project the latter pump trip was chosen to be the test case for code validation, but because the analysis of the latter transient may need data from the previous one, both the coast downs were reported.

In the test sequence MCP No. 3 was first switched off at full power and about 90 minutes later MCP No. 1 was switched off at the neutron power level of 65%. At this moment three pumps were operating, while the loop mass flow was reversed in one loop. ROM starts to decrease the power. The 10th control group moves down from its initial position of 73 % to the 55 % position, decreasing the reactor power from 65 % to 51.5 %. Turbine control system starts to unload the turbine, from 565 MW down to 415 MW in 300 s. The primary feed and bleed system maintains the pressurizer level. Further, the pressurizer spray valve opens twice at primary system pressure 15.89 MPa.

Amount of data collected is extensive, as concerns plant functions and time dependent plant data. Some discrepancies were noticed between different measuring system concerning the primary flow rates. The time dependent core data is limited, but the initial and final states of the transients are documented.

## *3.2 Calculation specification*

The Kozloduy data collection report /ref. 3/ gives the main ideas to perform the calculations for the validation of the coupled codes. Due to differing interpretation of measured data and confusion of several measurements for same parameters, some recommendations were given (appendix 1) to ensure the reasonable comparison of validation calculations.

The circulation loop mass flow is not directly measured at the plant, but derived from pressure difference measurements. In Kozloduy this is done in three systems. The recommendations for Kozloduy calculations confirms the data given in data collection report /ref. 3/ to be according to SVRK or UVS measurement system, according to which the reversed flow rate is about three times higher than measured in SVRK-VMPO system. To ensure the right initial mass flow rates, also one reference for the homologous pump characteristics was given /ref. 5/. An example of MCP coast down for the second pump trip was also given in the recommendations, because the measurements include the pump speed only for 40 seconds of one of 1 of 3 MCP stop transients.

In appendix 1 the pressurizer level control was informed to be based on a function that depends of the mean value of the hot and cold leg temperatures in those loops where MCPs are working. Such a function enables increase of the pressurizer control set point, although power decreases in the transient. Also the time constant of 10 seconds for temperature measurement simulation was decided to be used in the data comparison, in line with the earlier SRR1-95-project /ref. 4/.

### *3.3 Used codes and models*

The Kozloduy transient was calculated in five institutes, at VTT, KI, FZK, SSTCN and INRNE with three different coupled codes. The used codes and the basic models are summarised in Table 3.1 and the reactor data in Table 3.2.

All the code coupling types are used. Practically this kind of transient needs modelling of all the circulation loops separately, but symmetry of the core may be used. Also the 'open' core without shrouds around the assemblies stabilize distributions in the core. The whole core modelling has been used here only in KI calculations. Hence, mixing in the pressure vessel could have had meaning only in the KI calculations, but the total mixing was assumed in KI calculations.

**Table 3.1 Basic data in the Kozloduy calculations**

| | VTT | KI | FZR | SSTCN | INRNE |
|---|---|---|---|---|---|
| Neutron kinetic code | HEXTRAN 2.8 | BIBR8KN | DYN3D | DYN3D | DYN3D |
| Thermal hydraulic code | SMABRE 4.7 | ATHLET | ATHLET 1.2A | ATHLET 1.2C | ATHLET |
| Type of coupling, internal, external, parallel | Parallel | Internal | External | External | External |
| Used symmetry in core | 60° | 360° | 60° | 60° | 60° |
| Number of fluid channels in core in thermal hydraulic code | 4 | 163 | - | - | - |
| Number of fluid channels in core in neutron kinetic code | 28 | - | 28 | 28 | 28 |
| Number of assemblies in neutron kinetic code | 163 | 163 | 163 | 163 | 163 |
| Total core bypass flow of active part of core (%) | 3.0 | 4.04 | 3.0 | 3.0 | 3.0 |
| Number of circulation loops | 4 | 4 | 4 | 4 | 4 |
| Used boundary conditions | ~ control rod group 10 position | - | Steam header pressure, control rod group 10 position | Steam header pressure, control rod group 10 position | Steam header pressure, control rod group 10, spray valve position |

**Table 3.2 Reactor data in the Kozloduy calculations**

| | VTT | KI | FZR | SSTCN | INRNE |
|---|---|---|---|---|---|
| Neutron kinetic code | HEXTRAN 2.8 | BIBR8KN | DYN3D | DYN3D | DYN3D |
| Cross section calculations | CASMO-4 | KASSETA | NESSEL | NESSEL | |
| Initial neutron power (MW) | 1947. | 1945. | 1947. | 1948. | 1931. |
| Initial xenon | Non-stationary | Non-stationary | Stationary * | Non-stationary | Stationary * |
| Initial boron concentration (g/kg) | 3.15 | 2.60 | 2.89 | 2.63 | 2.98 |
| Fuel average temperature (ºC)<br>at initial state<br>at final state | <br>514.<br>480. | | <br>506.<br>470. | <br>566.<br>518. | |
| Maximum fuel center line temperature (ºC)<br>at initial state<br>at final state | <br>756.<br>701. | <br>836.13 | <br>829.<br>749. | <br>960.<br>863. | |
| Used gas gap model, constant htc ($W/m^2K$) or dependency of temperature or burnup ... | temp. dep. | constant | temp. dep. | temp. dep. | Constant |

* Xenon imbalance compensated by boron change

### *3.4 Results*

The first MCP was stopped already ninety minutes before the calculated case, one out of tree MCP stop. The time between these is not enough to total stabilization of the whole primary system, but may be treated such as in the calculations except for the core xenon content.

The time histories of the Kozloduy transient compared to the measurements are shown in Figure 3.2 to Figure 3.22. Typically the measurements are reported stepwise due to reading dependent measuring system. Then values values immediately after the steps are the 'true' points. In the figures typically three curves for circulation loop parameters are compared: the value of the loop number 3 with initially reversed flow, loop 1 with the stopping MCP and the average of the loops 2 and 4 with still operating MCPs.

The transient starts with MCP 1 stop at time 0.0 s. This activates ROM to decrease the core power with the control rod group 10, and half a minute later to draw it back in order to stabilize the power. The measured and calculated control rod group positions are depicted in Figure 3.3. FRZ and SSTCN used CR positions directly as boundary condition, VTT simplified it with a few points and KI modelled the controller itself. After the drawing back phase KI has a difference of 7 % in the CR group position compared to measurement.

The core power, shown in Figure 3.2, is measured only in a few points. Generally the calculations follow the real behaviour, but all the calculations are below the measurement in the stabilization phase. KI has the nearest values due to above mentioned higher

control group positions. The differences between the measurements and the calculations are largest at 40 s, depending on the temperature and flow rate to the core. With the coldest and largest flow FZR has the smallest deviation to the measurement.

In the beginning the MCP 1 trip leads to flow decreases and finally flow reversal in loop 1. The reversed flow of the loo3 decreases slightly and there is an increase in the loops 2 and 4. According to the measurements the MCP speed at first increases for a few seconds after MCP stop. This may have happened also according to pressure difference measurements over the MCP's, shown in Figure 3.4. The deviations in the initial pressure differences between the calculated and the measured values of the SSTCN and VTT results indicate too large loss coefficients along the circulation loops, because the calculated pressure drops over the pressure vessel are about the measured ones (Figure 3.14). The shape of pressure difference during the transient indicates modified pump characteristic in FZR result.

The MCP 1 pressure differences (smallest values in Figure 3.4) and mass flows (initially negative values in Figure 3.7) behave identically in the calculations. Figure 3.7 shows the timing of flow reversal to be between 38.6 s in the SSTCN to 50 s in FZR calculations. This is a result of used pump coast down curve. The calculated pump speed is depicted in Figure 3.9 and compared to a few points, measured in an earlier transient.

The cold leg temperature is a result of secondary pressure until the flow is reversed. The smallest decrease in secondary pressure leads to smallest decrease in cold leg temperature in the VTT calculations in the Figure 3.6. Also the hot leg temperatures in the loop 1 start to decrease after flow reversal, Figure 3.5. The time constants of the temperature measurements are important when comparing to the measurements. The shape of the measured hot leg 1 temperature cannot be a result of the thermocouple time constants, but indicates that the measurement is disturbed by the wall temperature, which is decreasing more slowly than the fluid temperature. In the figure wall temperature from one calculation is shown.

The core mass deviates into two groups, VTT and FZR results are near to specification at initial state, 14 062 kg/s total flow and 3 % of core bypass. KI and SSTCN have lowered values. INRNE has slightly larger mass flows. The differences stay the whole transient (Figure 3.8).

In the secondary side three calculations assume steam header pressure as a boundary condition (Figure 3.17). The steam generators with stopped loop have lower pressures (Figure 3.18) and higher collapsed water levels (Figure 3.19), because there is no steam inside the water. From the secondary side, also the calculated steam mass flows (Figure 3.20), feed water mass flow in the feed water control valve (Figure 3.21) and turbine powers (Figure 3.22) are compared. The various types of secondary side modelling finally produce the cold leg temperature, which is a key boundary condition for core neutronics. In the beginning all the calculations except INRNE produce a good prediction for the cold leg temperature (Figure 3.6) and at the end all except KI are about 2 °C below the measurements. The temperature differences between the hot and cold legs are within measuring accuracy.

### 3.4.1 Pressurizer level and pressure control

Measured and calculated upper plenum pressure is shown in Figure 3.10. All the calculated pressures are much more sensitive than the measurement to the changes in primary loop just after MCP trip, similar to the 1-D codes generally. The measured pressure increases significantly after flow has reversed in loop 1 and reaches the spray valve set point for opening 15.89 MPa at 64 s (Figure 3.15).

The pressurizer water level is controlled by mean temperature of the primary circuit. Some uncertainty still exists how this temperature is calculated in the real plant. This has more meaning in the cases with reversed flows in some loops. As a consequence of pump trip the mean temperature increases and the set point level for make up and letdown systems increases (Figure 3.16). No special changes are shown in the measured data although the measured pressurizer level, Figure 3.12, increases sharply. The VTT and KI calculations resemble to the behaviour but more slowly.

Typically pressurizer spray valves operate like safety type valves, but are here operated more like relief valves, shown in Figure 3.15. In FZR and INRNE calculations timing and opening of the valves has been as boundary conditions. In the VTT calculation the valve stays open for the rest of the transient and in the KI calculation the safety type valve is modelled with higher opening and lower closing pressure as set points.

### 3.4.2 Pump characteristic

At the plant the mass flows are not measured, but calculated from the pressure differences, typically for V1000 over the main coolant pumps. Using of this pressure differences also for calculation of reversed flows may lead to wrong values. Further, in the calculation with a typical pump model of system codes, the mass flows are a result of used pump homologous curves, which define the relationships between a volumetric flow, pump speed, direction and a pump head. Pump coast down curve tells how pump speed is decreased as a function of time. These and all other pump data are experimental data and very difficult to measure at least near the pump operational limits. The data available is limited and typical values are used in calculations for several plants.

The homologous curves were not given in the Kozloduy data report /ref. 3/. Also, the recommended curves given in /ref. 5/ proved to be partly wrong and finally several modified references had to be used in calculations. The comparison between the initial mass flows of the circulation loops are shown in Table 2.3. Further, some difficulties were also encountered in the interpretation of the measurements. As a result of these phases a common understanding was reached to interpret the data.

**Table 3.3 Measured and calculated initial circulation loop mass flows and pressure increase in main coolant pumps.**

| | Data report /ref.3/ | VTT | KI | FZR | SSTCN | INRNE |
|---|---|---|---|---|---|---|
| Mass flow rate (kg/s) | | | | | | |
| - ave in loops 1, 2 and 4 | 5210.7 | 5170.4 | 4813.7 | 5015.5 | 4847.1 | 5490.3 |
| - loop 3 with stopped pump | -1569.5 | -1511.4 | -1651.5 | -1602.9 | -1712.0 | -1515.4 |
| Pressure increase (kPa) | | | | | | |
| - ave in MCP 1, 2 and 4 | 469.8 | 511.6 | 451.9 | 473.4 | 528.7 | 510.0 |
| - MCP 3 | 162.8 | 159.5 | 152.6 | 148.1 | 144.8 | 209.1 |
| MCP 1 stopping time (s) | | 115 | | 116 | 110 | 108 |

### 3.4.3 Core behaviour and radial distributions

The axial and radial power distribution and the core outlet temperature distributions are shown in Figure 3.23 to Figure 3.28. The calculation of xenon transient between two pump stops in the VTT and the SSTCN calculations lead to more downward peaked axial power profiles than in the KI calculation. In the FZR and the INRNE initial states the xenon change is compensated with increased boric acid concentration. For boric acid concentration two values were given, 2.85 g/kg according to measurements and a more probable value 3.15 g/kg from independent data sources from the protocols. The applied boric acid consentrations are shown in Table 3.2.

The calculated core outlet temperatures are systematically higher than the measured ones. The difference between calculated and measured seems to depend on the temperature. This is illustrated in Figure 3.1. A possible reason for temperature differences is the position of the measurement in the mid line of the bundle below the conical part of the fuel bundle head. The main flow bypasses the measuring point in the edge zone and flows through the holes in the conical part. The measured temperature could be at least partly disturbed by the colder water coming from the central tube. These reasons could explain why temperature difference is larger with higher assembly power. The difference to the measurements could be compensated with higher mass flow to the core. In Figure 3.1 and Figure 3.27 and Figure 3.28 it is shown that VTT, FZR and especially INRNE result are nearer to measured temperatures, mainly due to higher core inlet mass flows. The KI results have the biggest difference with the smallest mass flow. However, all the distributions seem to create a linear dependence with about the same slope.

The initial and final radial power distributions are shown in Figure 3.25 and Figure 3.26. In the initial state the average deviation between the measured and the calculated values are above 5 %, KI has somewhat lower, 3.4 %. At the final state results are better. In all the calculations the biggest differences are in the middle of the core. The measured data for assemblies with enrichments of 3 % has not been considered.

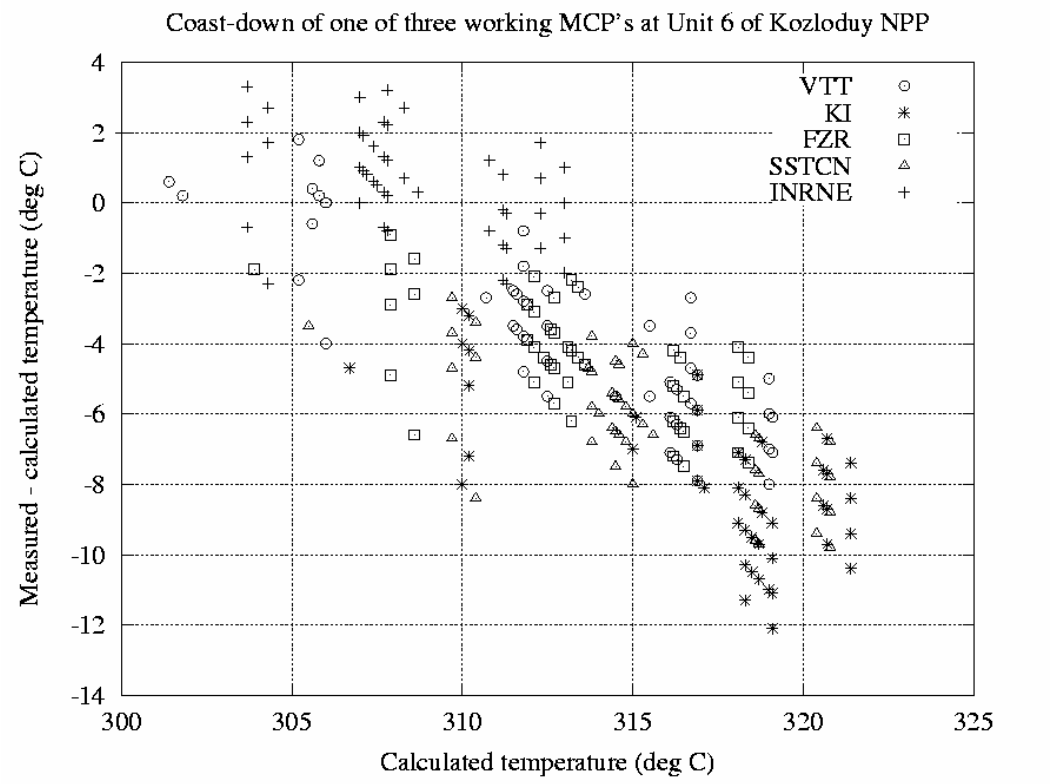


Figure 3.1 Calculated core outlet temperatures as a function of difference between measurement and calculations.

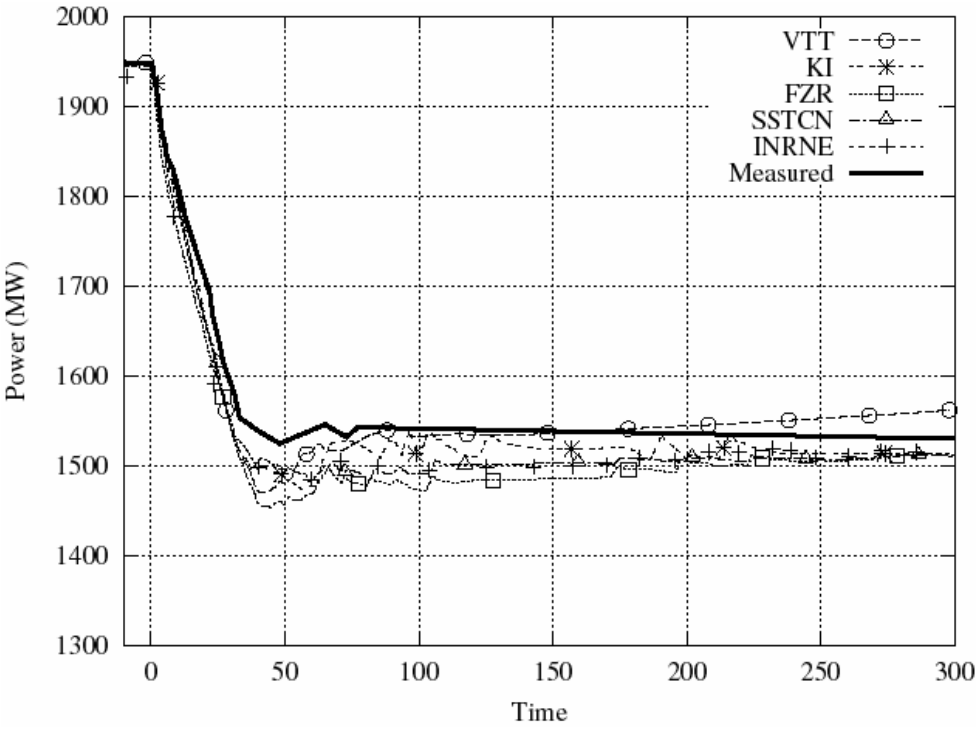


Figure 3.2 Calculated and measured neutron power.

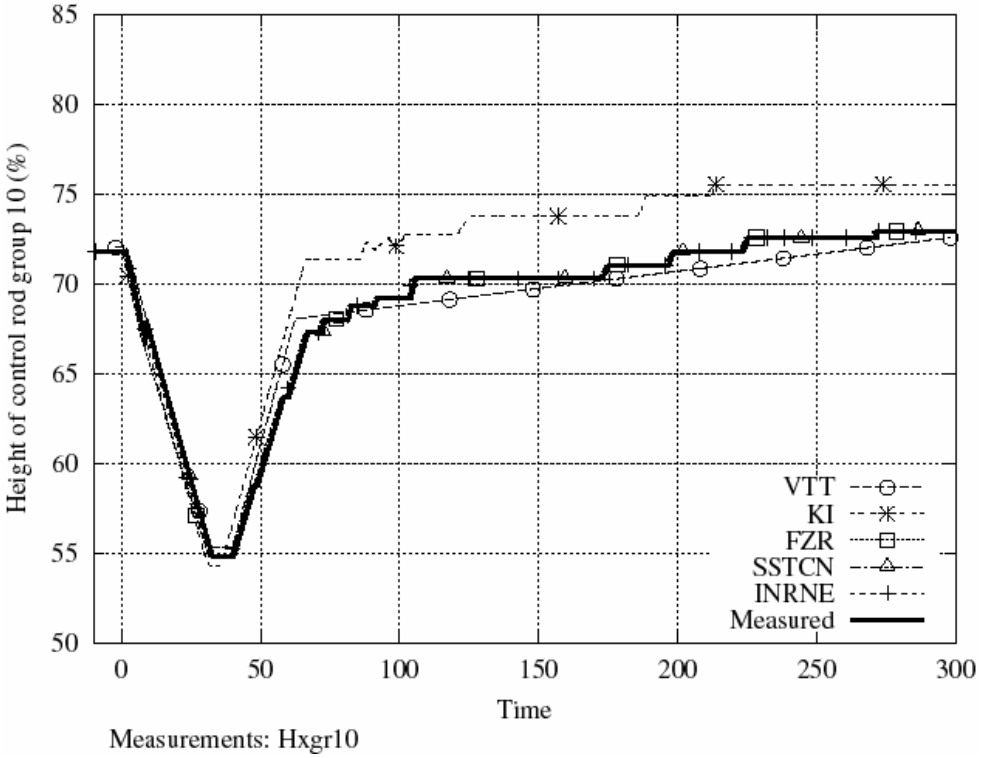


Figure 3.3 Calculated and measured axial position of control rod group 10.

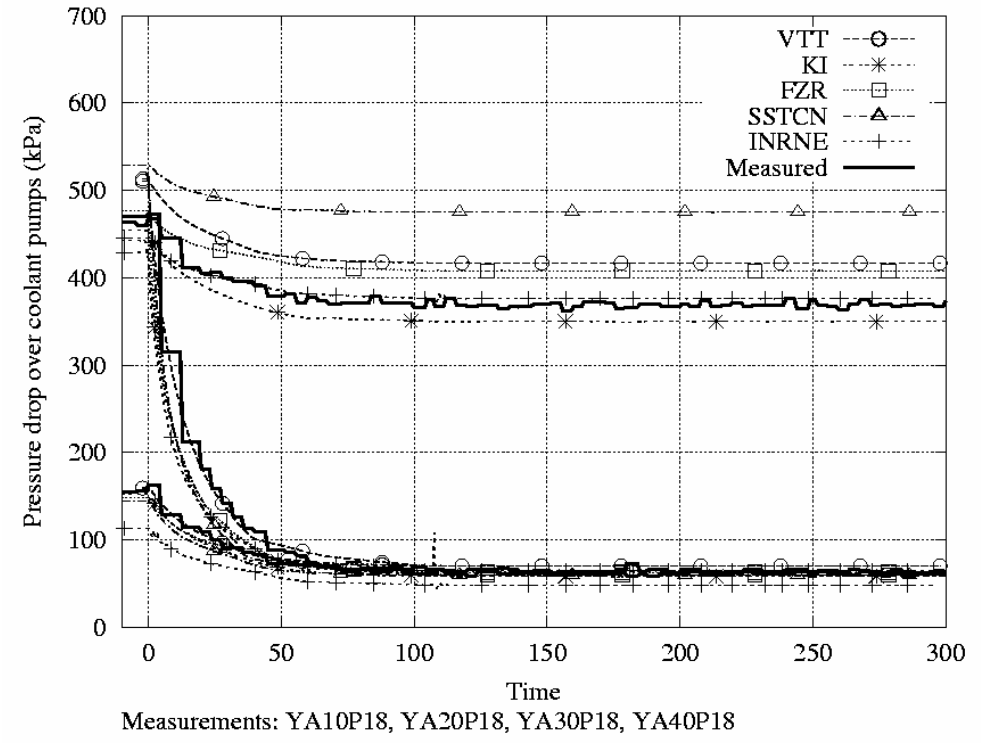


Figure 3.4 Calculated and measured pressure increase in main coolant pumps.

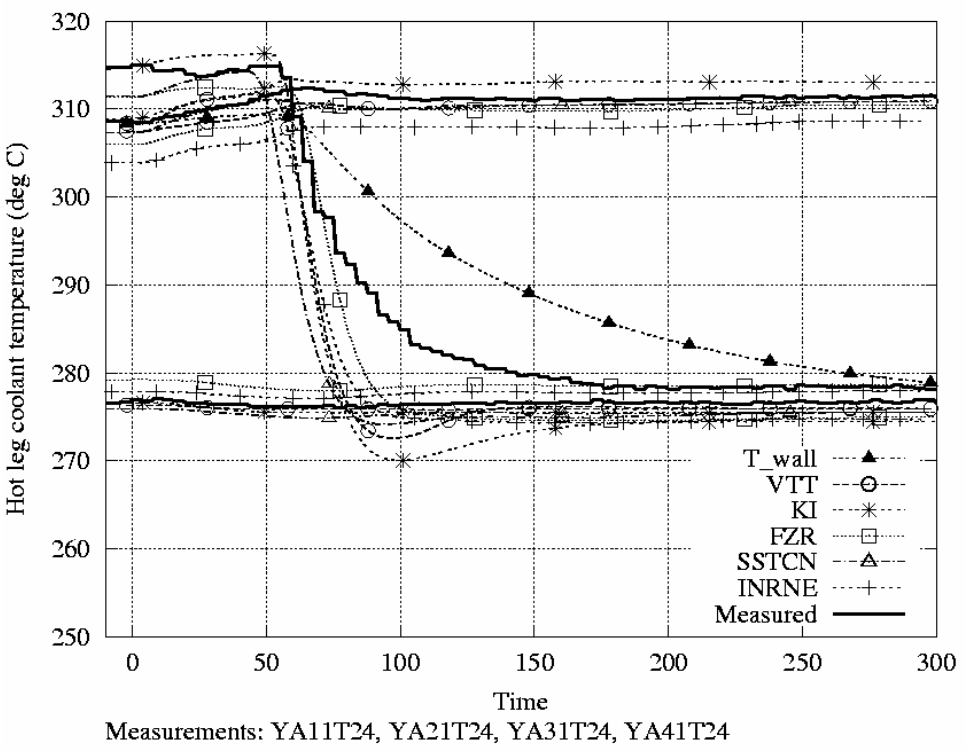


Figure 3.5 Calculated and measured temperatures in four hot legs.

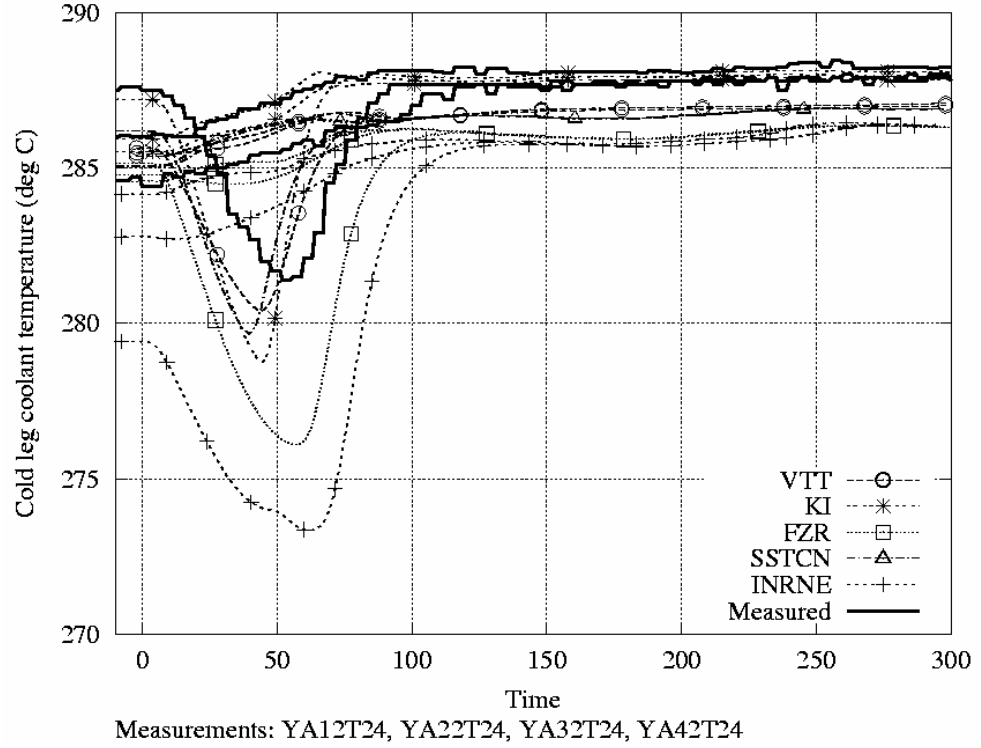


Figure 3.6 Calculated and measured temperatures in four cold legs.

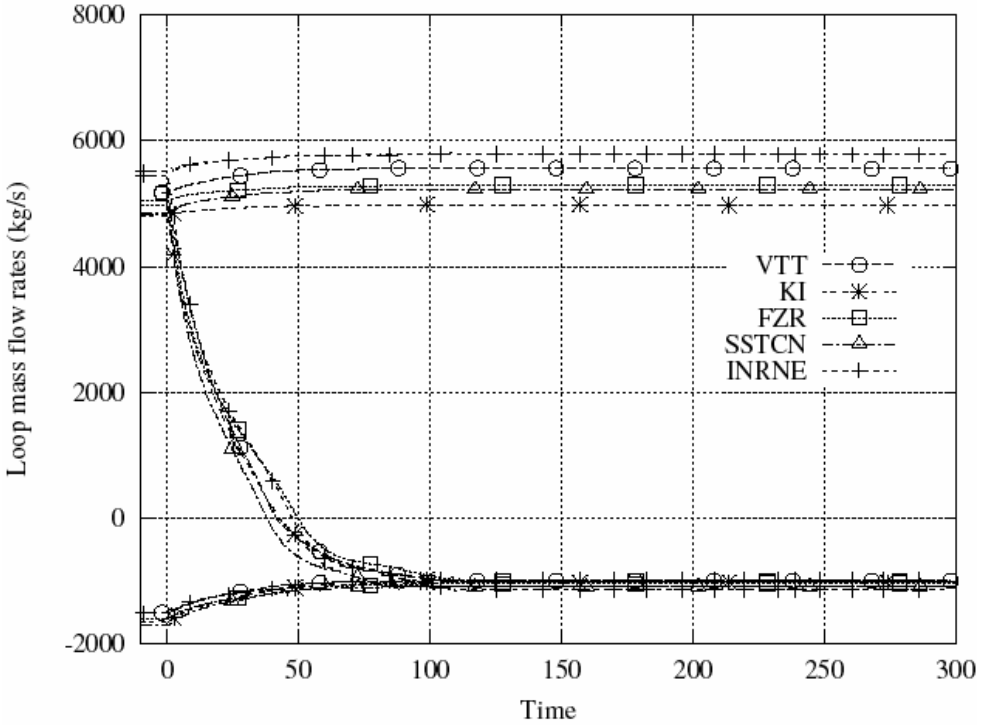


Figure 3.7 Calculated and measured mass flow rates in primary circuit loops.

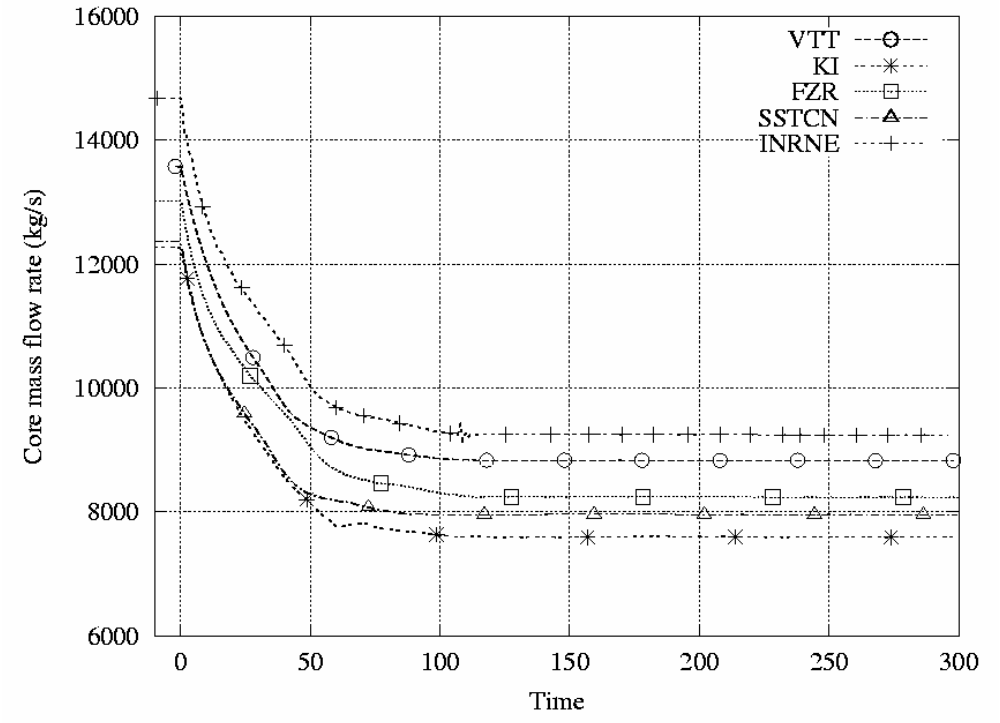


Figure 3.8 Calculated core inlet mass flow rates.

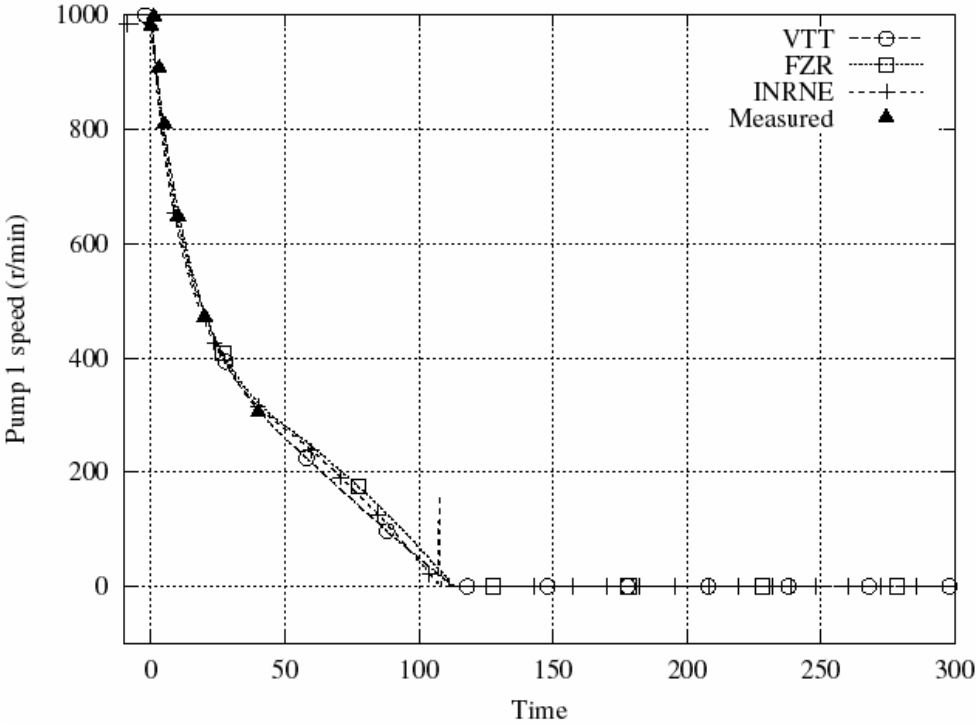


Figure 3.9 Main coolant pump 1 speed.

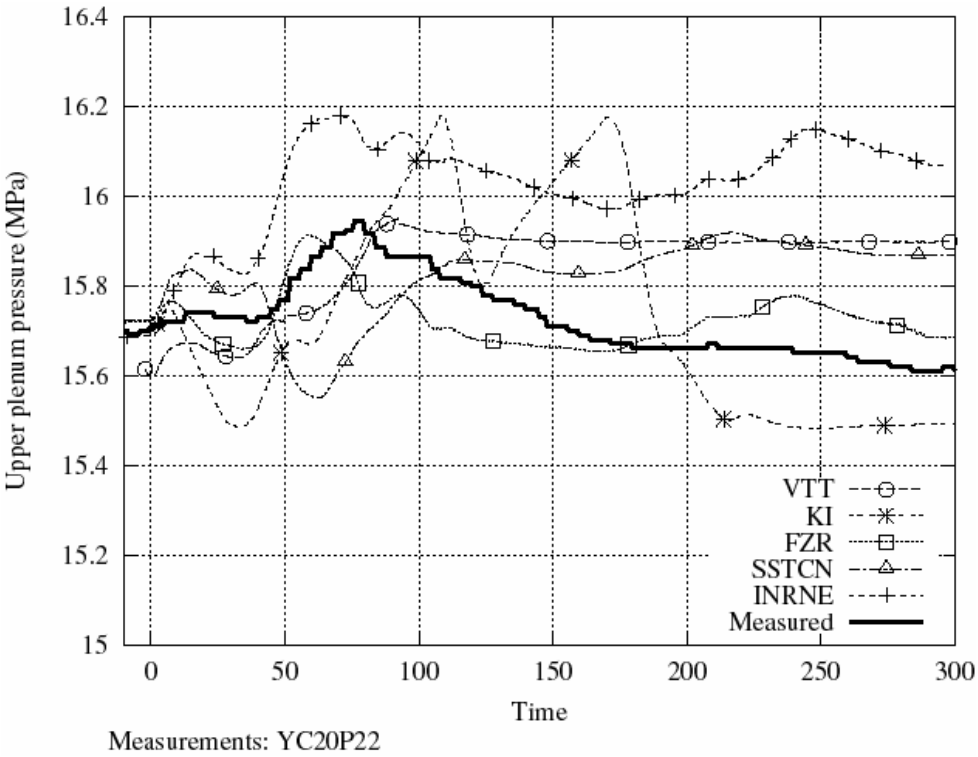


Figure 3.10 Calculated and measured upper plenum pressures.

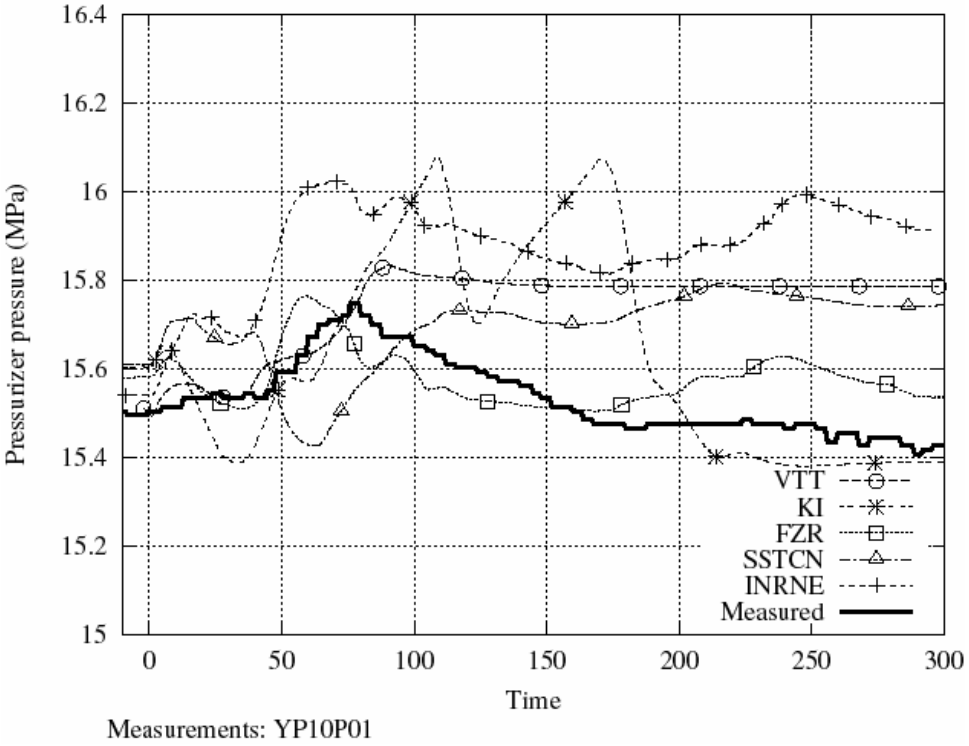


Figure 3.11 Calculated and measured pressurizer pressure.

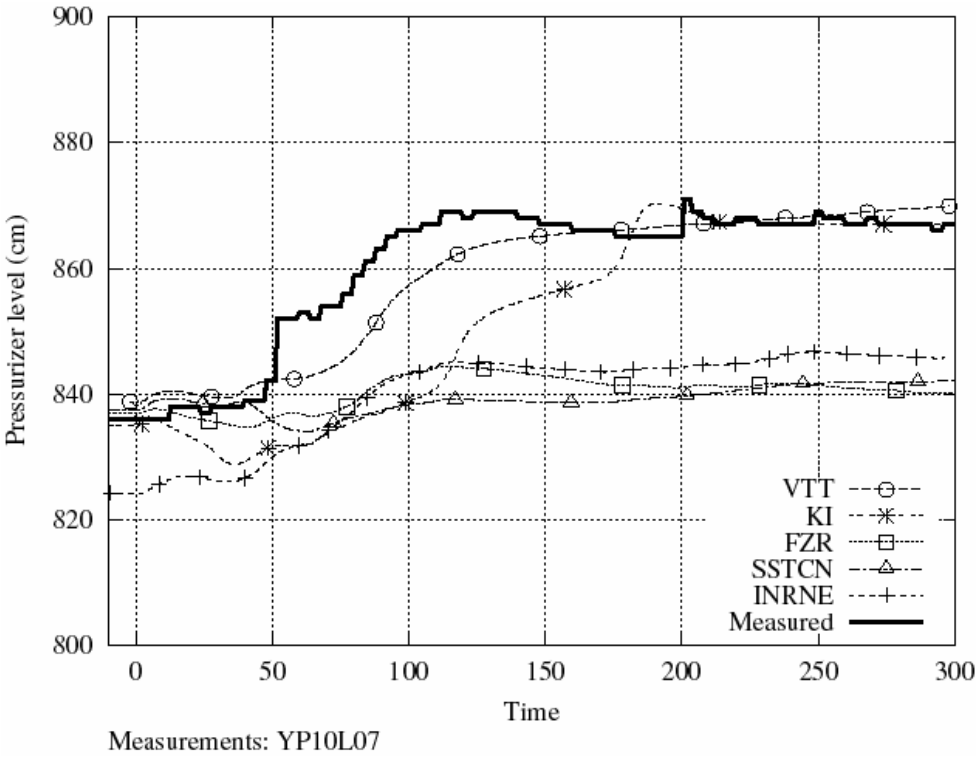


Figure 3.12 Calculated and measured water level in pressurizer.

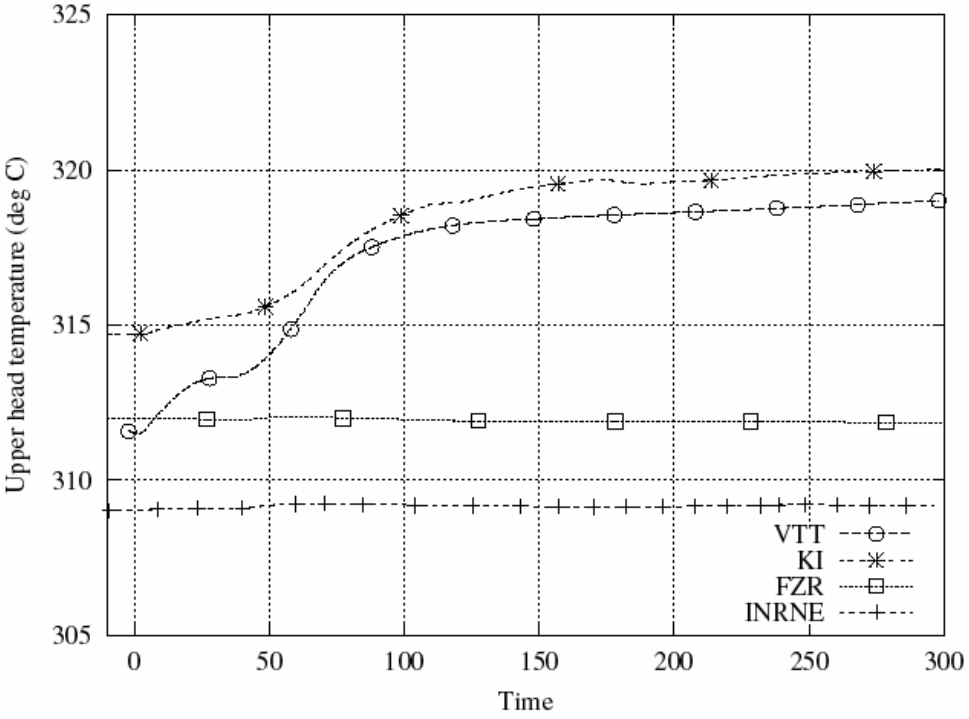


Figure 3.13 Calculated temperature in pressure vessel upper head.

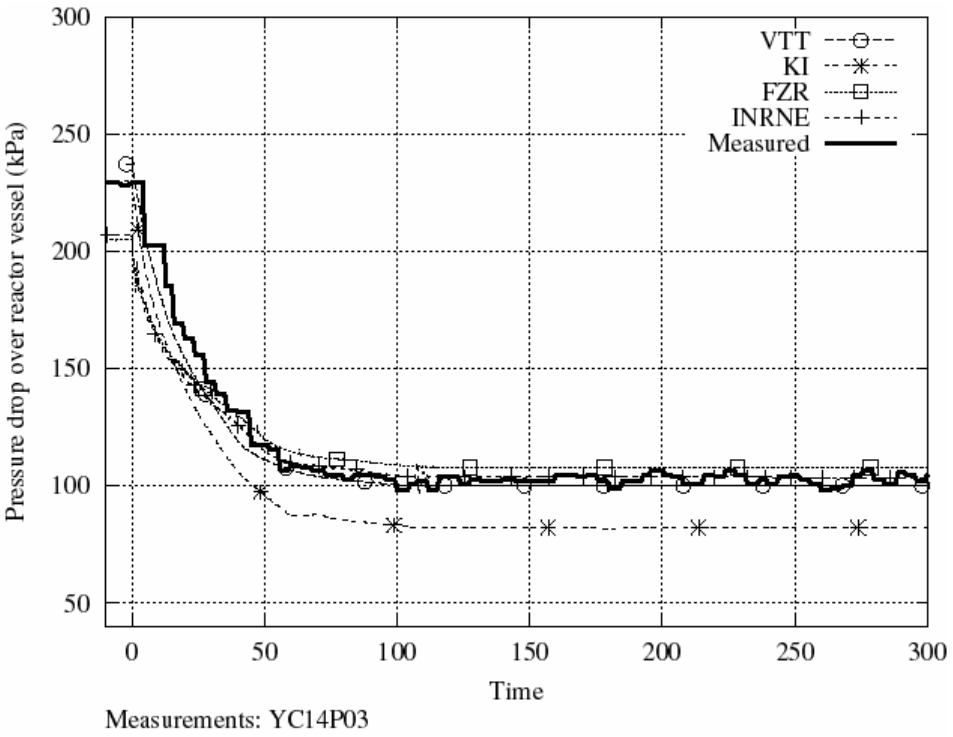


Figure 3.14 Calculated and measured pressure drop over core.

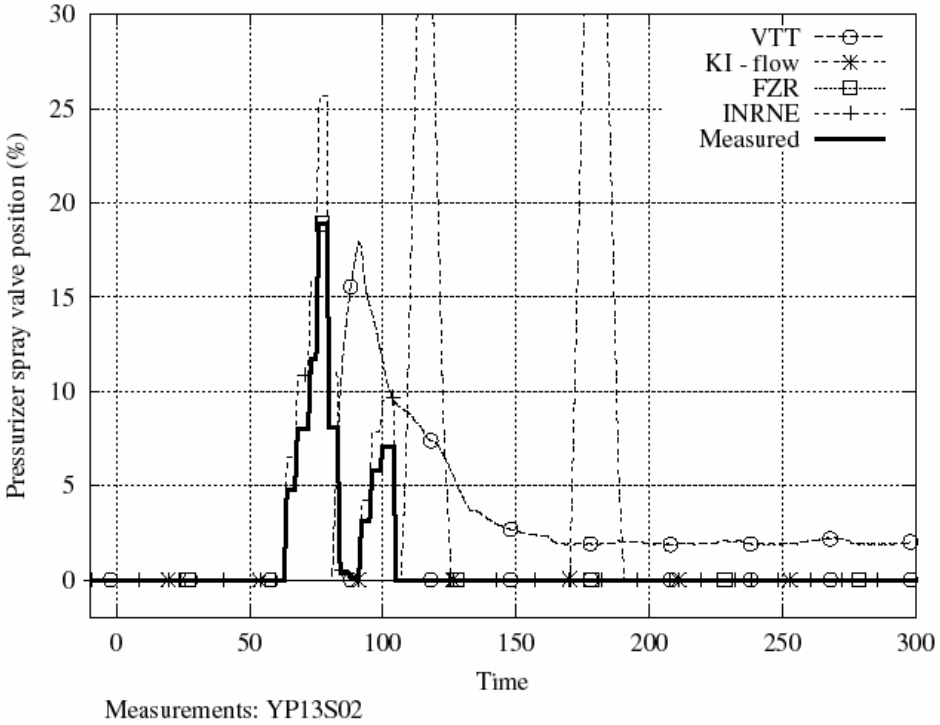


Figure 3.15 Measured and calculated spray valve opening.

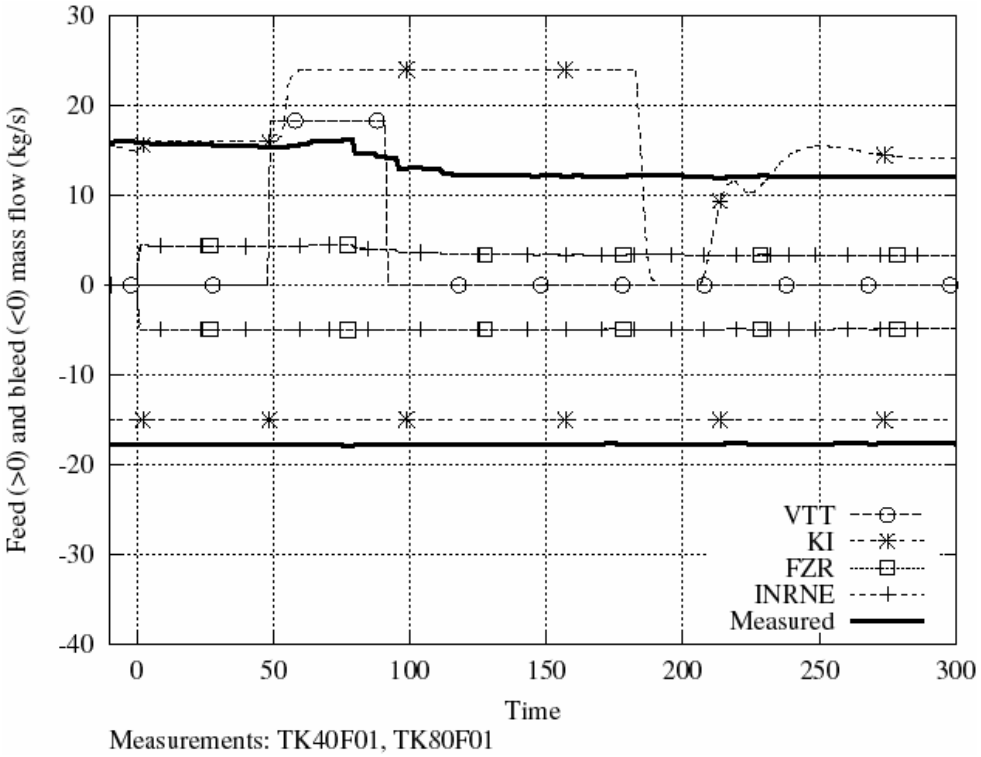


Figure 3.16 Measured and calculated feed and bleed mass flow**.**

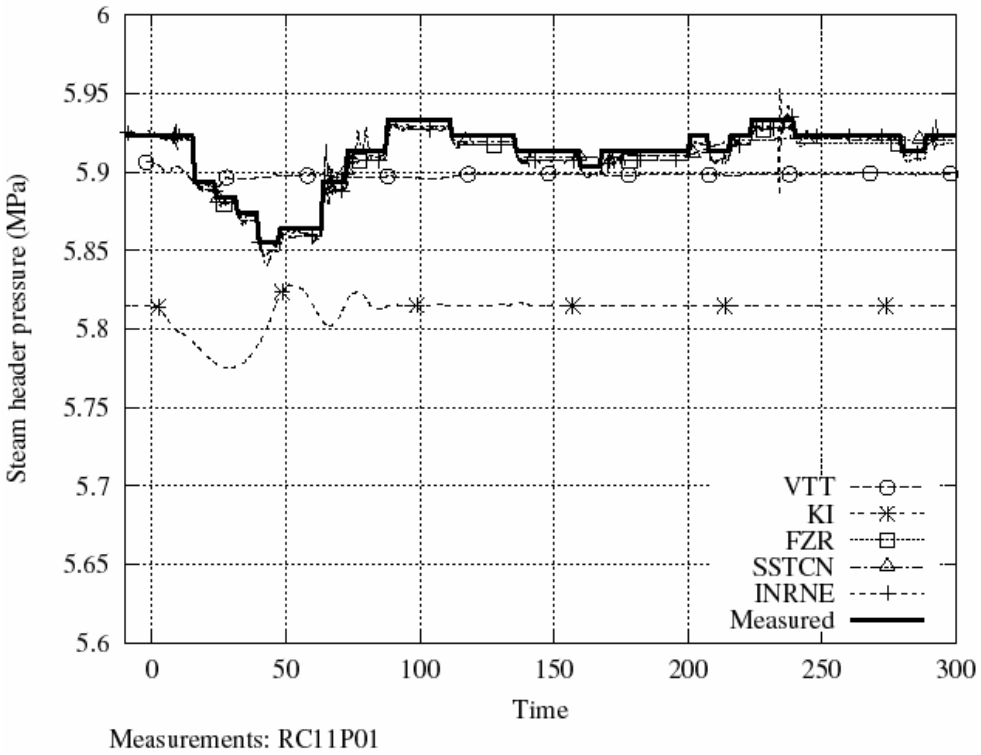


Figure 3.17 Calculated and measured pressure at steam headers.

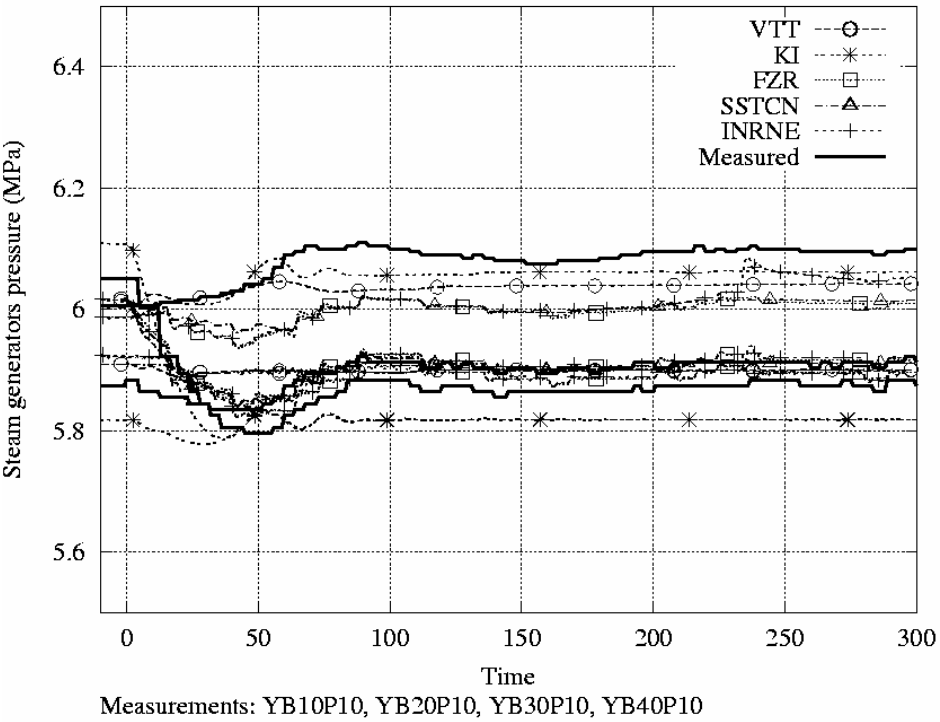


Figure 3.18 Calculated and measured pressure at steam generator secondary side.

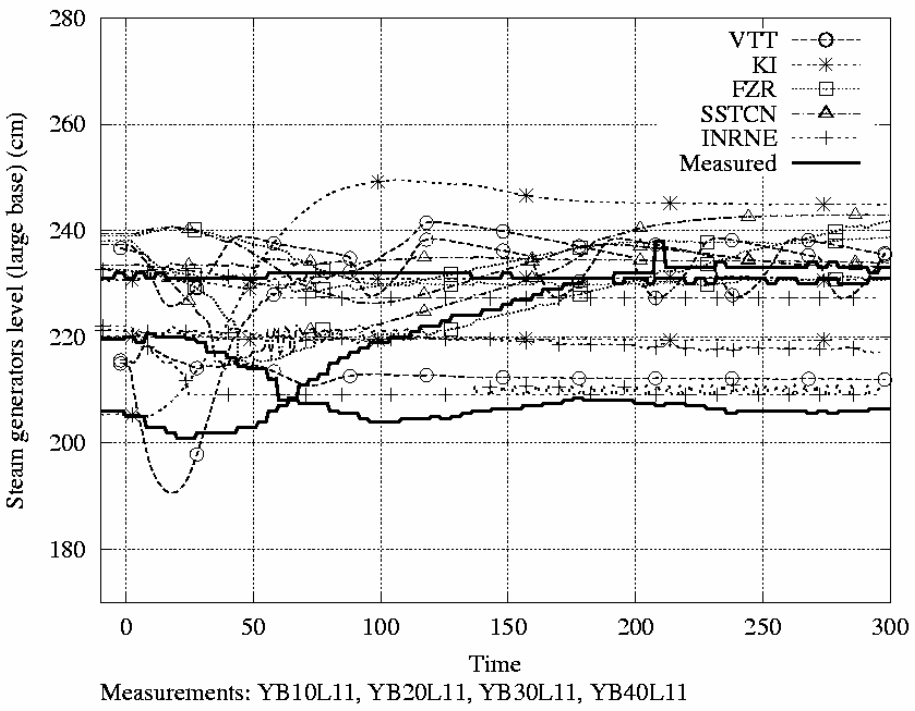


Figure 3.19 Calculated and measured collapsed water level in four steam generators.

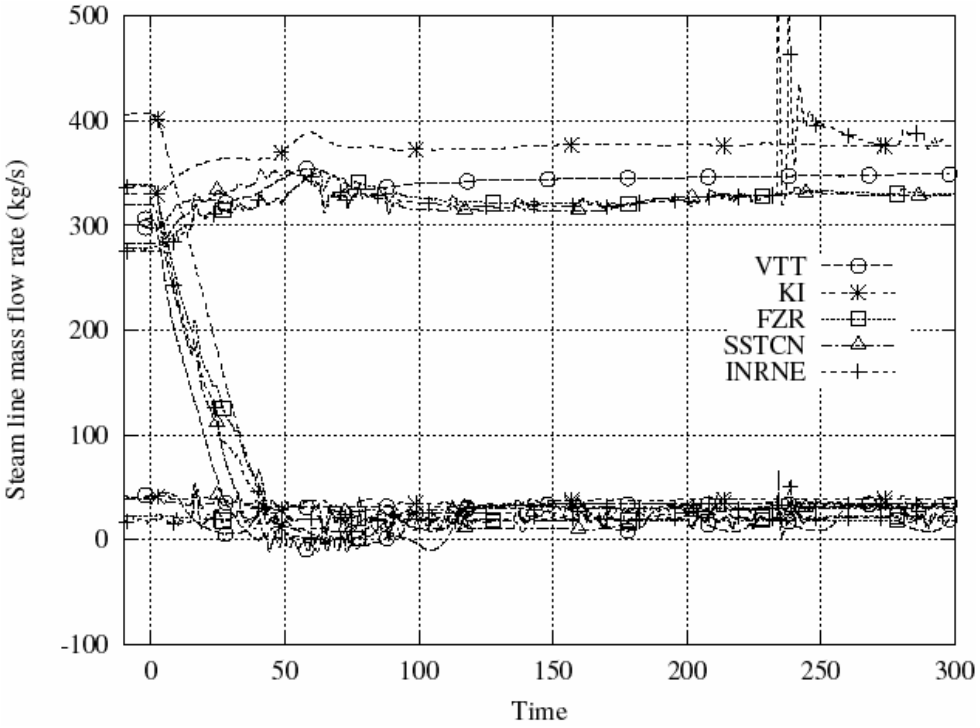


Figure 3.20 Calculated steam line mass flow.

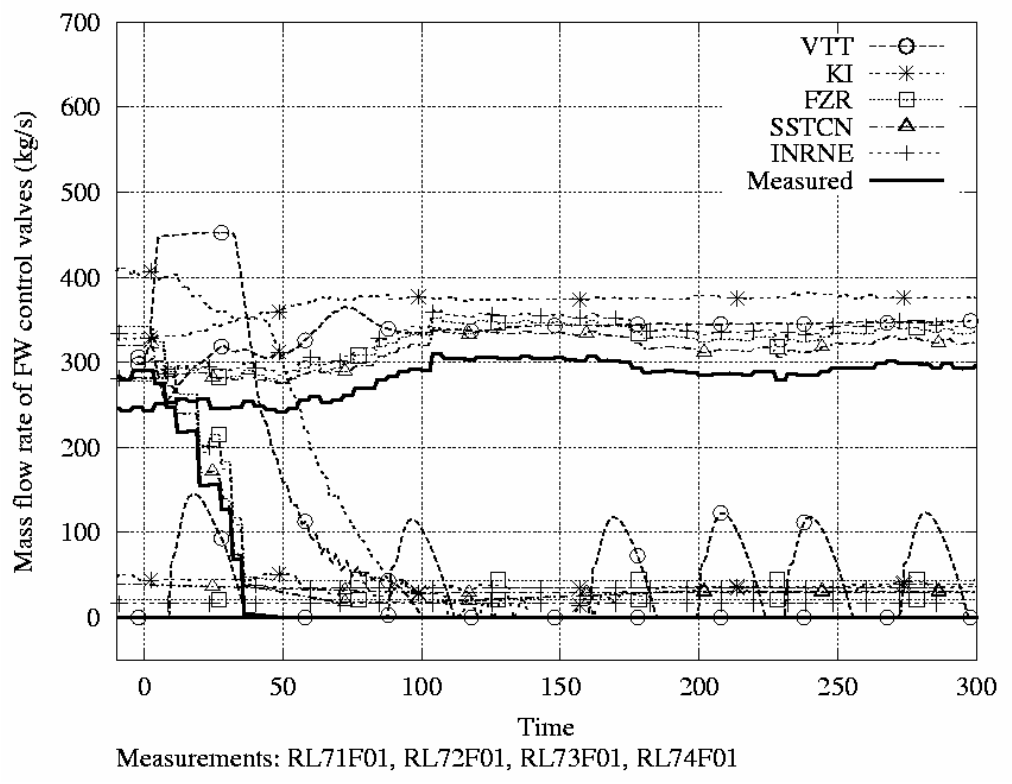


Figure 3.21 Measured and calculated feed water mass flow.

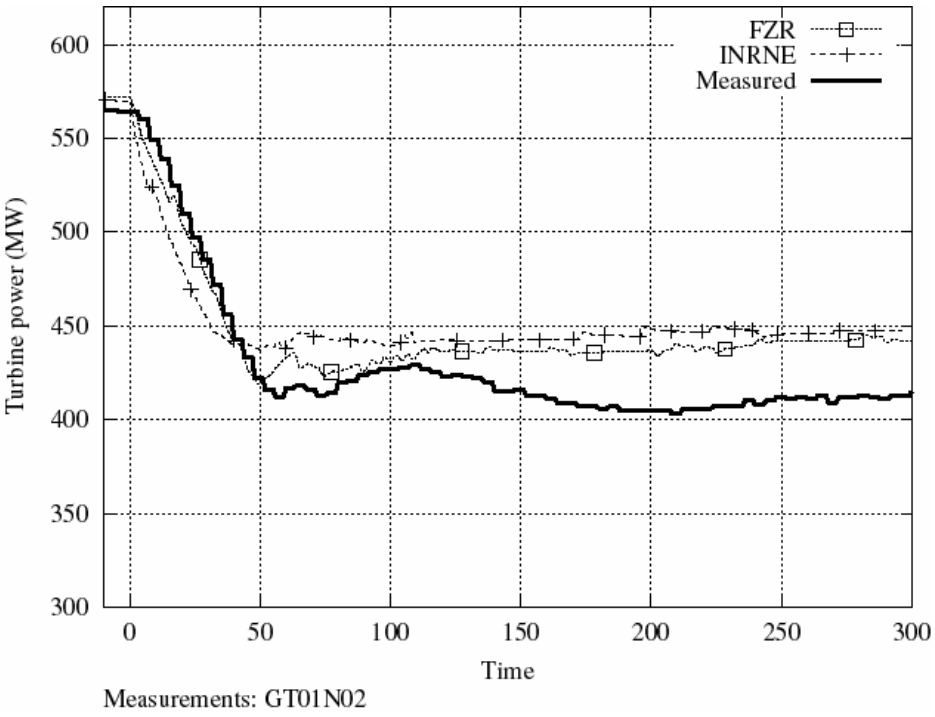


Figure 3.22 Measured and calculated turbine power.

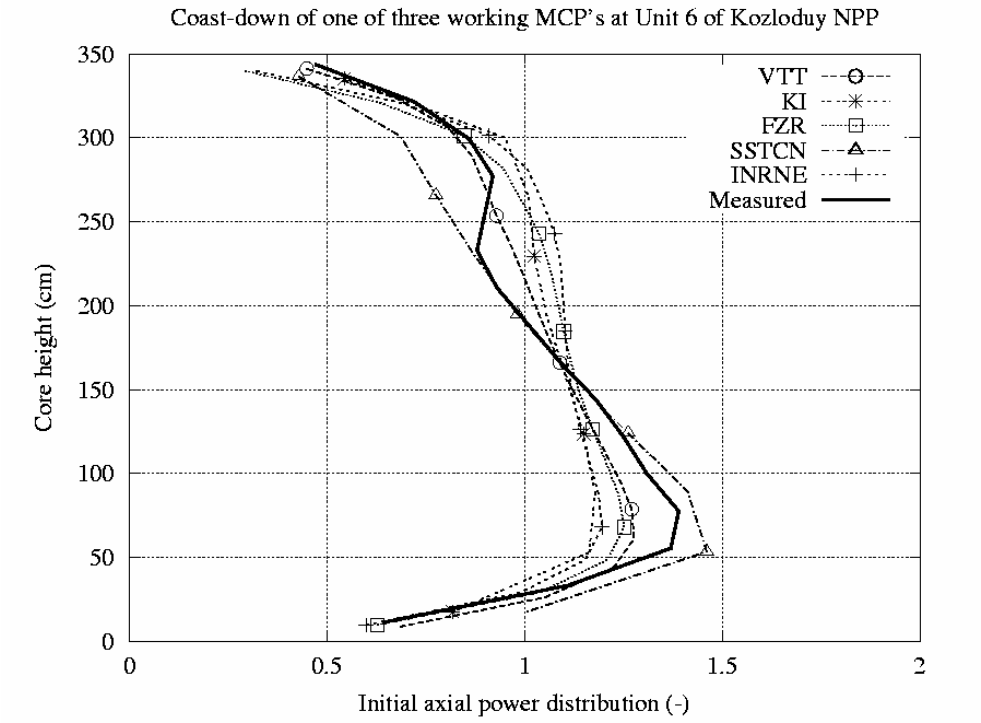


Figure 3.23 Measured and calculated initial axial power profile

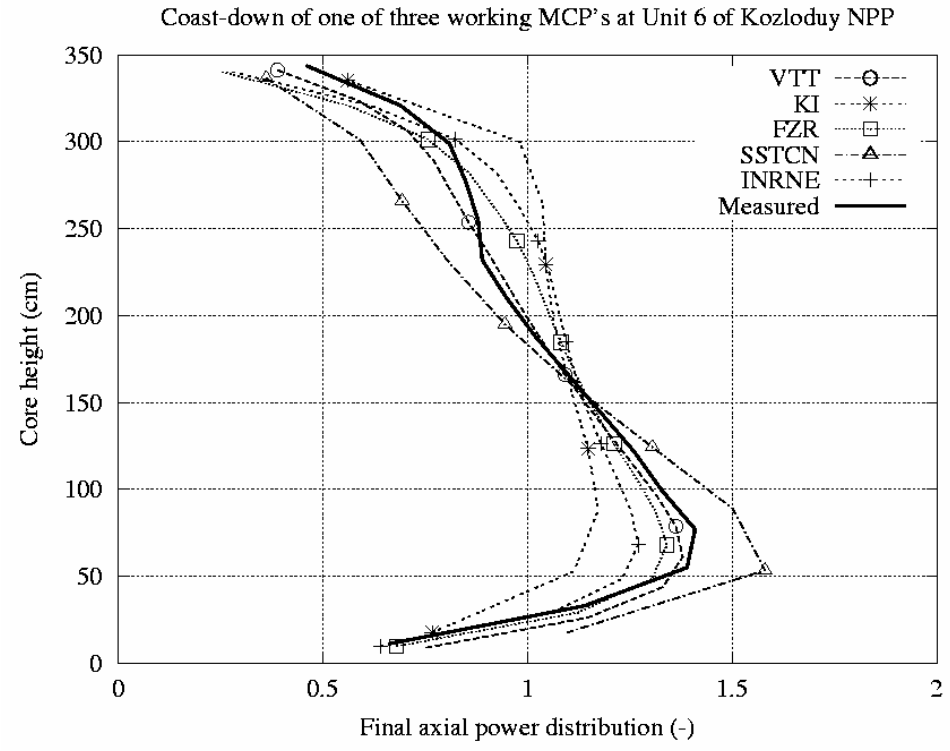


Figure 3.24 Measured and calculated final axial power profile

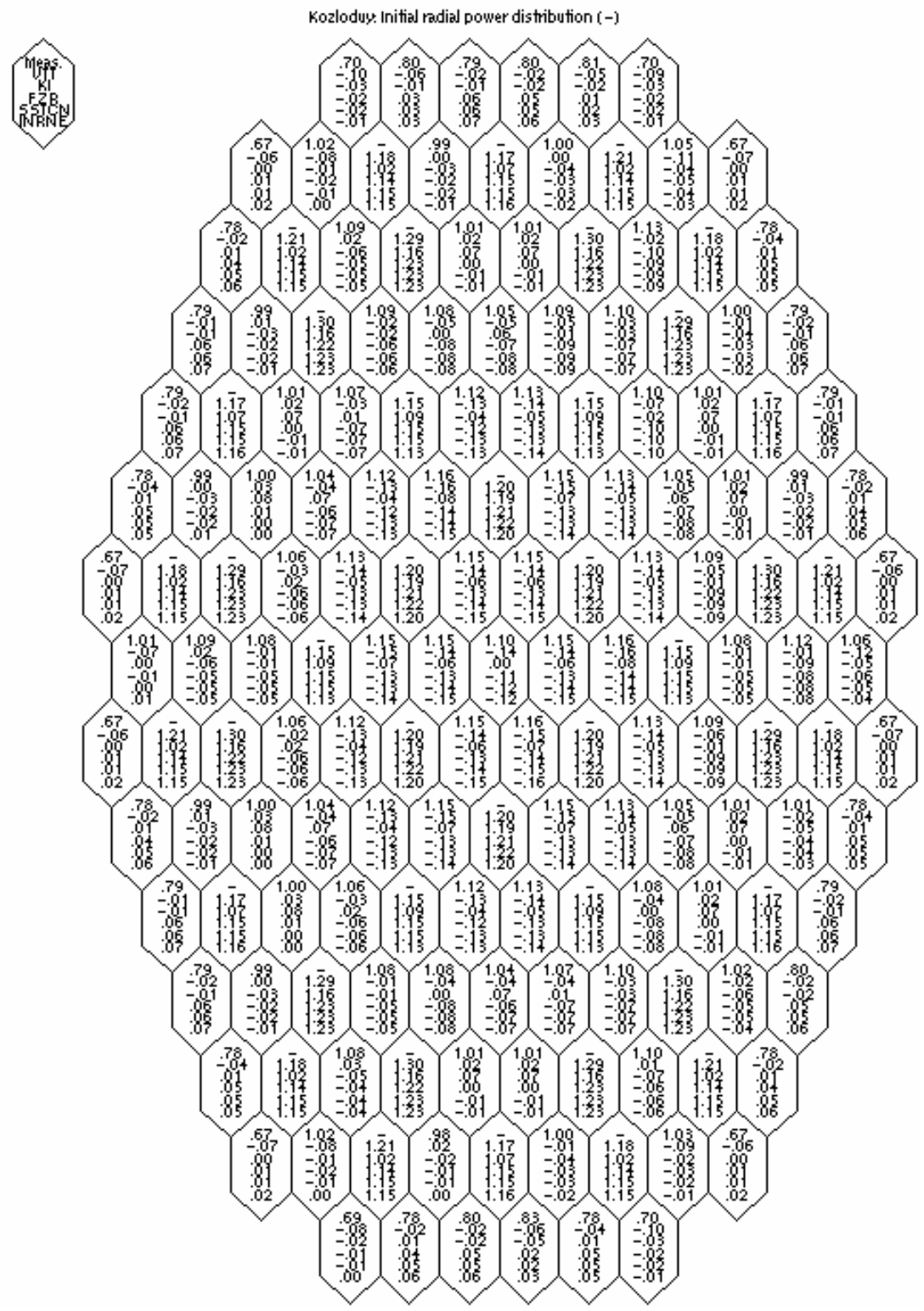


Figure 3.25 Calculated initial radial power distributions in Kozloduy case. Measured and deviation of calculations to measurements or just calculations if measurement is missing.

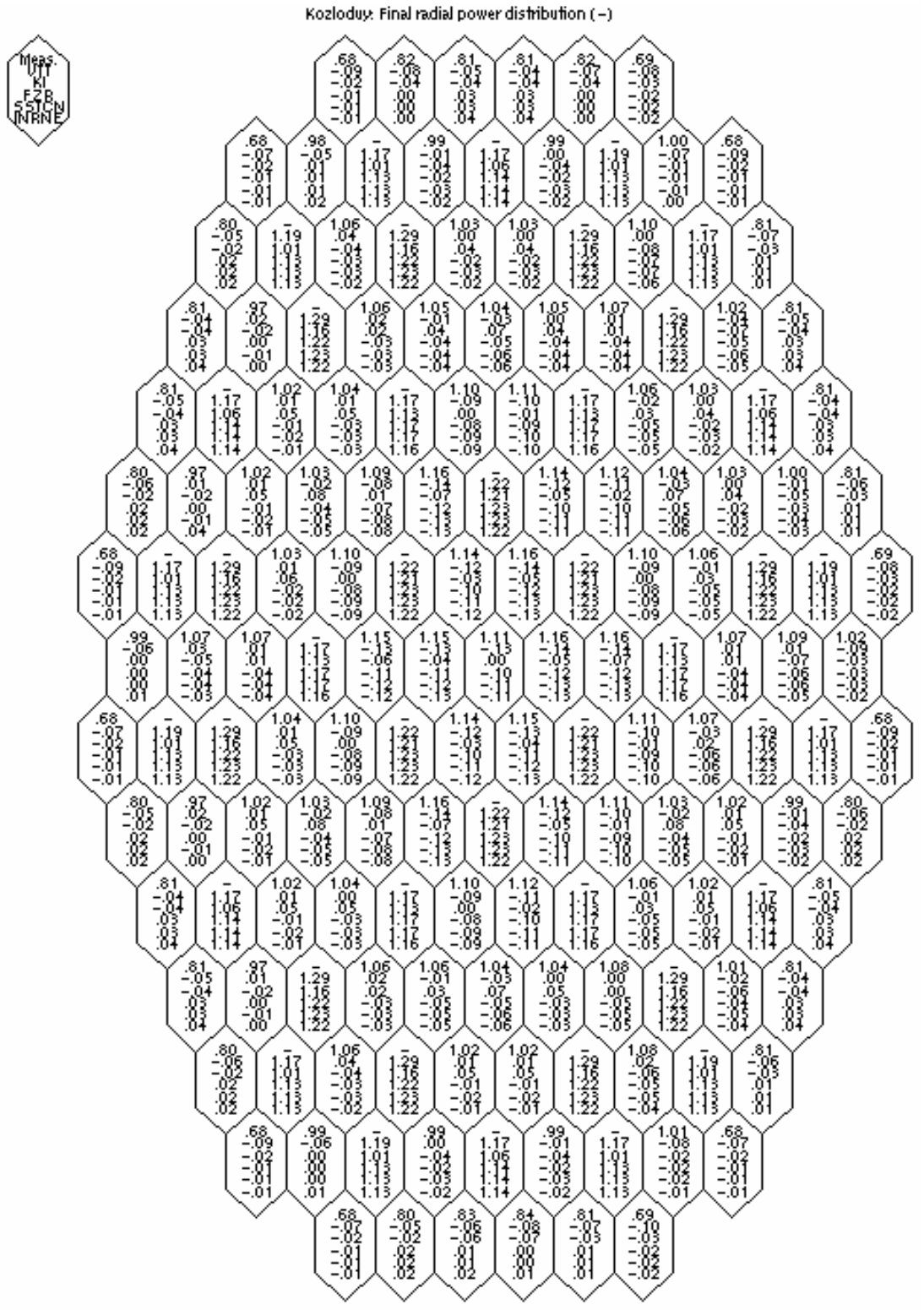


Figure 3.26 Calculated final radial power distributions in Kozloduy case. Measured and deviation of calculations to measurements or just calculations if measurement is missing.

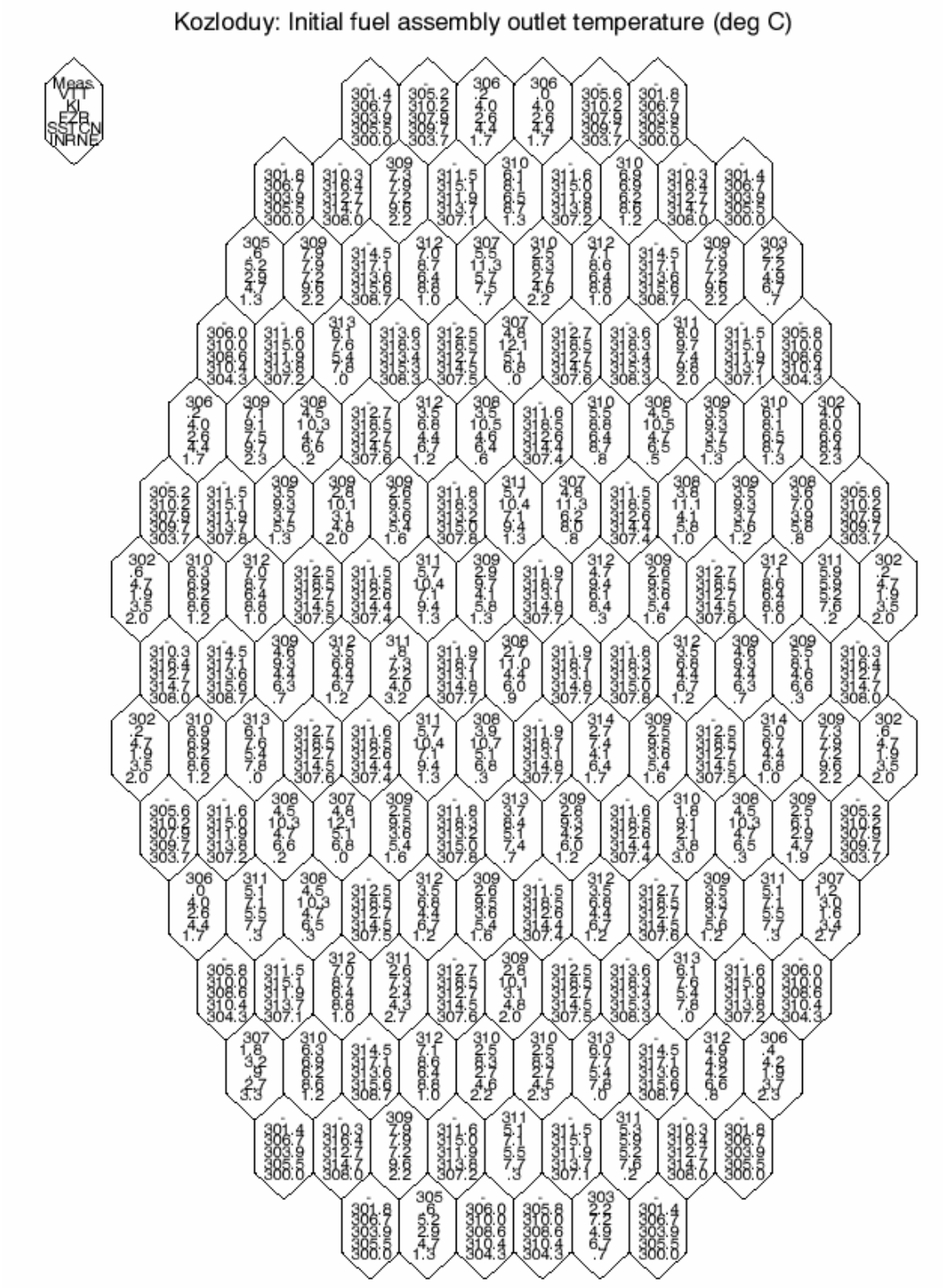


Figure 3.27 Measured and difference between calculated and measured initial fuel assembly outlet temperatures in Kozloduy case. Measured and deviation of calculations to measurements or just calculations if measurement is missing.

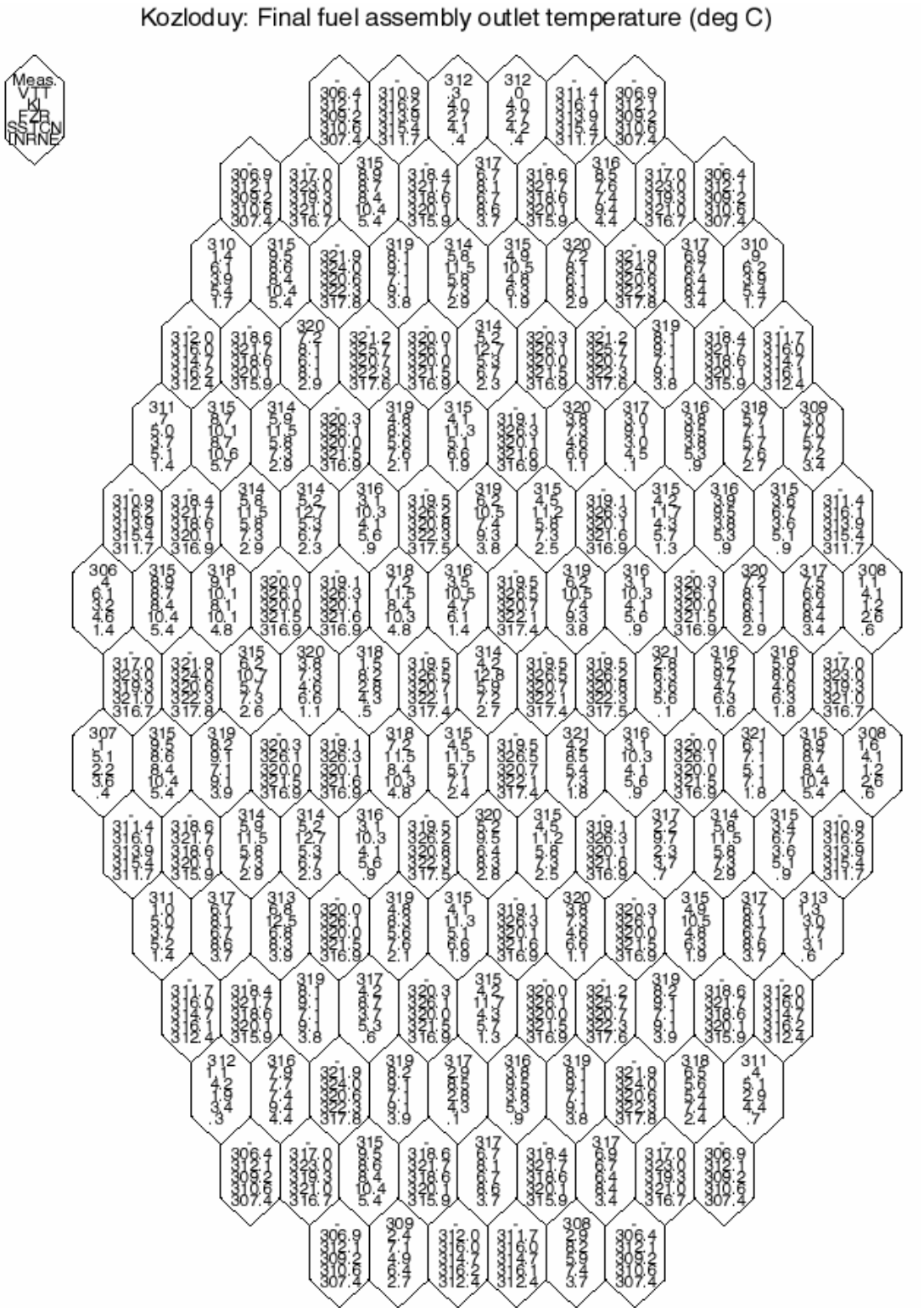


Figure 3.28 Measured and difference between calculated and measured final fuel assembly outlet temperatures in Kozloduy case. Measured and deviation of calculations to measurements or just calculations if measurement is missing.

# 4 CONCLUSION

In the Work Package 1 of the VALCO project a collection reports of five transients have been made and two of them, 'Drop of control rod at nominal power at Bohunice-3' for VVER-440 reactors and 'Coast-down of 1 from 3 working MCP:s at Kozloduy-6' for VVER –1000 reactor were selected for the code validation. The Bohunice case was an interesting and unexpected plant event, and Kozloduy was part of the plant start up tests. For the code validation eight institutes participated with five different coupled codes.

In the Bohunice case the behaviour of the core during the rod drop and during three minutes later starting control actions to reach 85 % power level is the most essential part for validation. General behaviour during the transients was quite well calculated with all the codes: both the power distribution changes and the fuel assembly outlet temperatures were mostly well reproduced. There were, however, differing results in the axial power profile, in the calculated control rod worth and in the level of fuel temperatures. The differences in the required control rod group movement to reach the final power were large. This may imply, that the fuel models need further attention.

The simultaneous measurements of the individual assembly outlet temperatures and the hot leg temperatures indicated that in the transient the coolant mixing in the upper plenum was weak. The result could be demonstrated with those codes that included a relevant mixing model and a detailed enough core channel model.

The features, that make the Kozloduy transient interesting, such as lowered power and reversed flow in the stopped loop in the initial state, also proved to be difficult both for data collection and for modelling. The data includes a longer history from full power nominal state, which in principle enables definition of the initial state for the calculations. Some more specific data would, however, have been needed about the pump characteristics and the control logics. Anyway, the general behaviour of the Kozloduy second pump trip was calculated satisfactorily with all the codes. In the comparison of the core outlet temperatures, a linear dependency between the assembly power and the difference between measured and the calculated temperatures could be observed in all the simulations.

Also in the Kozloduy case the initial fuel temperatures and the temperature differences during the transient vary remarkably. This paves the way for future needs of more accurate fuel models in the codes.

The comparison between the codes and validation against the measurements was successful and the results were acceptably accurate. The results were mainly obtained without additional corrections or a second round of calculations. The ability to interpret plant data has also increased among the participants.

## REFERENCES


1. Vanttola, T., Hämäläinen A., Measurement Data Collected For The Code Validation, VALCO/WP1/D1.0, 2002. VTT Processes, Finland.

2. Strmensky C., Darilek P., Hlbocky P., Suchon, M., Drop of control rod No. 287 in Unit 3 of NPP Bohunice, Data collection report, VALCO/WP1/EBO-VUJE-1, 2002. VUJE Trnava plc , NPP Bohunice, Slovak Republic.

3. Stefanova, S., Stoyanov, K., Passage, G., Hristova, V., Atanasova, B., Stoimenova, D., Collection, Evaluation And Documentation Of Measured Data From Two Transients At The Kozloduy Npp 6th Unit Incommissioning (1st Fuel Cycle), VALCO/WP1/INRNE-1, 2002. INRNE–BAS, Bulgaria.

4. Kyrki-Rajamäki R., Hämäläinen A., Kaloinen E., Additional data for drop of one turbine to house load level experiment on Loviisa-1 NPP, VTT/SRR195/LT1.0, 1999. VTT Energy, Finland.

5. Ivanov B., Ivanov K., Groudev P., Pavlova M., Hadjiev V., VVER-1000 Coolant Transient Benchmark, PHASE 1 (V1000CT-1) Vol. I: Main Coolant Pump (MCP) Switching On - Final Specifications, NEA/NSC/DOC(2002)6, 2002. OECD Nuclear Energy Agency, France.

6. Mittag R., Kliem, S., Weiss, F. P., Kyrki-Rajamäki, R., Hämäläinen, A., Langenbuch, S., Danilin, S., Hadek, J., Hegyi, G., Kuchin, A. & Panayotov, D. Validation of coupled neutron kinetic / thermal-hydraulic codes Part 1: Analysis of a VVER-1000 transient (Balakovo-4). Annals of Nuclear Energy, 2001. Vol. 28, pp. 857–873. ISSN 0306-4549.

7. Hämäläinen, A., Kyrki-Rajamäki, R., Mittag S., Kliem, S., Weiss, F. P., Langenbuch, S., Danilin, S., Hadek, J. & Hegyi, G. Validation of coupled neutron kinetic / thermal-hydraulic codes Part 2: Analysis of a VVER-440 transient (Loviisa-1). Annals of Nuclear Energy, 2002. Vol. 29, pp 215–321. ISSN 0306-4549.

**APPENDICES: CODE VALIDATION REPORTS IN VALCO:**

1) Hämäläinen, A., Vanttola, T., Recommendations for Calculations and Calculated Parameters for Comparisons from Bohunice and Kozloduy Transient, VALCO/WP1/GUIDE-3, 2002. VTT Processes, Finland.

2) Hämäläinen, A., Vanttola, T., Kaloinen, E., VTT Calculations of the Bohunice Rod Drop Transient, VALCO/WP1/VTT-BO-CALC, 2003. VTT processes, Finland.

3) Strmensky, C., Darilék, P., Kvizda, B., Suchon, M., Hlbocky, P., VUJE Calculations Of The Bohunice Rod Drop Transient, VALCO/WP1/VUJE-BO-CALC, 2003. VUJE ltd., SE EBO ltd., Slovakia.

4) Hádek. J., Lahovský, F., Macek. J., NRI Calculations of the Bohunice Rod Drop Transient, VALCO/WP1/NRI-BO-CALC-1, 2003. Nuclear Research Institute Řež plc, Czech Republic.

5) Hegyi, G, Keresztúri, A., Trosztel, I, Aeki Calculations Of The Bohunice Rod Drop Transient, VALCO/WP1/AEKI-BO-CALC, 2003. KFKI-AEKI-RAL, Hungary

6) Danilin, S., Nikonov, S., Lizorkin, M., KI Calculations Of The Bohunice Rod Drop Transient, VALCO/WP1/KI-BO-CALC, 2003. RRC "Kurchatov Institute", Institute of Nuclear Reactors, Russia.

7) Hämäläinen, A., Vanttola, T., Kaloinen, E., VTT Calculations of the Kozloduy Pump Trip Transient, VALCO/WP1/VTT-KO-CALC, 2003. VTT Processes, Finland

8) Danilin, S., Nikonov, S., Lizorkin, M., KI Calculations of the Kozloduy Pump Trip Transient, VALCO/WP1/KI-KO-CALC, 2003. RRC "Kurchatov Institute", Institute of Nuclear Reactors, Russia

9) Kliem, S., Kozmenkov, Y., Mittag, S., Weiss, F.-P., FZR Calculations of the Kozloduy MCP Switching off Transient, VALCO/WP1/FZR-K6-CALC, 2003. FZR, Germany

10) Kuchin, A., Khalimonchuk, V., SSTC NRS Calculations Of Coast-down of one of three working MCPs at Kozloduy, unit 6, VALCO/WP1/SSTC NRS-KOZ-CALC, 2003. SSTC NRS, Ukraine

11) Stefanova, S., INRNE Calculations of the Kozloduy Pump Trip Transient, VALCO/WP1/INRNE-KO-CALC, 2003. INRNE, Bulgaria. Not ready.